Teleskoppraktikum

Marco Müllner, Sebastian Panny, David Weßmayer & Sebastian Zieba

October 2018 -February 2019

Figure 1: RGB composite image of cluster M34 compiled from Johnson R,I and V filters taken with the Innsbruck 60 cm telescope.

Abstract

The Innsbruck 60 cm observatory provides an excellent opportunity for students to familiarize themselves with the operation, data acquisition and data reduction processes used in astronomy. In this work, we present our results of working with the instrument and the data acquired in the "Teleskoppraktikum" during the winter semester 2018/19 at the University of Innsbruck.

In particular we describe the instrument calibration, the data reduction for imaging and spectroscopy and the results of our observations of open clusters, a comet, as well as stellar spectra. Furthermore we touch on the subject of lucky imaging and use catalogue data to investigate the status of open cluster candidates.

Contents

1 Introduction

Learning how to operate a telescope and how to work with the data one can derive from observations of the sky is the primary goal of the "Teleskoppraktikum". The 60 cm Cassegrain telescope at the observatory of the University of Innsbruck and the instruments available there, are the tools used to achieve our first real foray into astronomy. This report takes us from the utter excitement during our first observations to the results accomplished by weeks of team work and individual efforts via a slight detour to our first setbacks and our learning process.

The Innsbruck 60 cm telescope is located atop the Victor Franz Hess building at the Technik campus of the University of Innsbruck (00h45m22.20s, 47°15′51.19″, 580 m above sea level). It is the only ground based observatory used for our work during the "Teleskoppraktikum".

The course takes place from late October 2018 to the end of February 2019, where the first few weeks are used for lectures on the basics of astronomy, telescope calibration and image reduction using tools like IRAF. From December on, we start with the actual observations, finishing in late January. Afterwards we work with the gathered data using a multitude of software tools and approaches to familiarize ourselves with the processes that are used regularly in astronomy.

Altogether six days are used for observations, of which two are used for gathering calibration data, one for spectroscopy using an Echelle spectrograph one for both imaging and spectroscopy using a Littrow spectrograph and two specifically for imaging alone. Additionally some data is taken by the lecturers during the semester and is provided to us and the other students.

This report showcases all the steps of our work during the "Teleskoppraktikum", starting with the calibration of the setup in section 2 and an overview of the reduction procedure in section 3. Where the first one explains the determination of the optimal CCD temperature and pixel binning for the different cameras used and the second one the reduction of the various imaging data taken during the observation runs during the course.

Next, in section 4, we describe the procdedure and hardships we encounter while using the telescope for imaging purposes. In particular the imaging of a comet close to Earth and open galactic clusters is explained in this section. We focus on the pocedure of extracting their position and brightness information of stars from an image, as well as the creation of Hertzsprung-Russell diagrams from images in several filters and the identification of probable members to the imaged clusters (and cluster candidates respectively) with data taken by the ESA spacecraft/mission Gaia.

In this section we additionally introduce lucky imaging as a method to counteract the influence of Earth's atmosphere on the image quality by reviewing the results of stacked images of Moon observations with a lucky imaging camera.

Finally, in section 5, the spectra taken during the course are analyzed and the procedure of taking a spectrum and reducing the data received, is explained with the aid of the spectra of two bright and well studied stars Vega and Deneb.

2 Calibration

In this first step we perform a calibration on camera 1 and 2, to find the good working temperatures for the cameras. We take multiple images for each temperature step, reducing statistical outliers and giving us a clearer picture on how the camera performs. We take images for all temperatures with a binning of 1 and 2.

2.1 Bias calibration

2.1.1 Camera 1

For camera 1 we get an initial set of 10 images for each temperature from −5 °C to −40 °C in 5 °C steps, with binning 1 and 2. These images are then combined, with outliers being clipped from the averaging process, giving us only real bias values. We then generate a master bias file for each temperature, that is then used for the dark calibration. Figure 2 and figure 3 show the resulting CCD images for binning 1 and 2.

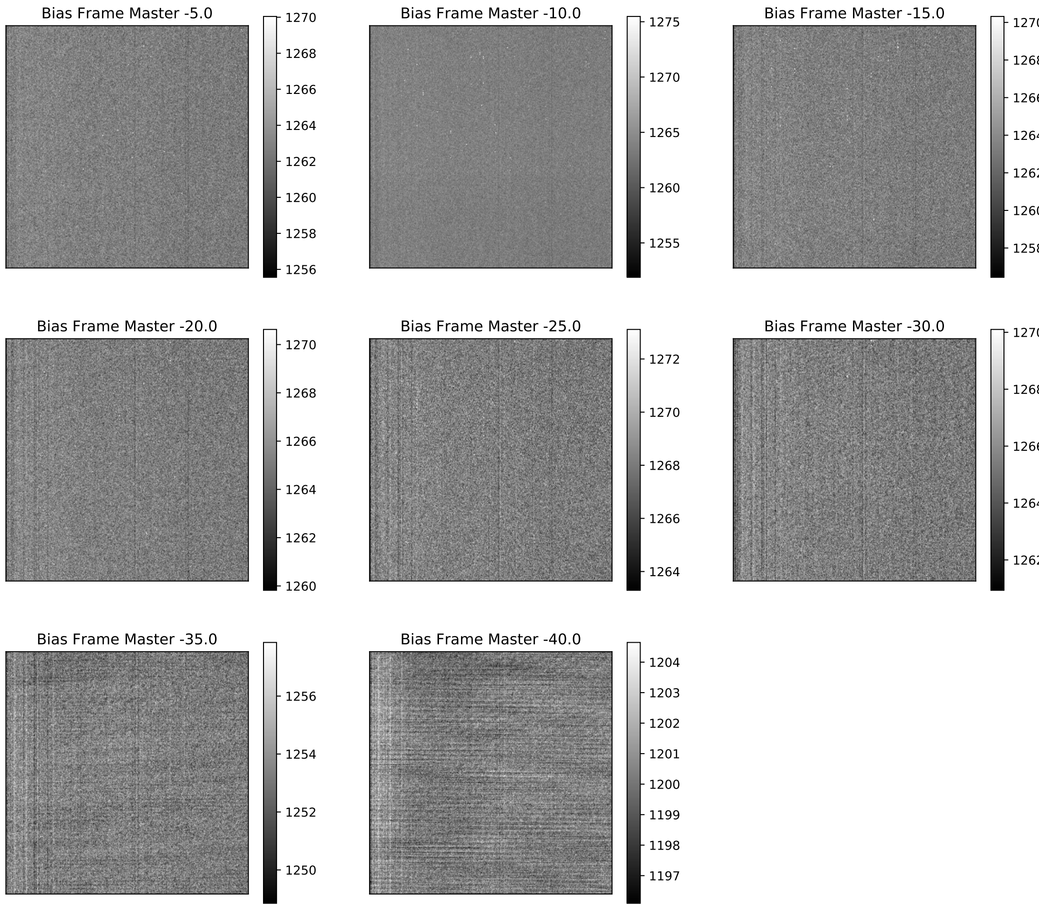

Figure 2: Bias images for camera 1 for different temperatures as noted in the titles with binning of 1. The biases show stronger structures, the lower the temperature is set.

Through visual inspection of these images, one can clearly see the emergence of a regular, horizontal pattern in the biases for lower temperatures. Clearly these lower temperatures are therefore not useable for proper imaging, as these will deform images and distort them. A clear reason for these vertical regularities was not found up to the point of writing this report. It is suspected that the shared power supply for the cameras is maybe to blame for this behaviour. We also can see some vertical regularities, from the first temperature step on. These are probably features of the CCD itself, and need to be noted and known in the further analysis. Looking at the behaviour of camera 1 with a binning of 2, this behaviour is persistent and even more expressed, again especially for lower temperatures. Figure 3 shows the CCD images for binning 2. Because of the clear worsening in the behaviour of the camera we decide to only use a binning of 1 from here on out.

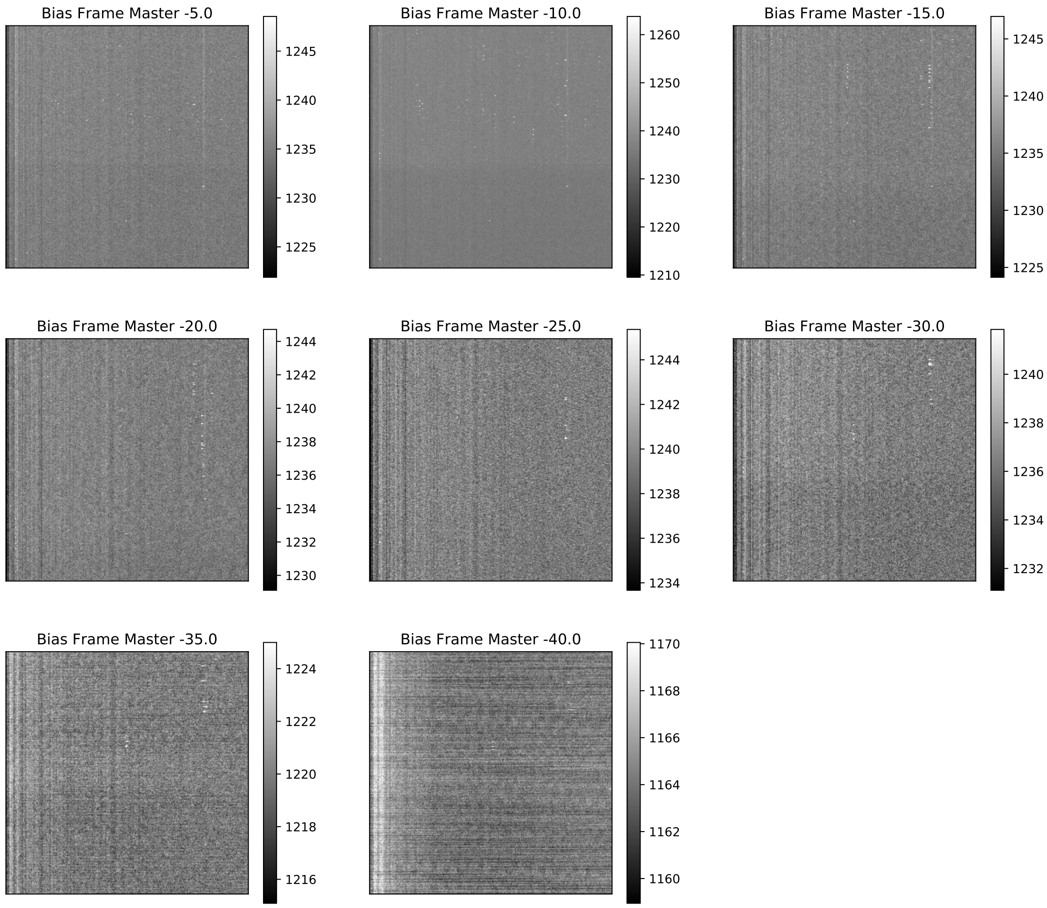

Figure 3: Same as figure 2 but with binning 2. A even more distinct expression of vertical and horizontal structures is present for this setting.

This effect in the biases lead us to the idea of disabling other cameras while taking images with the imager. We again take new biases for this camera, leading to the result shown in figure 4.

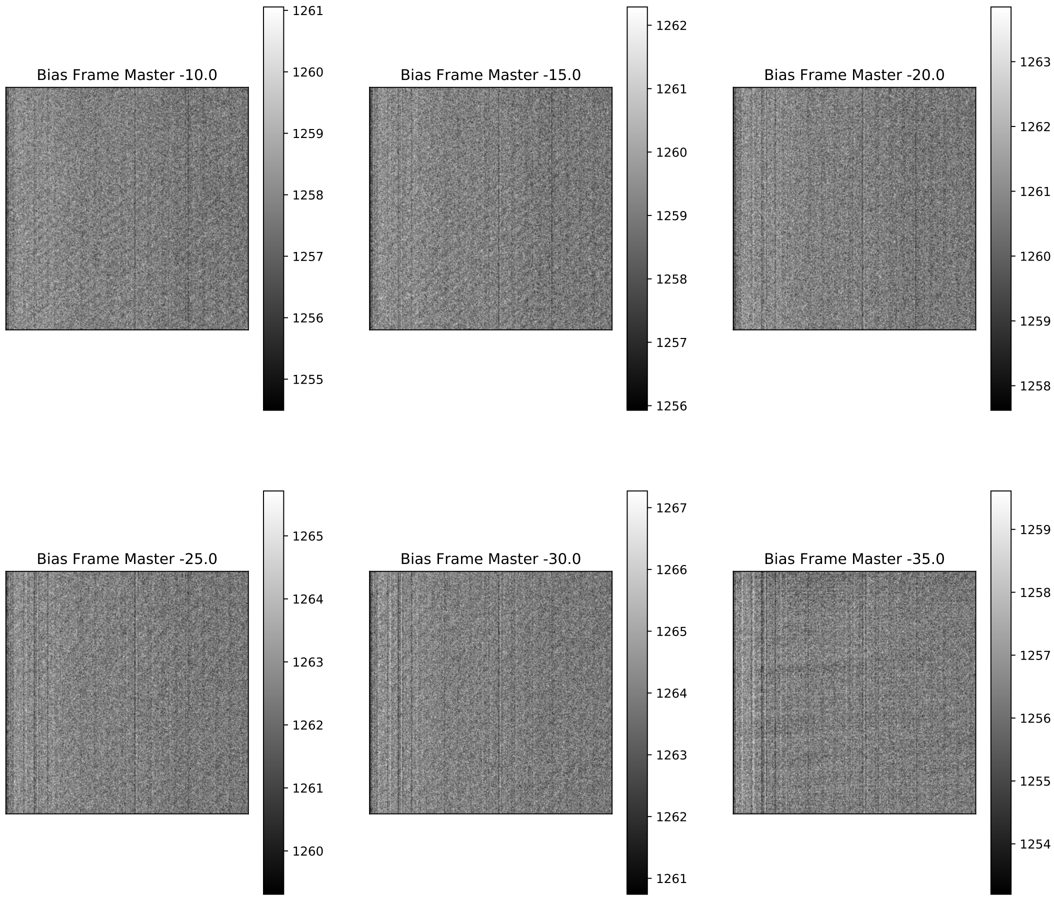

Figure 4: Bias images for camera 1 with reduced load on the power supply with binning 1. Vertical structures are still visible, horizontal structures begin to appear at $-35\,^{\circ}\mathrm{C}$.

This leads to an improved image in the biases. The horizontal lines at $-35\,^{\circ}\mathrm{C}$ are weaker than the ones done in the first batch, yet still visible, so the problem is not totally solved using this solution. All further analysis for camera 1 takes place using this new batch of images. Looking at the distributions of the pixel values in figure 5, we can see this behaviour as well. For the lowest temperature at $-35\,^{\circ}\mathrm{C}$ we can see some slight edging out in the distribution, while for the lower ones this behaviour seems to be mostly nonexistent. We find clear gaussian distributions for the pixel values. This is to be expected, as the process that creates the bias should lead to normally distributed pixel values.

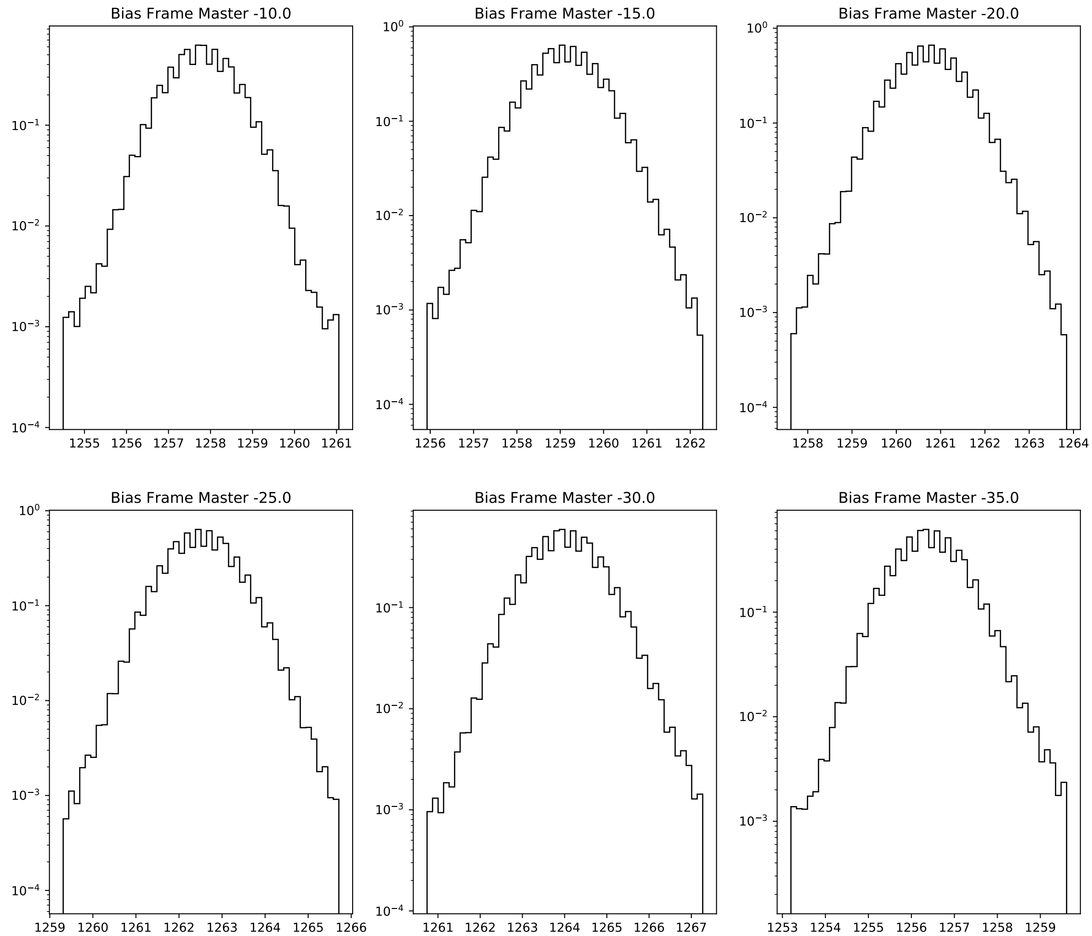

Figure 5: Distribution of pixel values for the different temperatures. The y axis for all plots is logarithmically plotted to better see the features of the dataset.

2.1.2 Camera 2

While we use camera 1 fairly extensively throughout this work, the second camera was rarely used. We therefore lack some practical experience using this camera. Similarly to camera 1 we get a batch of biases and darks to perform a calibration on the camera. We again use multiple bias images for a temperature range between 0 °C and −45 °C for binning 1 and 2.
Visual inspection of the biases shows the emergence of vertical patterns on the CCD as seen in figure 6. By looking at the distribution of pixel values, as seen in figure 7, the structural behaviour of this is clearly discernible at −45 °C. Looking at these distributions, a temperature in the middle ranges is preferable, as these seem to reproduce the best behaviour of camera 2.

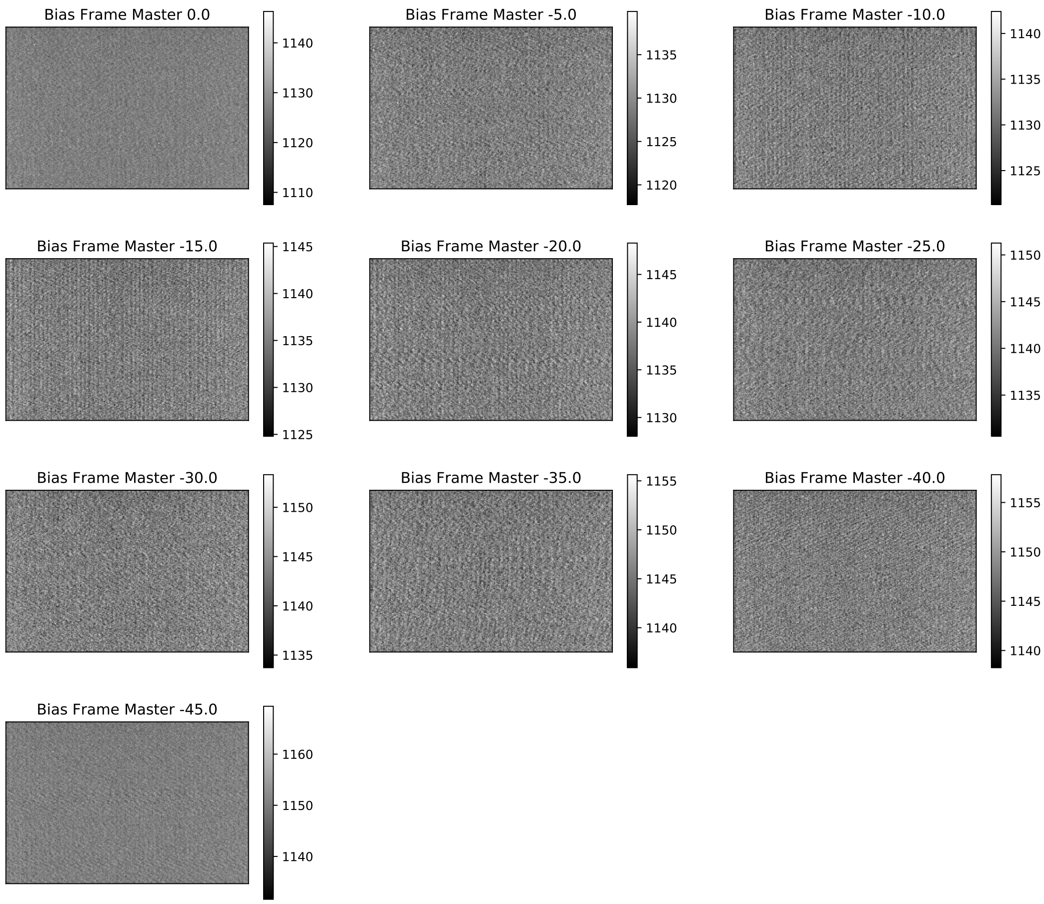

Figure 6: CCD images for camera 2 with binning 1, with different temperatures. We can clearly see more vertical structures on the CCD than on camera 1.

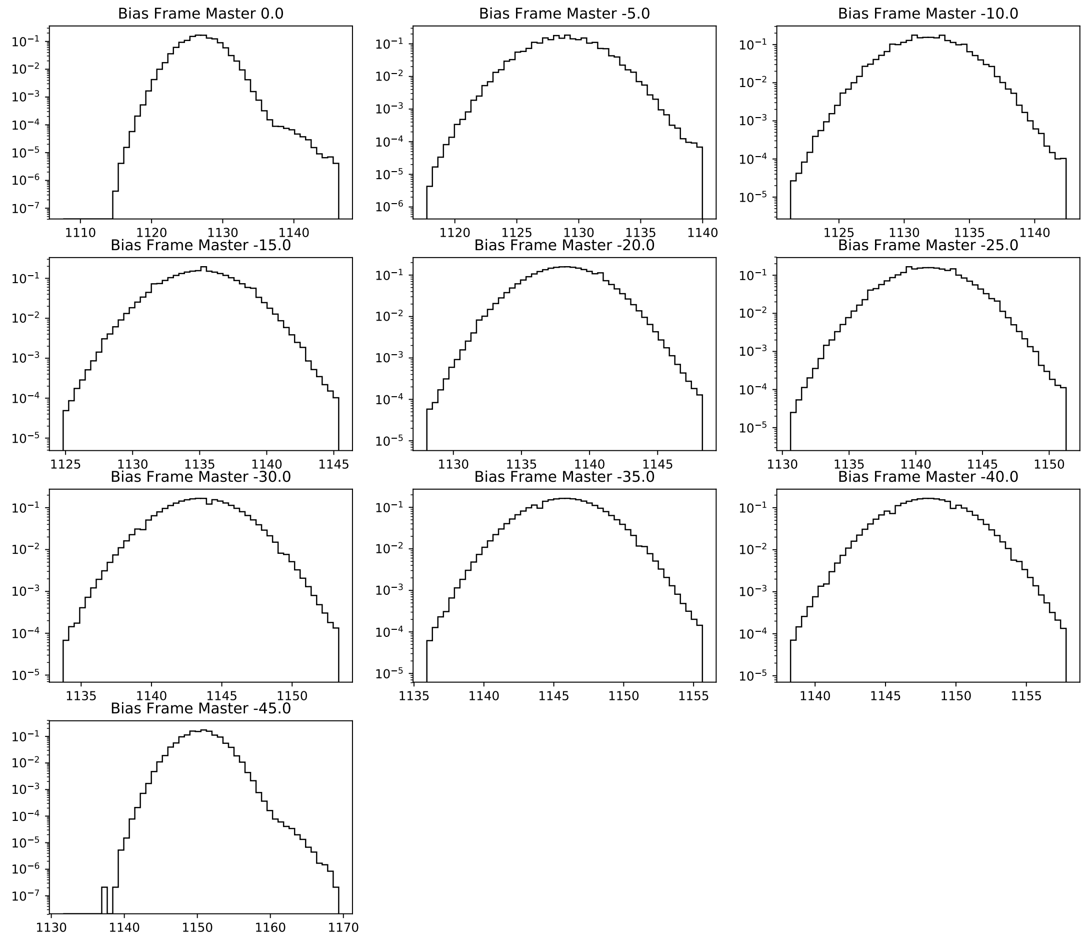

Figure 7: Distribution of pixel values for camera 2 with binning 1, with different temperatures. The pixel values are again logarithmically plotted. The best distributions for these temperatures can be found at $-20\,^{\circ}$C, $-30\,^{\circ}$C, $-35\,^{\circ}$C and $-40\,^{\circ}$C. These show nice normal distributions for their pixel values. The rest has some deformities in their distributions, especially at $-45\,^{\circ}$C.

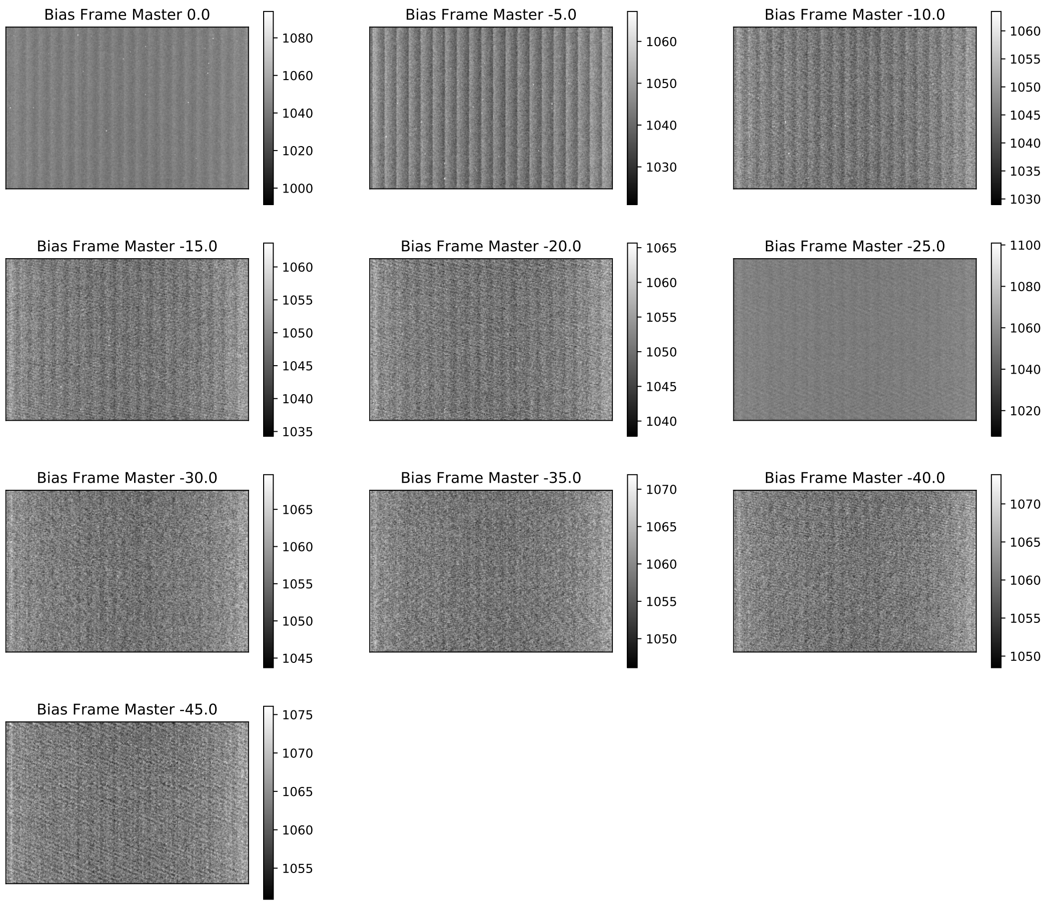

Figure 8: Same as figure 6 but with a binning of 2. The structure of the CCDs does not resemble a bias anymore, but rather a very regular structural pattern, that shows vertical and diagonal structures.

We also look at the behaviour of camera 2 with binning 2. This reproduces the by far worst result of all of them. We have a column like structure, that is overlapped by a diagonal structure at lower temperatures as seen in figure 8. Clearly there is a massive problem using this mode of the camera, making it useless for observations.

2.2 Dark calibration

With the analysis of the biases in different temperature ranges complete, we conclude that we will only use a binning of 1 for the further analysis of the dark current. To get a statistically good view on the dataset, we first combine a set of different dark images to one using an average combine again, similar to the bias procedure. We then remove the bias from the CCD, gathered through the analysis in section 2.1. After this step the image is divided by the exposure time, as this is what we use as a master dark in a real observation. All pixel values after this process that are < 0 are set to zero, to not introduce weird behaviour for the darks.
We checked camera 1 with temperatures between $-5\,^{\circ}\mathrm{C}$ and $-40\,^{\circ}\mathrm{C}$. As expected the mean dark current decreases with decreasing temperature. Of course, through the structures visible in the bias frames (see section 2.1) at lower temperatures, this also creates structures in the dark frame. Figure 9 shows the dark frames at different temperatures. A better view on the structure of the dark frames is visible through the distribution of pixel values.

Figure 10 shows the distribution of pixel values of the dark frames. Looking at these distributions, the optimal temperature for camera 1 would be $-30\,^{\circ}\mathrm{C}$.

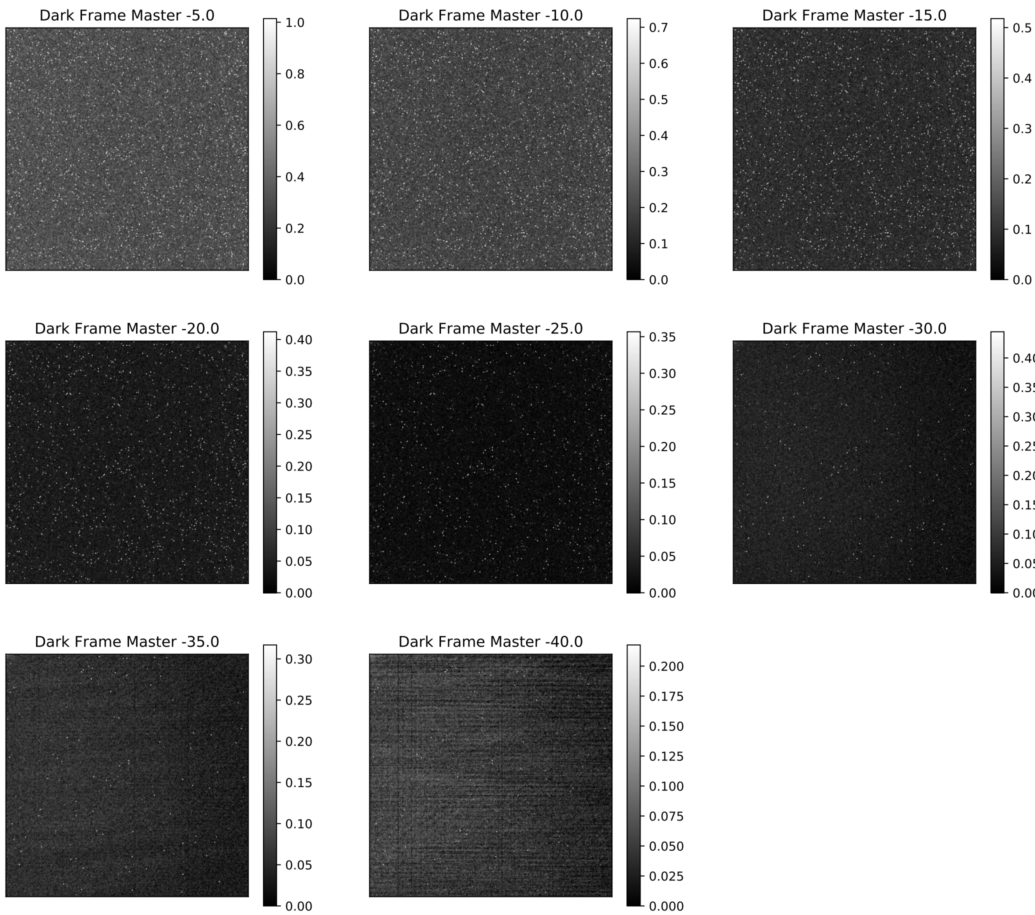

Figure 9: Dark frames for camera 1 with binning 1 for different temperatures. As expected, the dark current falls with falling temperatures on the CCD. Clear structures are visible on the CCD from $-35\,^{\circ}\mathrm{C}$ on, making smaller temperatures not useful as a working temperature.

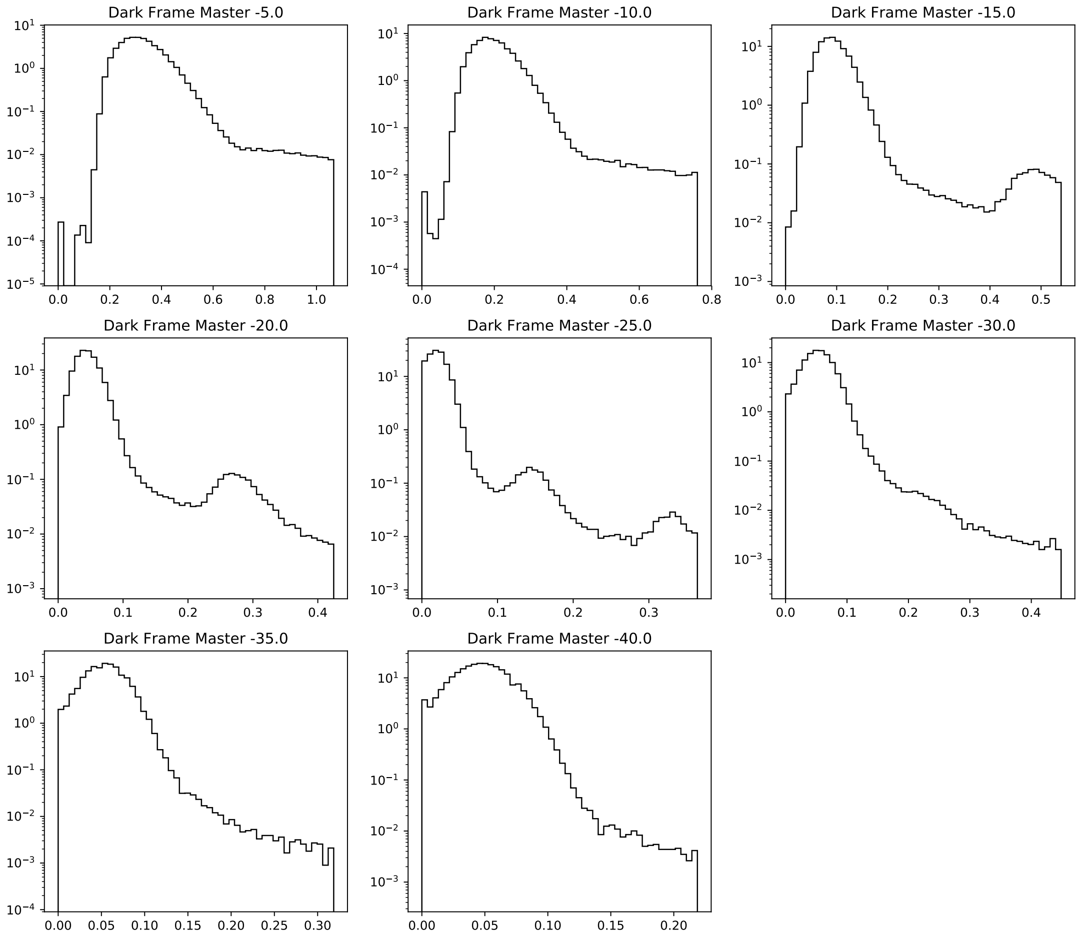

Figure 10: Pixel value distribution for the dark current of camera 1 with a binning of 1. We see multiple peaks between $-15\,°C$ to $-25\,°C$. These peaks are probably due to the reduction of the images, where some pixels show a higher value for some pixels than would be expected and are not matched by the clipping process. They then vanish for lower temperatures.

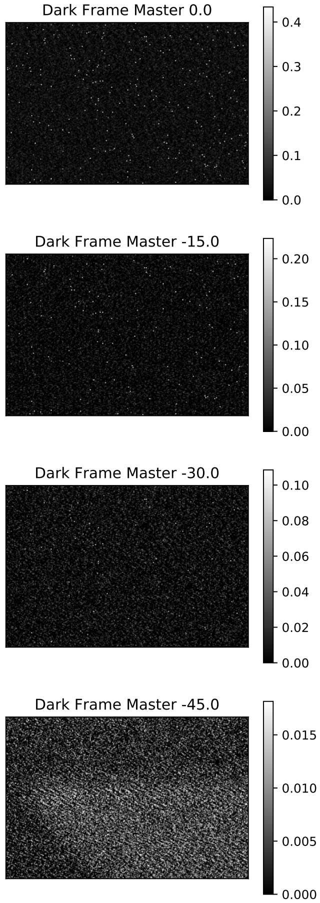

Figure 11: Same as figure 9 but for camera 2. Clearly there is a strange behaviour with this camera, as the image shows shadowing for the lower right part of the CCD, where a significantly higher dark current is visible. This structure is probably persistent through all temperatures, but only visible for these lower temperatures.

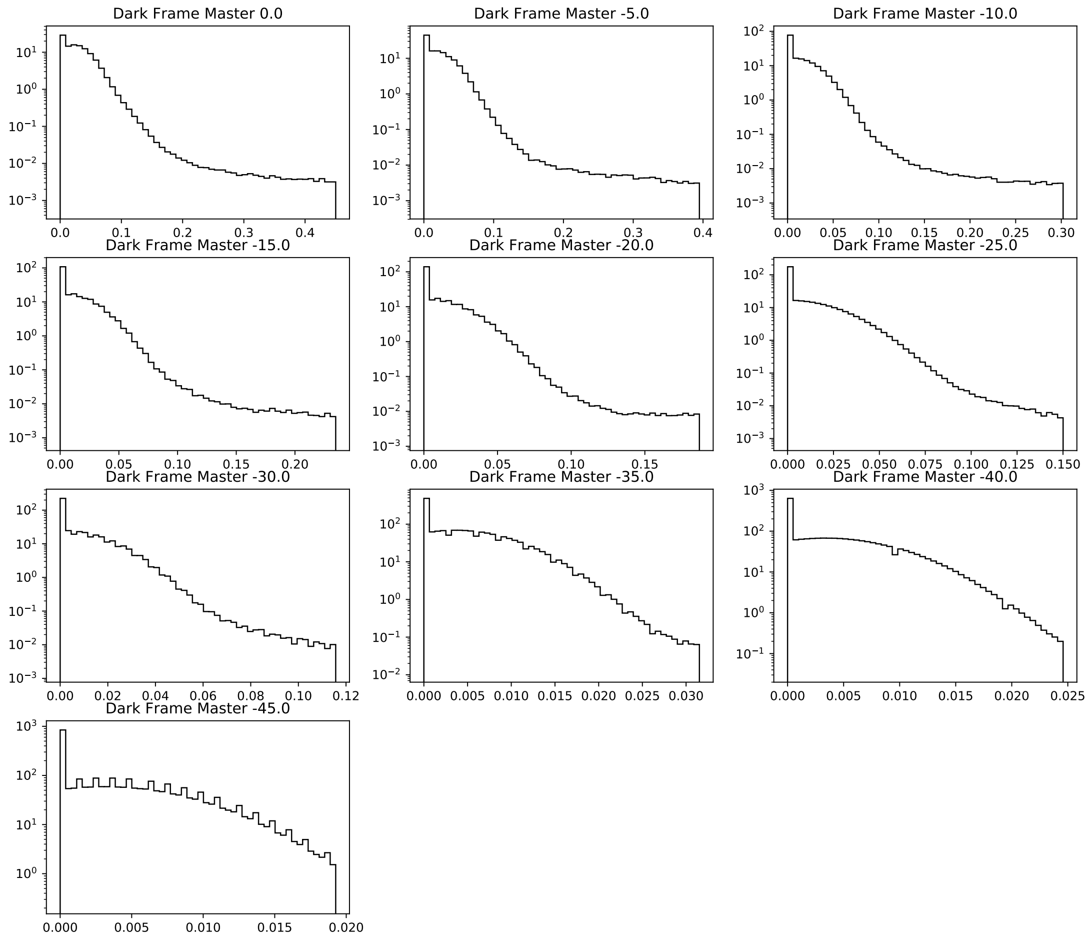

Figure 12: Same as figure 10 but for camera 2. We see a flattening out of the initial peak in the distribution for lower temperatures, giving us a broader dark current distribution.

For camera 2 we performed the same analysis with temperatures between $0\,^{\circ}\mathrm{C}$ and $-45\,^{\circ}\mathrm{C}$. The behaviour of camera 2 is similar to camera 1. Its dark current decreases as the temperature decreases, as seen in figure 12. There is a significant shadowing effect on the CCD though from around $-35\,^{\circ}\mathrm{C}$ onwards, as seen in figure 11. This again leads us to the conclusion, that the best operating temperature of camera 2 is $-30\,^{\circ}\mathrm{C}$.

3 Reduction

Reduction of observed images with a modern telescope (imaging on a CCD) is a very integral part for the quality of the dataset. To perform this reduction, multiple steps need to be taken, as will be explained in the following. We will first describe a theoretical reduction of a given dataset, continuing with a more practical approach as well as the technical details for the developed custom pipeline written in Python.

3.1 Theoretical reduction

For this theoretical reduction we assume a more or less ideal CCD with no hot pixels, no cosmic rays or other problems in the dataset. This is of course not the case for a real life CCD, yet this is the fundamental block we will

work with.
The first step in the reduction is the capturing of a bias image. This is usually done by simply reading out the CCD without opening the shutter of the camera. In theory, this is simply a constant value caused by the constant voltage applied to the detector itself. We call this value σ_{b}. The next step consists of taking a dark frame image. This gives us the dark current σ_{d} in the dataset, representing the thermal electrons that are read out from the CCD through the ambient temperature of the chip. This effect is reduced to a minimum through the cooling of the chip (see section 2). To compute the dark frame image, we expose the chip with the shutter closed for a given time (we usually choose around 30 s). In the reduction, we then subtract the bias from the dark current and divide the image through its exposure time. The dark current is therefore

$$\sigma_{\mathrm{d}} = (\sigma'_{\mathrm{d}} - \sigma_{\mathrm{b}})/t_{\mathrm{exposure}} \tag{1}$$

The last part that is needed is the so called flat field σ_{f}. Pixels on a CCD are not perfectly equally sensitive to exposure. There might be some structure in the CCD, stemming from the production of the chip or the readout electronics might have an effect. This means that any image exposed on the chip will not be uniformly well lit out, which is corrected using the flat field. To get a flat field image, multiple techniques are possible. For example we could use an evenly illuminated white flat surface which is then exposed on the CCD. This of course is a bit difficult, as the focal length of the telescope might not be perfectly aligned with such an object. We therefore chose to perform the second method for most of our later observations. For this, one starts the observations a bit earlier in twilight. We then take an image of the twilight in the horizon, giving us a decent enough lit out flat field of the CCD. To get the final flat field, we take this image and subtract the master bias and dark multiplied by the exposure time. This gives us

$$\sigma'_{\mathrm{f}} = (\sigma''_{\mathrm{f}} - \sigma_{\mathrm{b}} - \sigma_{\mathrm{d}} * t_{\mathrm{exposure}}) \tag{2}$$

This, of course, is not enough, as we want to multiply the flat field with the observations of our target. We therefore divide the flat field through the median.

$$\sigma_{\mathrm{f}} = \sigma'_{\mathrm{f}}/\widetilde{\sigma'_{\mathrm{f}}} \tag{3}$$

The median is used, because we don't want to massively change the true pixel values of the dataset in our observations. Using the maximum could lead to non sensical pixel values in the CCD.
Finally, our observations can be reduced using these values. To reduce an observation, one subtracts the bias and dark current from the image and divides the image through the flat field. So to get real observational data we need to perform

$$\mathrm{IMG} = (\mathrm{IMG}' - \sigma_{\mathrm{b}} - \sigma_{\mathrm{d}} * t_{\mathrm{exposure}})/\sigma_{\mathrm{f}} \tag{4}$$

which gives us the reduced CCD data.

3.2 Practical application

In practice, the CCD is of course not perfect. There are therefore multiple other steps that need to be taken to ensure a well enough reduction of the data set. To reduce statistical uncertainty in the data, we take multiple bias frames and dark frames. We then remove cosmics and outliers through the median and only accept values within a given range. These values are than averaged, giving us a good idea of the bias and dark frames.
In principle, the twilight flat fields are a good method to get decent flats for the CCD. But we also need to take multiple images here, as even in twilight, stars are clearly visible in the image. We move the telescope slightly before each flat field, and perform the same combination method used for darks and bias images. We also need to create a flat field for every filter that is used in the observation, as these filters can have a significant impact on the image. It should be also noted, that temperatures need to be constant for this whole process, which is due to the different behaviour at different temperatures in the CCD.
This whole process was automated using a custom pipeline written in Python. This pipeline reads the images from a given folder, and given that this folder contains bias, dark and flat field frames, it computes a master dark, master bias and master flat for all filters in this folder and reduces all light frames. The information for each file is read out through the fits header of the file. We first combine the biases using an average combine method, and generate a master bias for a given data set. It then creates the dark by subtracting the master bias from every single dark frame, and combines them using the average combine technique. The flat images are created for every single filter and this is applied to the light frames taken for our targets.

4 Imaging

Imaging is the main objective of the second half of our "Teleskoppraktikum". The primary goal is to take images of several open clusters and possible candidates in different filters. From these images color magnitude diagrams are created. Additionally one can search for proper motion and distance information for the imaged stars in catalogues and use this information and the color of the stars to check their membership to the given open cluster or open cluster candidate. If these parameters can be gathered for enough stars, one can conclude whether the imaged cluster candidate is in fact an open cluster. Furthermore one can also get information on the size of the clusters with this technique.

In addition to the imaging of clusters and cluster candidates we image comet 46P/Wirtanen as a target of opportunity. We also use the lucky imaging technique to image the moon in higher quality than would be possible with a classic imager.

4.1 Imaging of a comet

On December 13$^{\text{th}}$ the weather conditions allow us to try to image comet 46P/Wirtanen, which had its closest approach to Earth around that time. The seeing is mediocre during the observation and the observation direction right towards the city does not help the image quality either. Furthermore the behaviour of the imaging camera (Camera 1) was not entirely understood at the time, which challenges us greatly during the reconstruction of the images. The comet is seen over Innsbruck at a right ascension of 3[illegible]m 20 s and a declination of 11°45′26" at around 18:00 CET. Therefore the observations are done at a very low angle above the city which explains the high background noise in all images taken of 46P.

Searching for 46P/Wirtanen on the sky is done by interpolating between data points given in an ephemeris table [Wie18] of the comet and manually pointing the telescope to the calculated coordinates. After finding the comet, the telescope position has to be readjusted occasionally as the comet is of course moving with respect to the reference frame of the stars which the telescope is tracking. Two 90 s exposures of the comet are taken for each of the filters Johnson V, I and R. Furthermore we take bias and dark frames as well as flat fields for all three filters. In addition we then try to take a spectrum of the comet using camera 2 but unfortunately the comet is too faint and the conditions too bad to get usable data. The V, I and R images are also of mediocre quality, especially the V filter shows a very bad signal to background ratio.

The reduction of the images is performed using our pipeline. Unfortunately the flat fields taken during the observation night are unusable as we did not complete the calibration of the camera, and chose a wrong temperature for the observation. To temporarily work around this and to be able to at least show a somewhat reduced image of 46P/Wirtanen we replace the flats with ones taken in January at a different temperature which of course only removes influence of dust on the filter wheels but not the influence of the CCD at the time of observation. The three color composition of the "reduced" V,I and R images can be seen in figure 13. Obviously this is not a true RGB composition but rather a stack of the individual colorized images but a true composition is unfortunately rather bad, as one can see in figure 14 which also shows the original unmatched V, I and R channels overlaid. These are fairly nice to look at, but are of little scientific value.

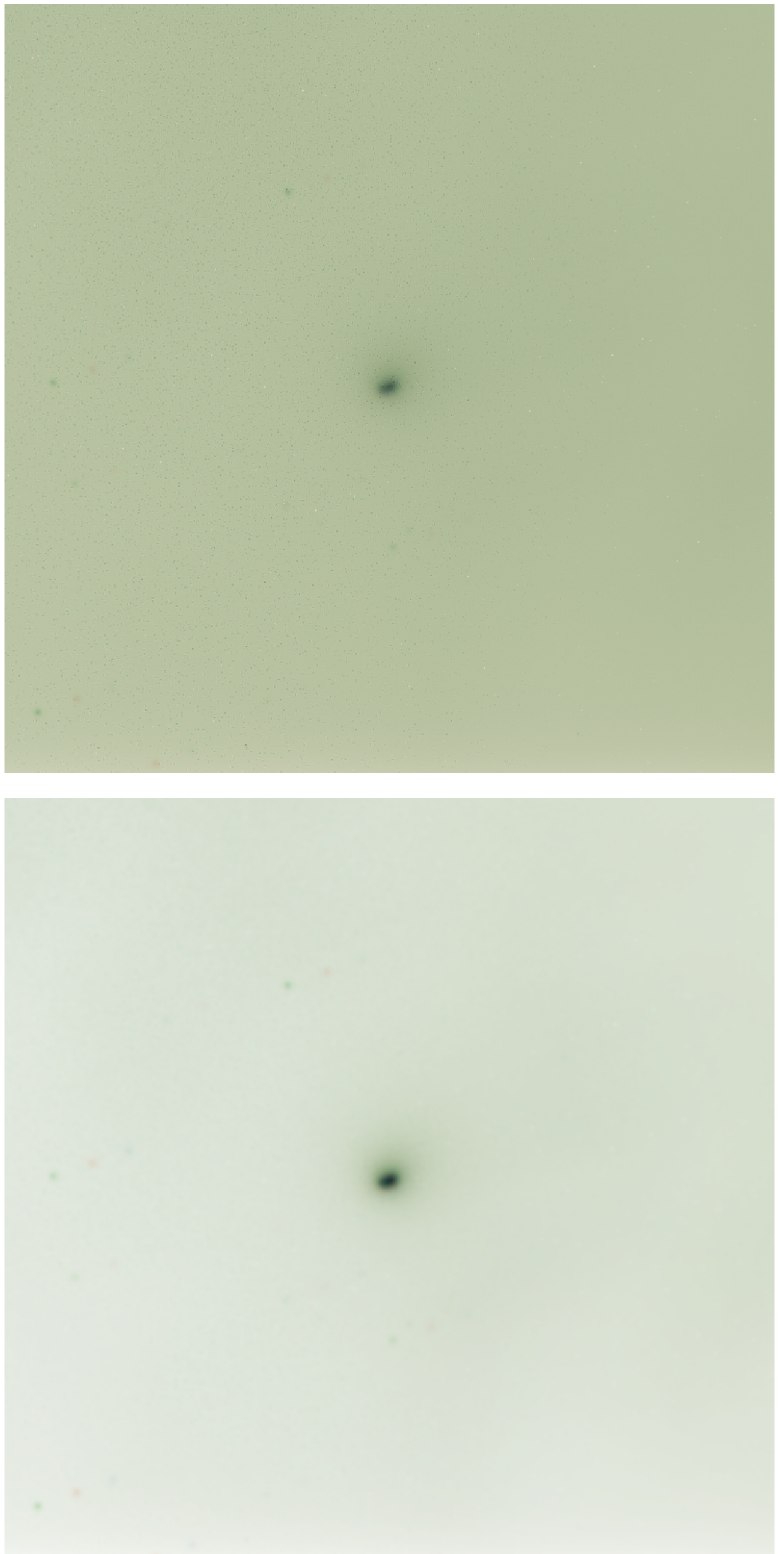

Figure 13: Comet 46P/Wirtanen in a three color composite from Johnson I,V and R images taken on 2018-12-13 with the Innsbruck 60cm telescope. The lower image was smoothed by convoluting a 5 by 5 pixel 2D-Gaussian filter of order 0. The stars in the background appear once in every colour as the comet moved significantly between each exposure, while the telescope was tracking the stars. Due to the movement of the comet during the exposures the position match up for the composition is not perfect.

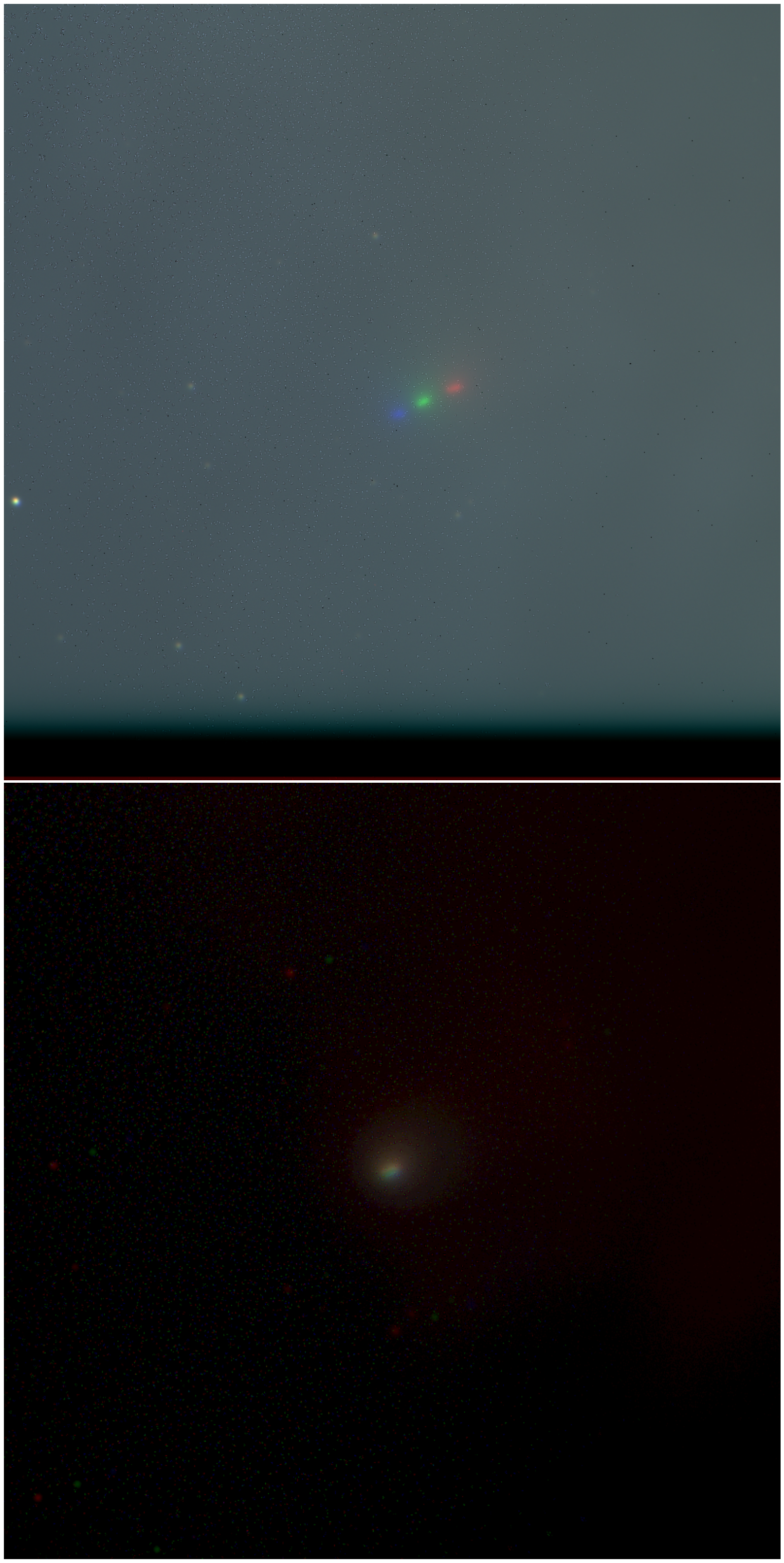

Figure 14: Top: initial unmatched image of 46P/Wirtanen from the three filters. Bottom: Highly edited RGB composition matched on the comet position. A smoothed version was produced but the comet is very faint and therefore hardly visible.

From the offset of the comet in different images and the known times at which the images are taken one can try to reconstruct the velocity of the comet across the sky. When doing this we encounter the problem that our imaging software does not include the telescope pointing position in the FITS header which means that we have no reference which pixel in the image corresponds to which position on the sky. Adding this information later is complicated as there are distortions on the projected image from the telescope optics and the spherical sky which rules out a linear conversion from identifying two stars and using their position to convert from pixels to right ascension and declination.

Therefore we use the Astrometry.net tool [Lan+10] to find the world coordinate system (WCS) for our images. For this the tool uses a geometric hash code of four parameters which characterize the position on the sky of four stars independent of the image scale and rotation. The definition of these four parameters can be seen in figure 15. Astrometry.net extracts the sources in the input image and builds a set of these parameters for every combination of four stars detected. These parameter sets are then compared with a database of index files which has been generated from several star catalogues like Tycho-2, 2Mass and USNO-B. If the parameters from the input image match the ones in the database, the position, rotation and scale of the world coordinate system is known and therefore the WCS is added to the header of the input .fits file. Surprisingly this nifty technique works, despite the image quality and low number of visible stars, for five of the six images of 46P/Wirtanen.

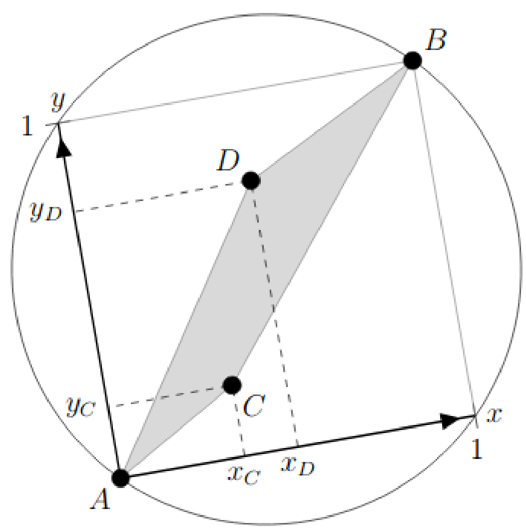

Figure 15: Definition of the geometric hash code parameters x_C, x_D, y_C and y_D used by the Astrometry.net tool for world coordinate system calculation. Image taken from [Lan+10].

As the output of Astrometry.net gives the star positions but no brightness of the objects we use SExtractor [BA96] on all five images with a WCS to get the brightness in instrumental magnitudes and the position both in pixel and in right ascension and declination for the detected stars and the comet. From the time the image was taken (which is included in the .fits header) and the difference in the comet's position we can determine the proper motion of 46P/Wirtanen. Using this technique we determine an absolute value of the proper motion vector of $p_{46P} = 2.2(13)\,''\,\mathrm{min}^{-1}$ which is significantly lower than the value expected from the ephemeris table of $9.83\,''\,\mathrm{min}^{-1}$ given in [Wie18]. Possible reasons for this include the difficult extraction of the actual comet position as the exposure time is long enough for the comet to smear out in the image and the comet potentially being actually slower than expected.

4.2 Imaging of open clusters

We image open galactic clusters in order to create Hertzsprung-Russell (HR) diagrams and study the membership of the individual stars to the clusters. The studied objects are M34, Teutsch 55, C0001+557 (also known as Stock 19) and Patchick 78. While the first one, M34, is very well studied the other three are not. All of them are located on the northern sky and therefore readily observable from Innsbruck. Two observation nights on the 16^{th} and 22^{nd}

of January 2019 are used to observe these objects. M34 and Patchick 78 are only observed during the first night, C0001+557 only during the second night and Teutsch55 during both nights. While observing Patchick 78 it quickly becomes clear that the members of this cluster are mostly too faint and therefore observations of it are stopped immediately in favor of Teutsch 55. Prolonging the exposure time for Patchick 78 is not possible as the images become too background dominated.

The images of the clusters are reduced using our reduction pipeline and then given a world coordinate system using the Astrometry.net tool. As the observation conditions during the two nights in January were much better than the one where 46P/Wirtanen was imaged in December, all images have a unique solution for their world coordinate system. This leads to the possibility of automatically searching the Gaia DR2 catalogue with the coordinates of all cluster stars derived from the WCS. For this automatic Gaia query we use the Python package astroquery [Gin+18]. This procedure will be discussed in more detail in section 4.2.2. A RGB composite image of one of the studied clusters can be seen in figure 1 on the title page.

4.2.1 Hertzsprung-Russell diagrams

As we image the open clusters in four different filters we can create HR diagrams in the form of color-magnitude-diagrams. The lack of magnitude calibration/zero point for our telescope does not affect these as only differences of colors are relevant, which of course do not depend on the absolute scale of the brightness of the stars. To create the observational HR diagrams we extract the sources from four images in the different filters (Johnson V,I,R,B) using SExtractor [BA96]. This gives us the extracted position and brightness of the imaged stars in every filter. Some stars are only visible in part of the images, as they are for example brighter in the blue and therefore fainter or even not visible in the redder filters. This, of course, has to be taken into account when creating HR-diagrams. Therefore we only use extracted stars which can be found in all filters on the same pixel position in the image (with a tolerance of $\pm 3\,\mathrm{px}$).

The number of sources extracted varies greatly with the input parameters of the source extraction process. Primarily the threshold above which a pixel is counted as non background and the minimum area of joint pixels above this threshold indicate whether a bright spot in the image is a star or not. Furthermore, the seeing can be (in part) compensated by allowing for objects with a rather high FWHM to be still considered stars and not extended objects. The level of the background can also be adjusted individually for each filter. If the parameters chosen are too constricting no stars are extracted from the image, however if they are not constricting enough, large areas of the background are detected as extended sources. Both of which is unwanted and therefore compensated by redoing the analysis with different input parameters.

SExtractor has hundreds of possible return values of which we are interested in mainly three: the position of the extracted source in pixels (for x and y direction respectively) and the brightness of the source in uncalibrated instrumental magnitudes. The position is used for matching the stars between different filters and the brightness is then used for the HR-diagrams. These are simple plots of the difference of brightness in two filters versus the brightness in one of the filters, for example B-V versus V. The resulting diagrams are shown in figure 16 for the clusters M34, Teutsch 55 and Stock 19. Especially the one for M34 clearly shows the main sequence as expected.

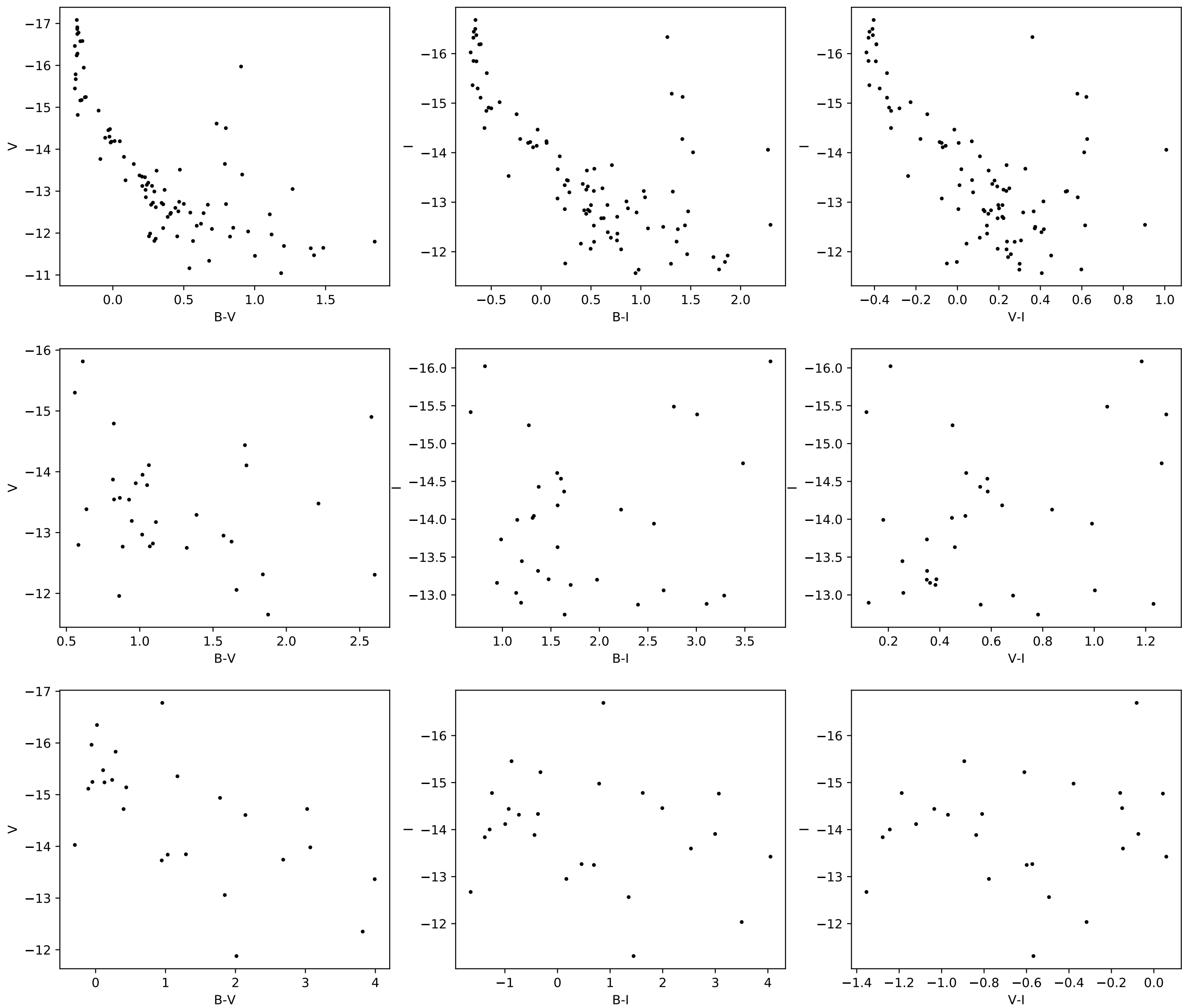

Figure 16: Hertzsprung Russell diagrams from the four filters Johnson B,V,I and R for the stars in the image frams for the clusters M34 (top), Teutsch 55 (middle) and Stock19 (bottom).

4.2.2 Determination of cluster membership using Gaia

The automatic query search for Gaia DR2 entries for the extracted stars is done using the Python/astropy package astroquery [Gin+18]. The tool searches the online Gaia DR2 catalog for the positions extracted by SExtractor for the given clusters. The query returns the complete Gaia entry of the star which includes the source ID, position, proper motion, parallax, and other parameters depending on which were measured by Gaia.

As the Gaia DR2 catalog has a lot of entries often times the query returns more than one Gaia entry for an extracted position. In this case we ignore the star at the extracted position for the further analysis as it is often not possible to tell which of the entries is the correct one. In very rare cases we can not find a Gaia entry for a extracted position which also leads to us skipping the position.

The whole process is done only for the sources which are present in all four filters for each cluster candidate as we want to be able to use the color of the stars as an indicator of their cluster membership. Unfortunately this also means that there are very little sources for which we have a Gaia entry and a color, especially for Teutsch 55 and Stock 19 (under 20 stars in both cases). Therefore we decide to not go further into this automated search but rather use the old fashioned way of looking at the images, numbering the stars, looking up their Gaia ID and finding their parameters this way (i.e. using a human SExtractor). Of course this unfortunately removes the color information as the reverse process of looking up the stars in all our images is tedious and error prone. Therefore we decide to solely rely on proper motion and distance information for determining cluster membership. The manual method proves to be the vastly superior one, although the immense time consumption is usually very hard to justify.

So in order to determine the membership of the imaged stars to a cluster, we followed the following procedure shown in the flowchart (figure 17). It and the followed analysis will be quickly summarized in the following:

1. We take an observation and make as many light sources visible as possible. It turned out that the red filter was in every case the filter with the most sources visible; blue was always the worst one.
2. Check if the light source of our observation is also visible in the Digitized Sky Survey (DSS2) on *Aladin*[BF14].
3. If it is visible in both images, put a number on this star (cf. 18 and 19).
4. Use *Aladin* in order to find the corresponding *Gaia DR2 source IDs* (SIDs) to those stars. However, if there were multiple sources very close to each other, this source was not used.
5. Import those extracted *SID*s in the *ESA Gaia archive*[1] ([Gai+16], [Gai+18]).
6. Extract valuable properties like: right ascension, declination, the proper motion in those directions, the Gaia magnitude, the parallax and the errors of those values.
7. Using the position and magnitude of every light source we can reconstruct our observation image (cf. 20). The proper motion can also be illustrated by arrows originating from the corresponding star.
8. Now we can take a look at the distribution of distances and proper motions using a histogram (cf. 21). We can exclude outliers in distance and the proper motions using an iterative three sigma clipping procedure. Meaning, we removed all stars outside the three sigma regime with respect to the median. This eliminated outliers with high or low distances or proper motions. This clipping was repeated until nothing was 'clipable' anymore. Notice that having the right distance is not enough; you also need the right proper motion. Using a Gaussian fit on the remaining stars, which will be called cluster members (CMs) from here on, gives us our guess for the distance and the mean proper motion of this cluster.
9. As an independent check we also have a look at the radial velocities of our CMs (cf. 22). Our CMs should not be seen as outliers here.
10. As additional information, we also provide a histogram of the magnitudes of our extracted sources and our CMs (cf. 23).
11. Followed by a new reconstruction of our observation image just containing the CMs and their proper motions (cf. 25).
12. Finally, we show the distribution of the proper motions together with the mean and standard deviation in the proper motions of the cluster extracted from the gaussian fit (cf. 24).

[1] `https://gea.esac.esa.int/archive/`

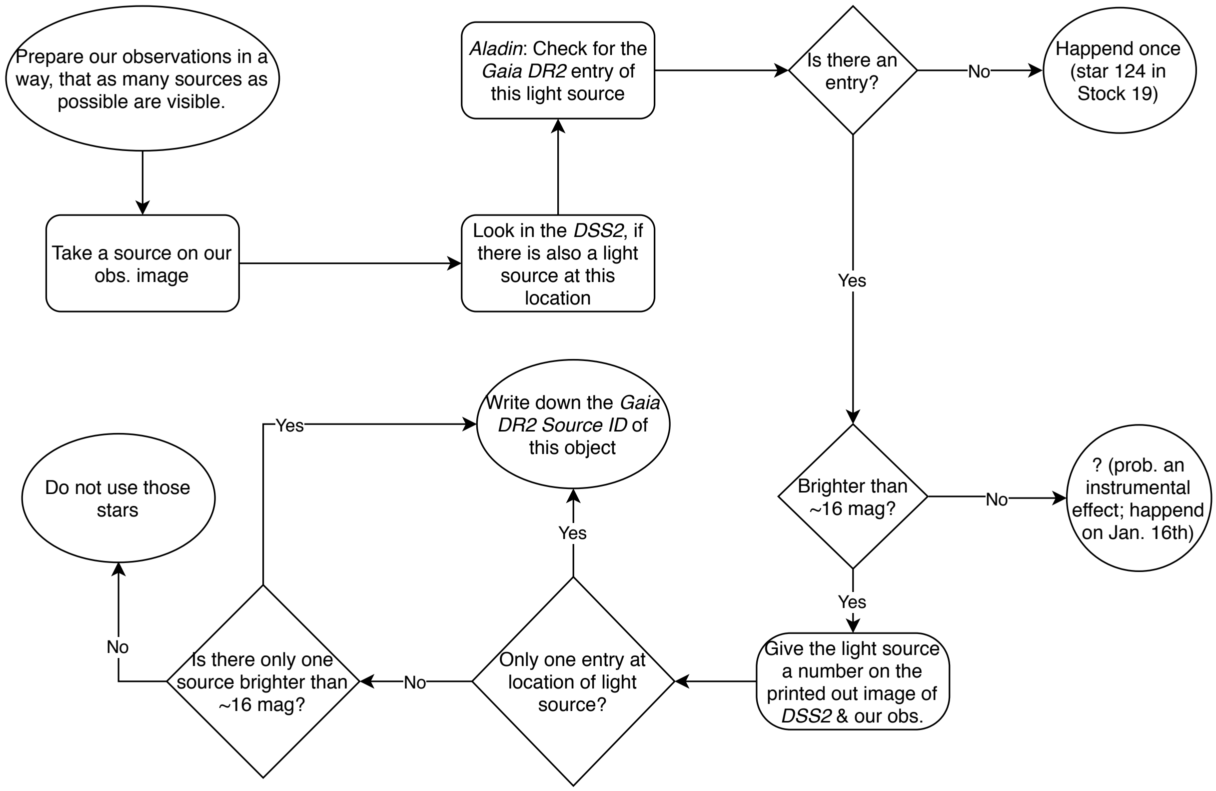

Figure 17: This flowchart summarizes the procedure, which was used in order to extract the sources from our observations.

Table 1: **Num. stars**: Number of extracted sources from our observations for every cluster. **Not used**: Number of sources not used, because the existence of two or more *Gaia DR2* entries very close by. **Two parameter sol.**: Some stars are lacking the full five parameter solution (position on the sky in RA and Dec, proper motions and parallax), but only have a two parameter sol. (RA and Dec). Those stars were not used in the following analysis. **Neg. parallax**: Stars with negative parallaxes were also excluded from the analysis. Those stars also typically have big uncertainties in their parallax or proper motions. **Analysed stars**: The final number of analyzed stars. **RV stars**: Number of extracted sources with a radial velocity value. It was only available for a small number of stars.

	M34	Teutsch 55	Stock 19
Obs. date	Jan. 16th	Jan. 16th	Jan. 22nd
Filter	R	R	R
Exposure time (s)	150	300	200
Num. stars	195	191	208
No Gaia DR2 entry	0	0	1
Not used	6	5	0
Two parameter sol.	3	3	2
Neg. parallax	2	0	2
Analysed stars	185	184	203
RV stars	28	33	37

In the appendix (A) one finds the Gaia data of all extracted stars -the cluster members, the non-cluster members and the stars, which were not analyzed.

4.2.2.1 M34

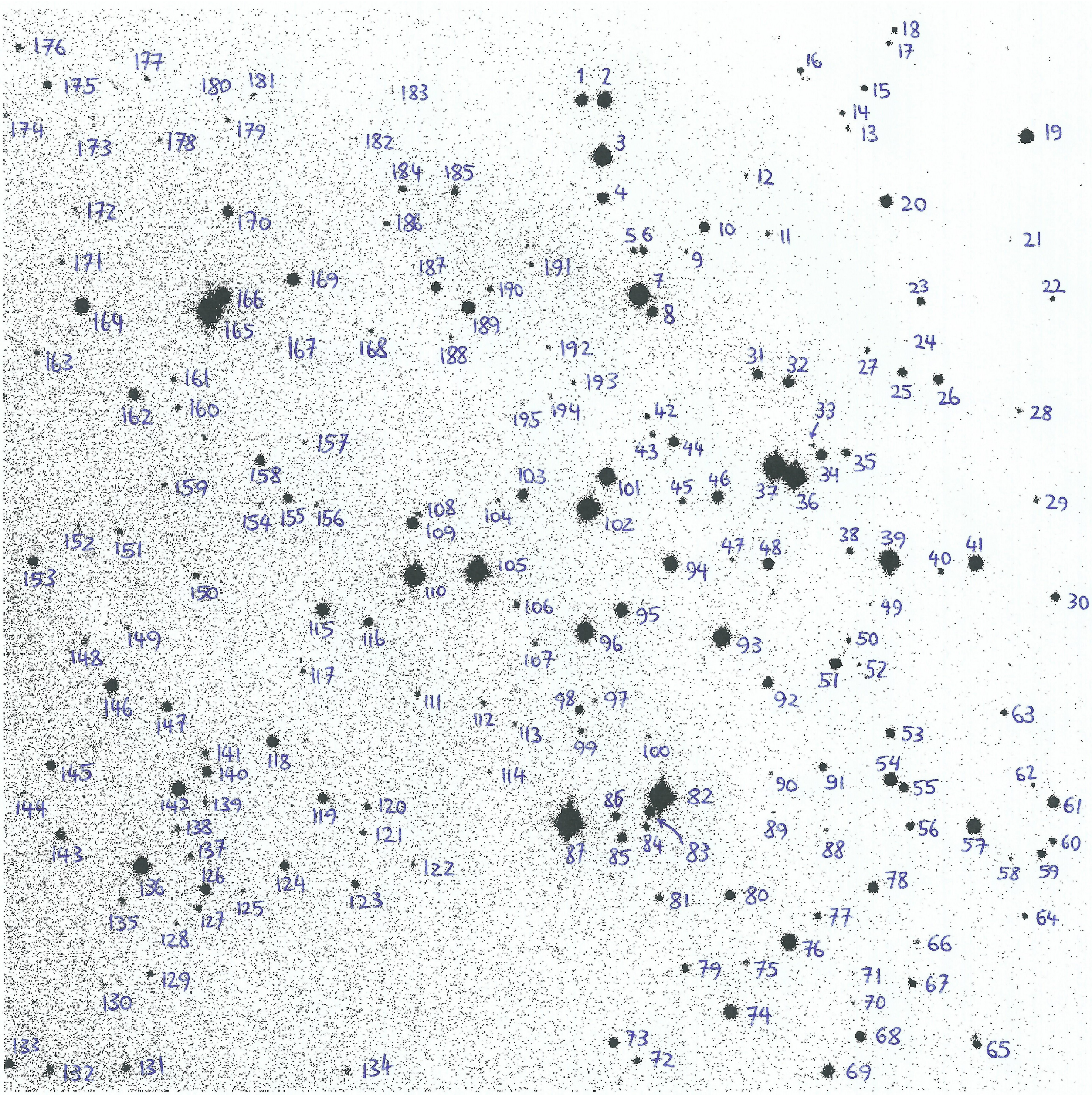

Figure 18: Our observation of M34 in the red filter with an exposure time of 150 seconds. The numbers are in correspondence with those in image 19.

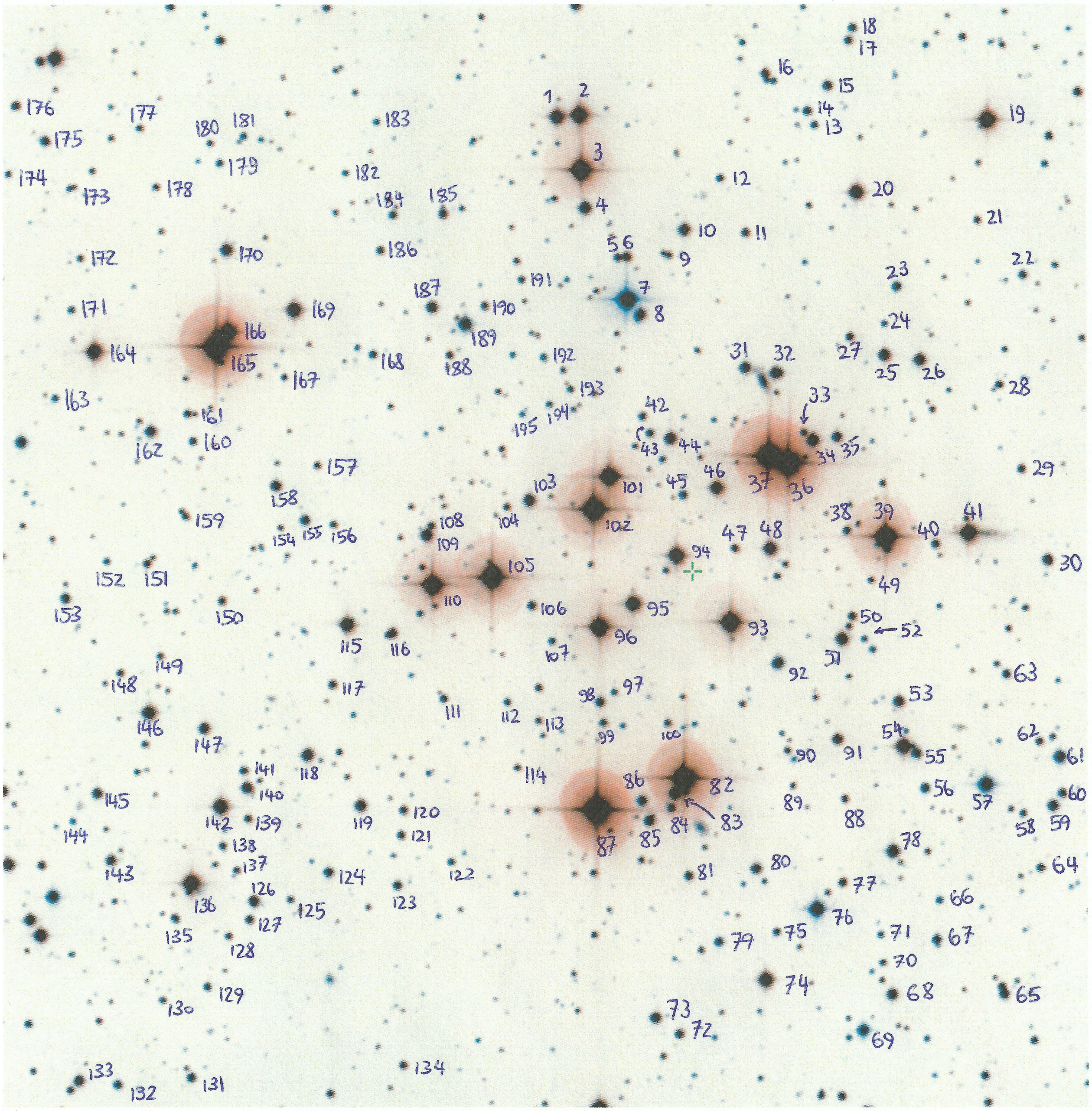

Figure 19: The negative of the observation of M34 by the DSS2. This picture was extracted from *Aladin*. The numbers are in correspondence with those in image 18.

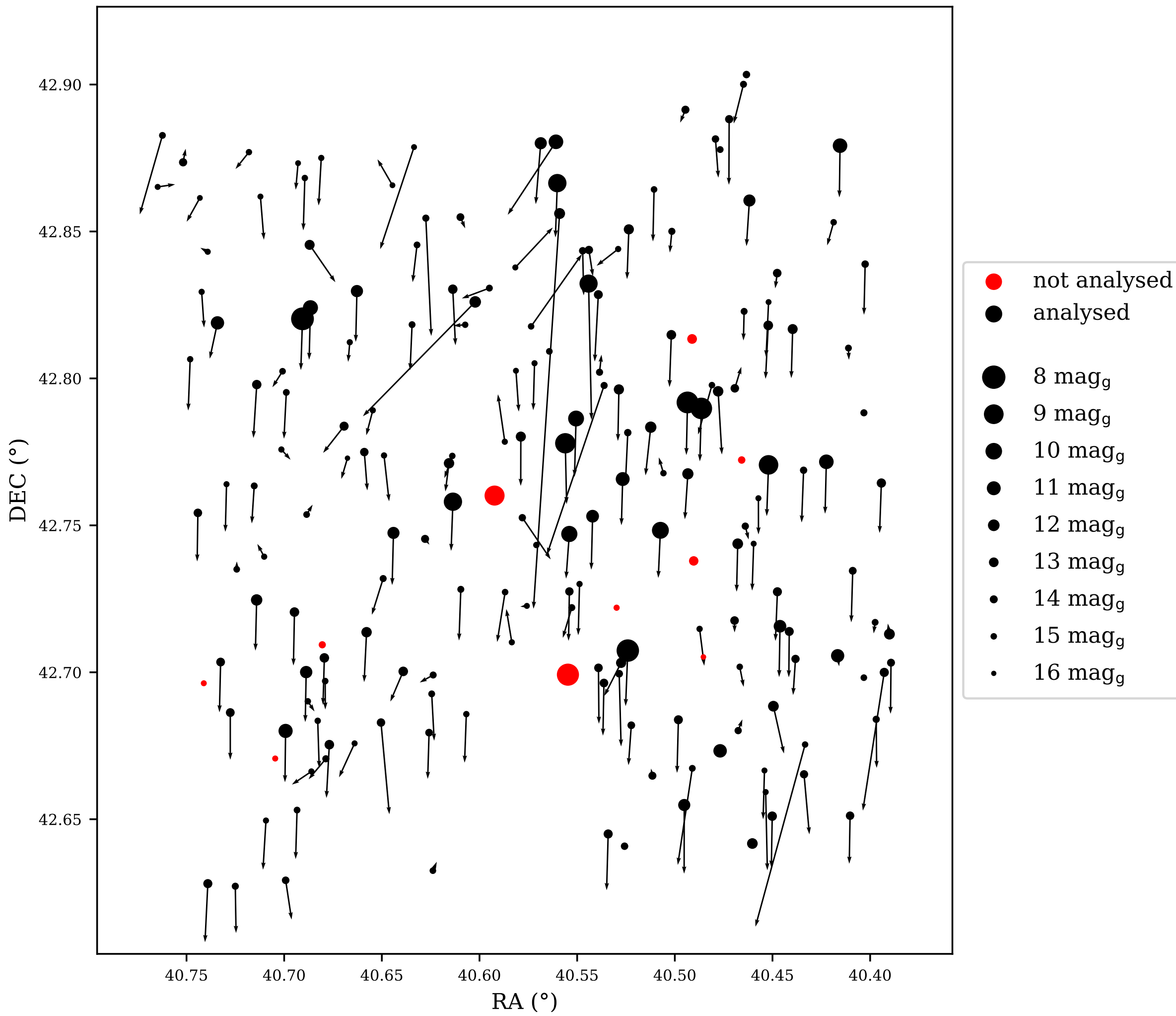

Figure 20: Every point is an extracted source. The size corresponds to the Gaia magnitude. The arrows illustrate the direction of the proper motion. A star was for example not analysed if the proper motions were missing.

This figure 20 already illustrates that most stars are moving in the negative declination direction. One can also see some high proper motion stars.

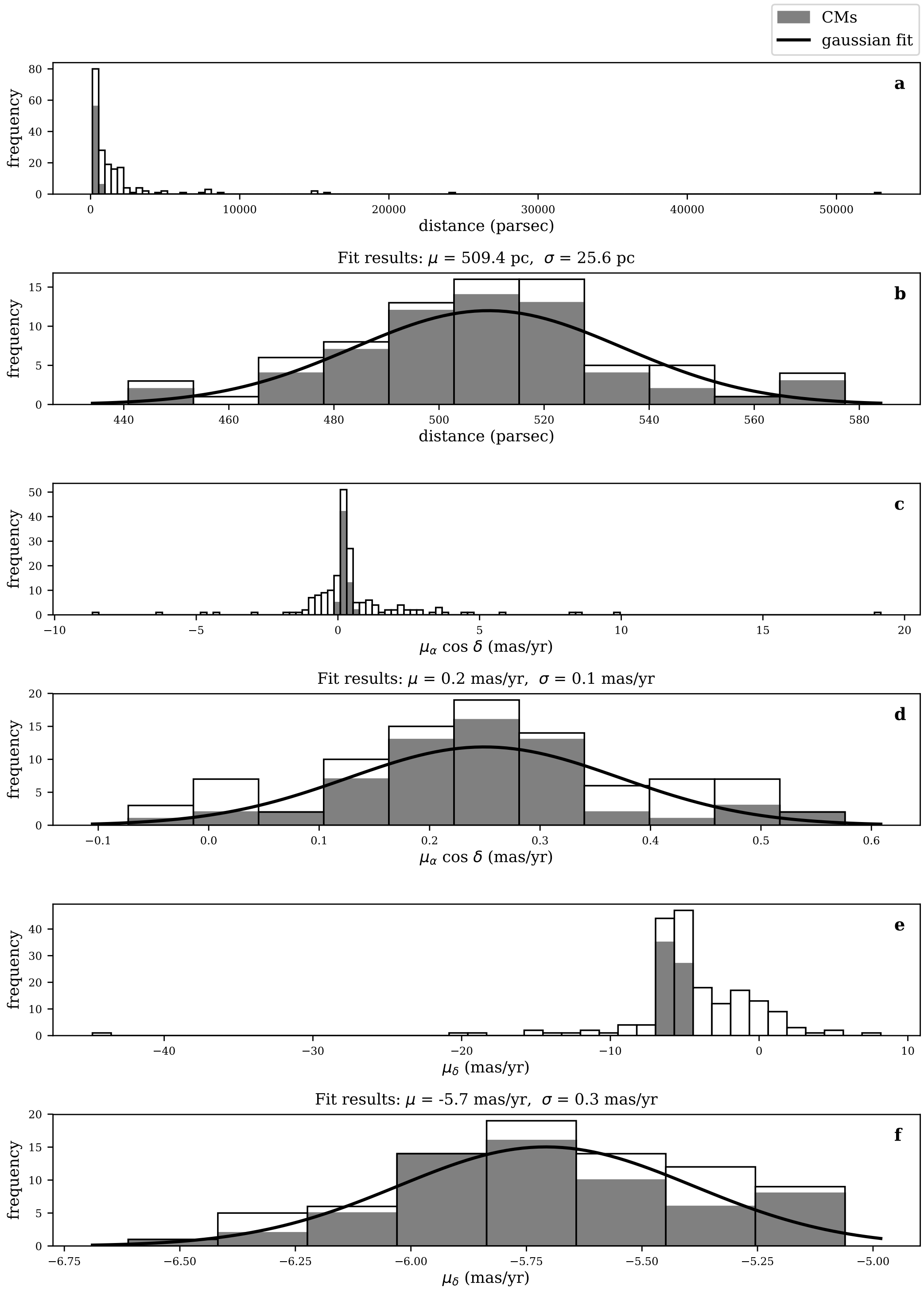

Figure 21: Histogram of the analysed stars. In order to determine the Cluster members (CMs) an iterative sigma clipping procedure was applied (see point 8 in section 4.2.2). **a, c, e**: The distances and proper motions for all stars and the CMs (in gray). **b, d, f**: This zoom-in also includes a gaussian fit of the CMs. Above those plots the mean and standard deviation of this gaussian.

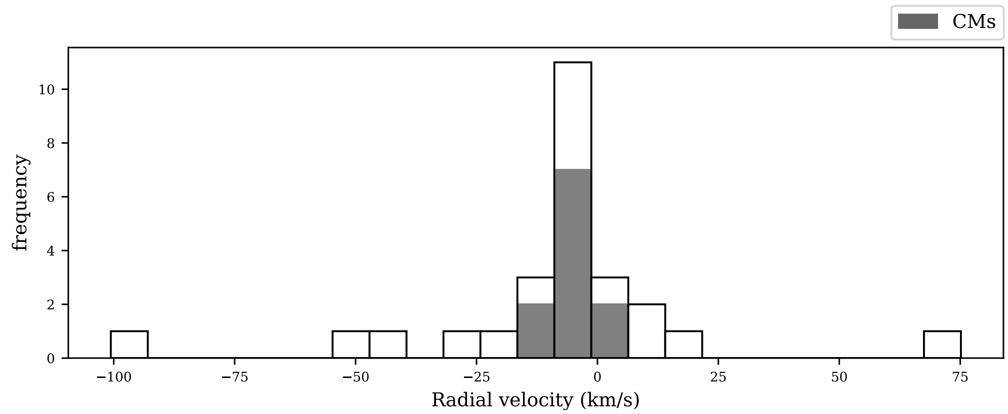

Figure 22: An histogram of the radial velocities. In gray our cluster members determined with figure 21. We see that non of the outliers are also CMs. This is what we would expect.

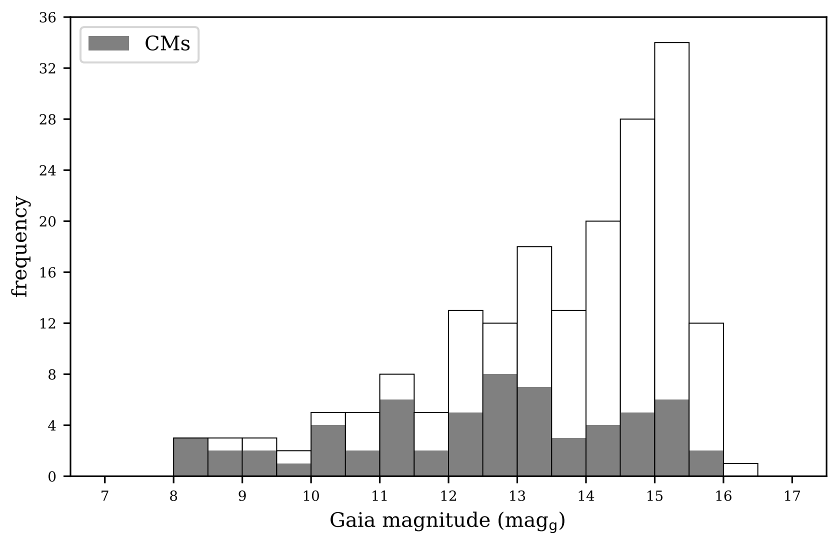

Figure 23: The distribution of Gaia magnitudes of the analyzed stars.

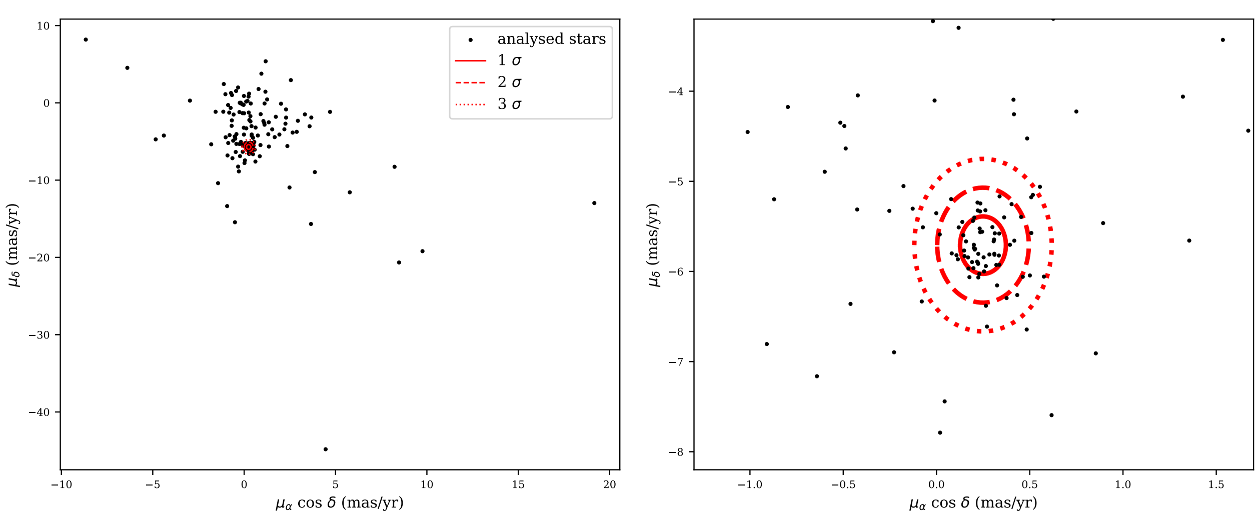

Figure 24: The proper motions of all analyzed stars including the proper motion of the cluster (red) extracted in figure 21. The right side is a zoom-in of the left side.

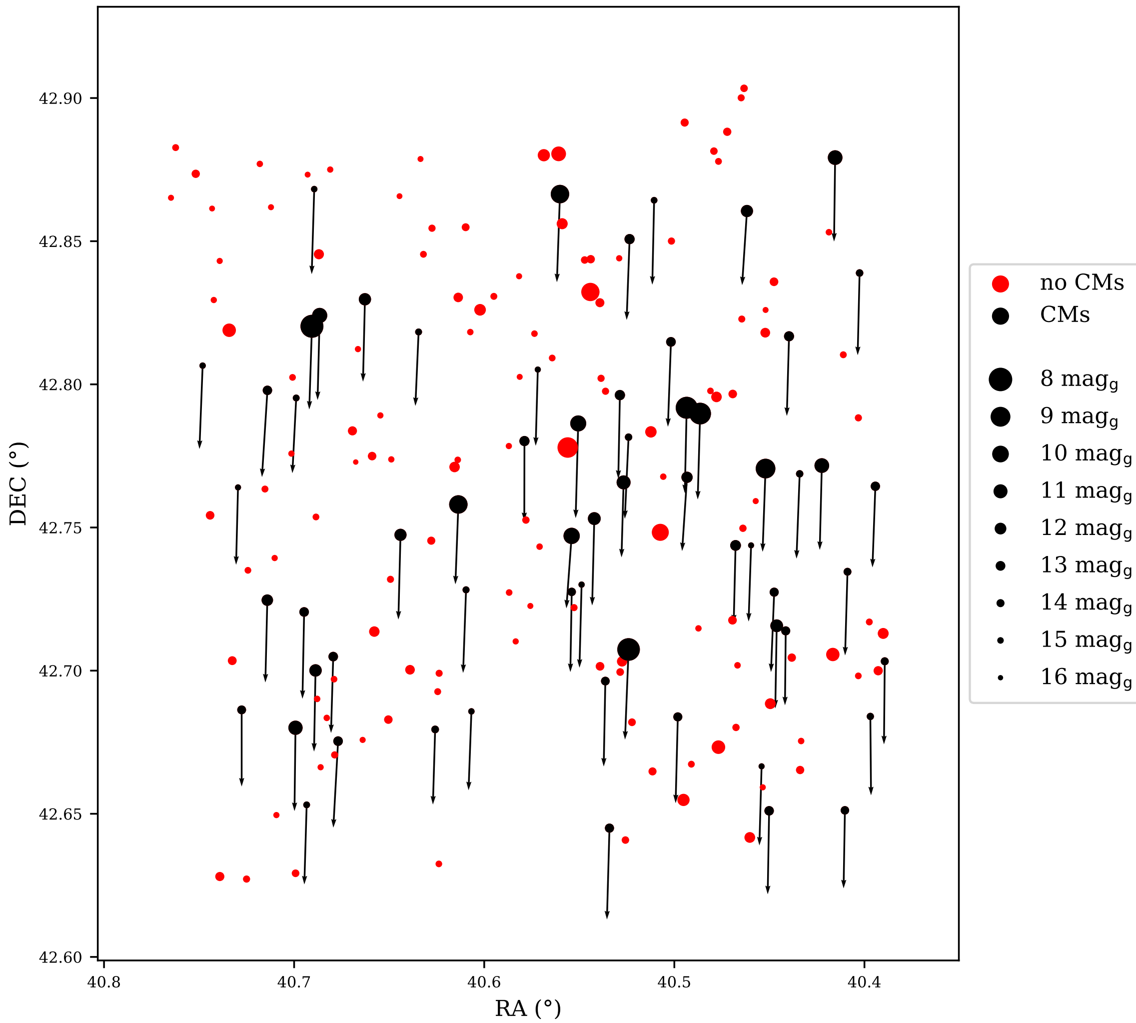

Figure 25: Similar to figure 20 yet just including our cluster members (CMs).

Those last few plots clearly shows us that those stars really make us a cluster. Our cluster distance of (509 ± 26) pc agrees with the literature value of 513 pc [Can+18]. We want to bring up that SIMBAD incorrectly classifies some stars as member stars of M34 e.g. *Gaia DR2 337177889338182400*[2] -this star has an distance of (126 ± 1) pc according to *Gaia*. This would be about 400 parsec away from the core of the cluster.

[2] `http://simbad.u-strasbg.fr/simbad/sim-basic?Ident=Gaia+DR2+337177889338182400&submit=SIMBAD+search`

4.2.2.2 Teutsch 55

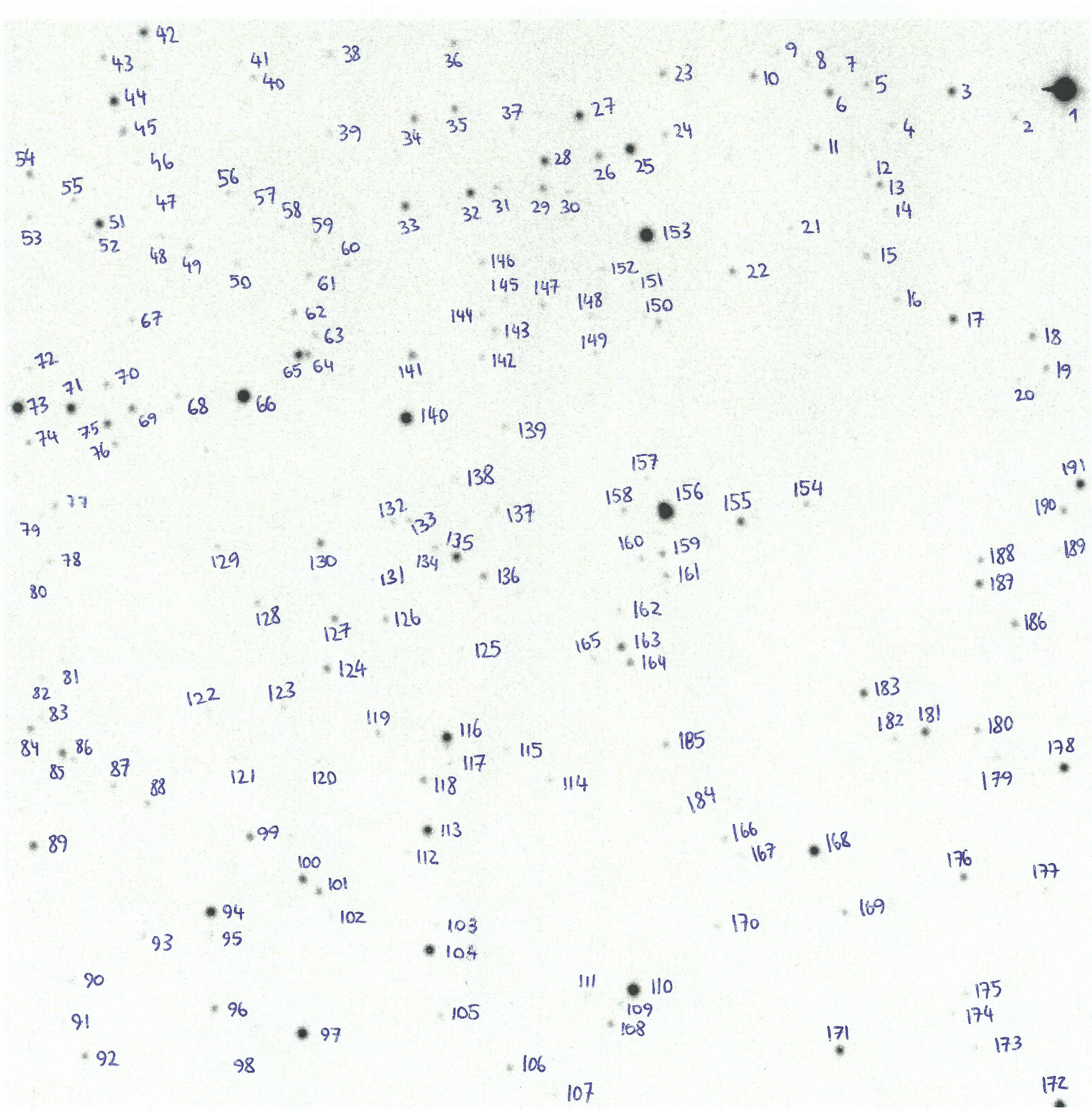

Figure 26: Our observation of Teutsch 55 in the red filter with an exposure time of 300 seconds. The numbers are in correspondence with those in image 27.

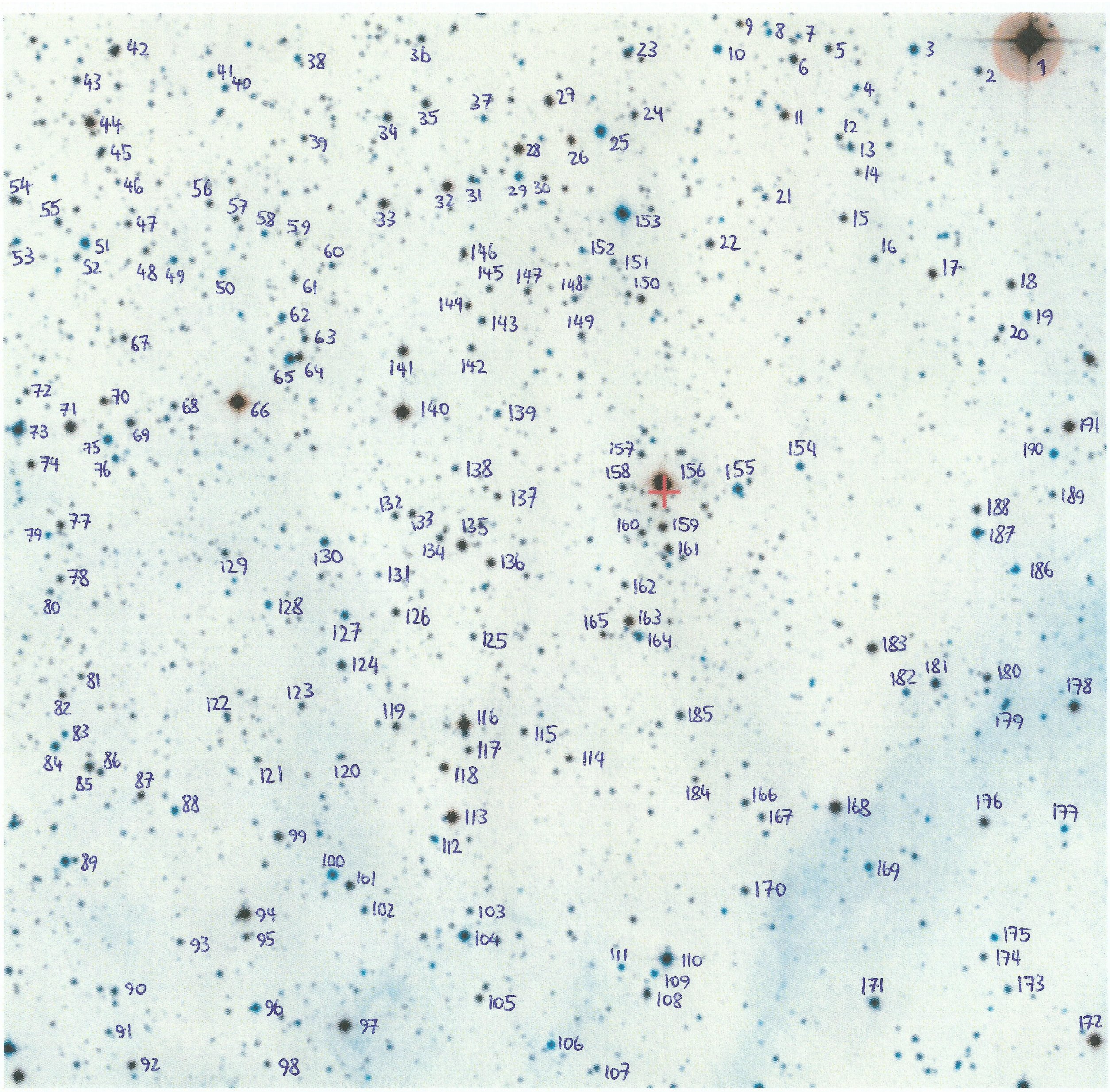

Figure 27: The negative of the observation of Teutsch 55 by the DSS2. This picture was extracted from *Aladin*. The numbers are in correspondence with those in image 26.

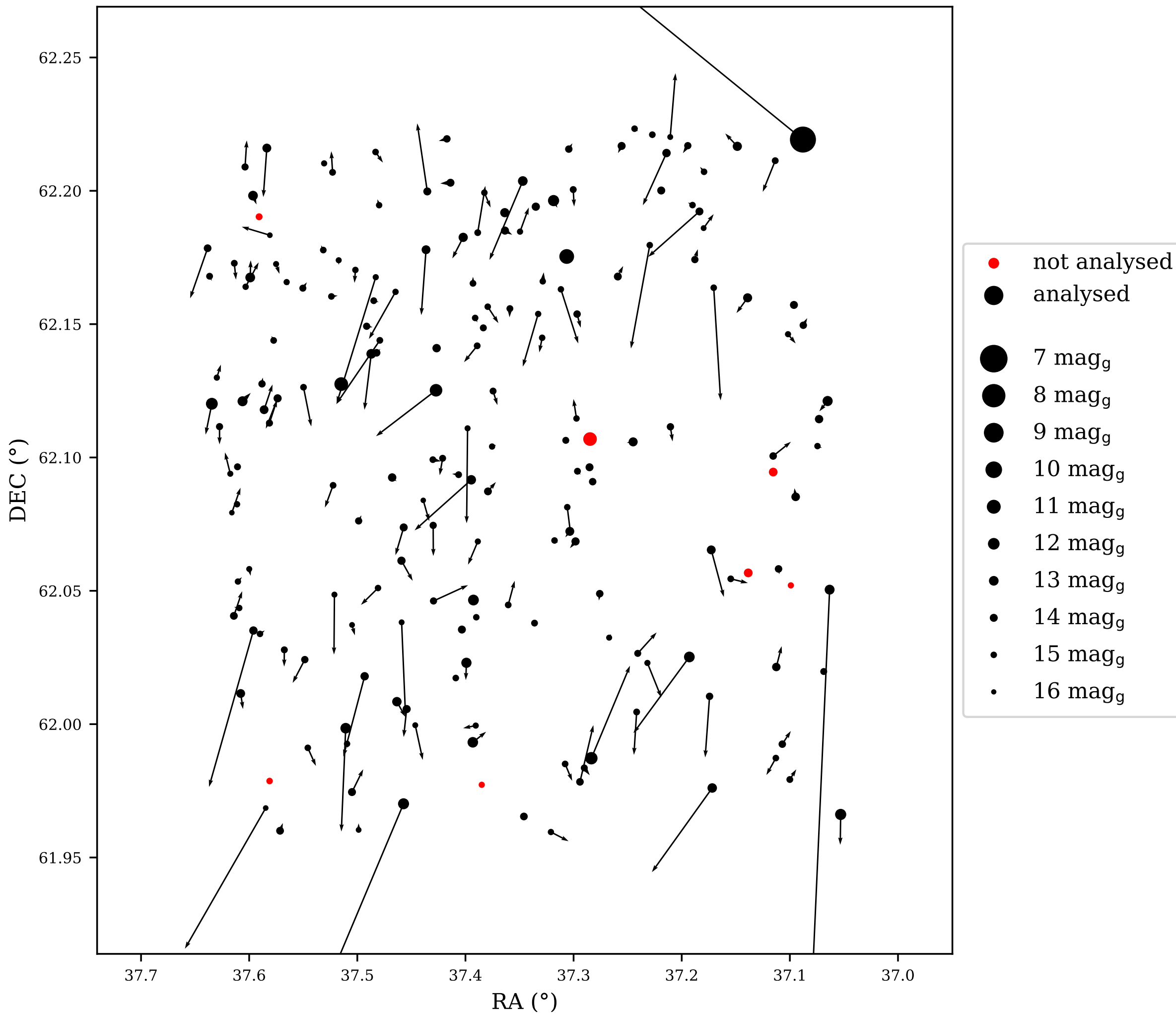

Figure 28: Every point is an extracted source. The size corresponds to the Gaia magnitude. The arrows illustrate the direction of the proper motion. A star was for example not analyzed if the proper motions were missing.

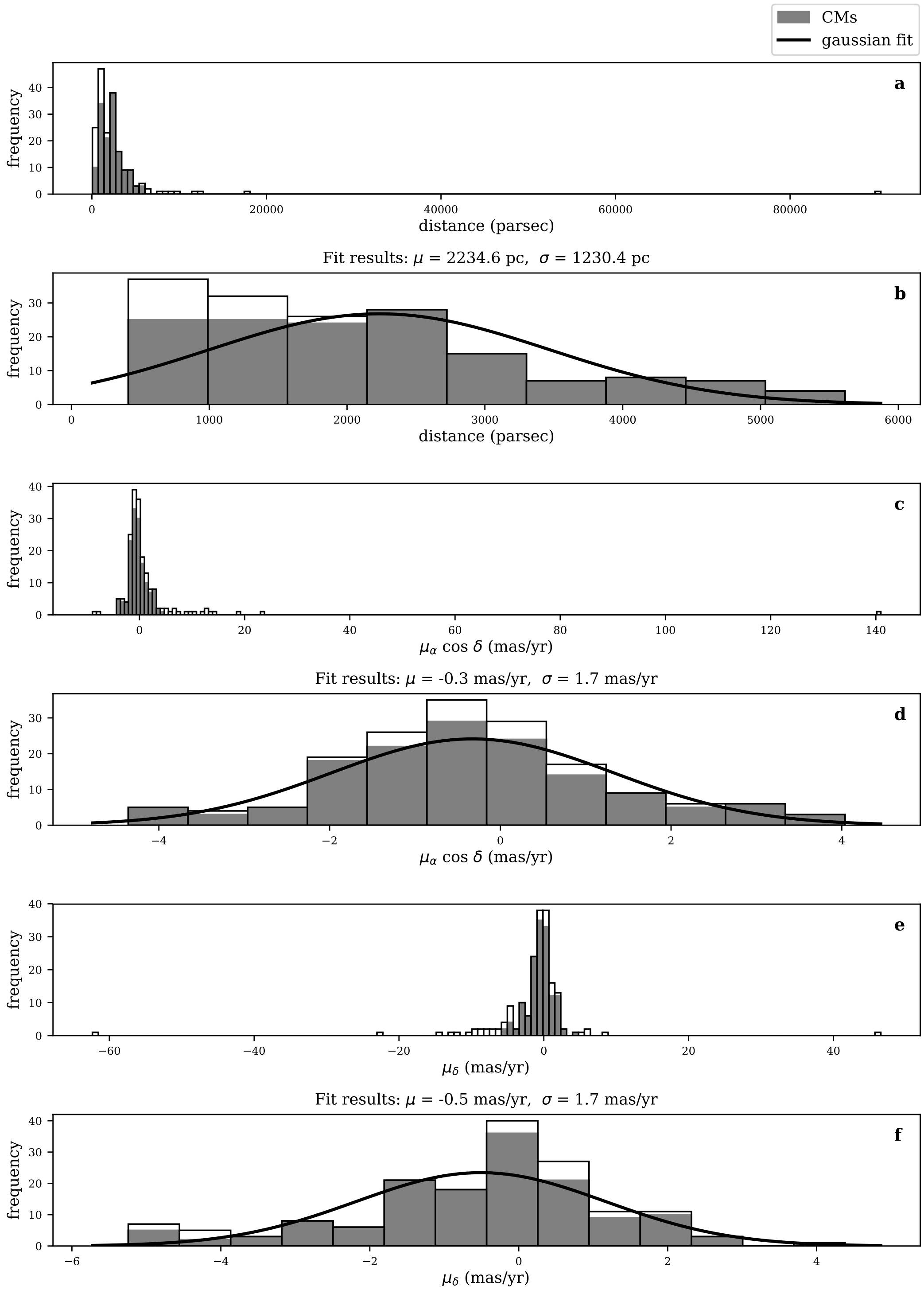

Figure 29: Histogram of the analysed stars. In order to determine the Cluster members (CMs) an iterative sigma clipping procedure was applied (see point 8 in section 4.2.2). **a, c, e**: The distances and proper motions for all stars and the CMs (in gray). **b, d, f**: This zoom-in also includes a gaussian fit of the CMs. Above those plots the mean and standard deviation of this gaussian.

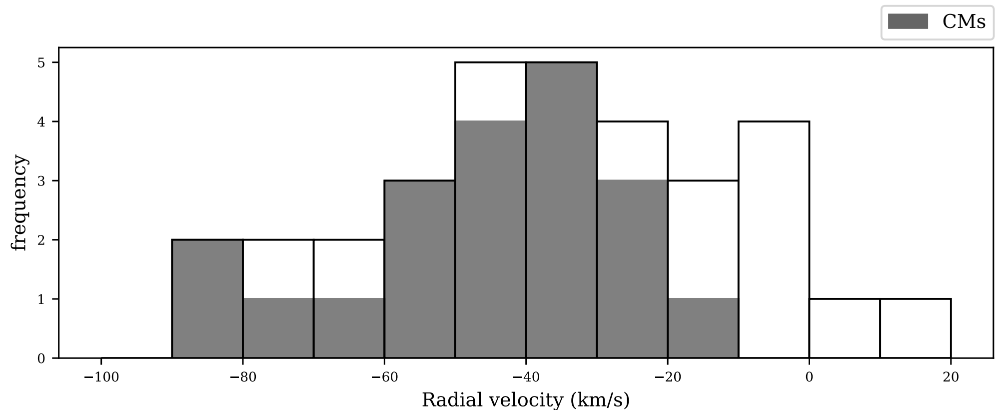

Figure 30: A histogram of the radial velocities. In gray our cluster members determined with figure 29. We see that non of the outliers are also CMs. This is what we would expect.

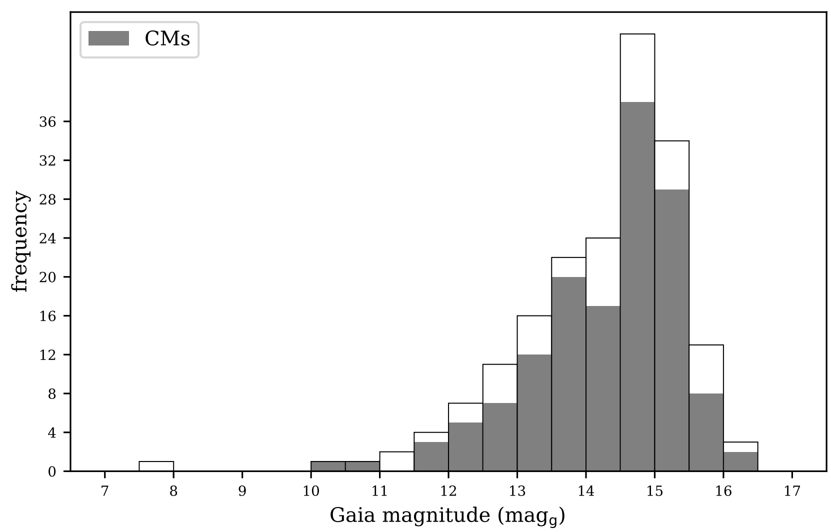

Figure 31: The distribution of Gaia magnitudes of the analyzed stars.

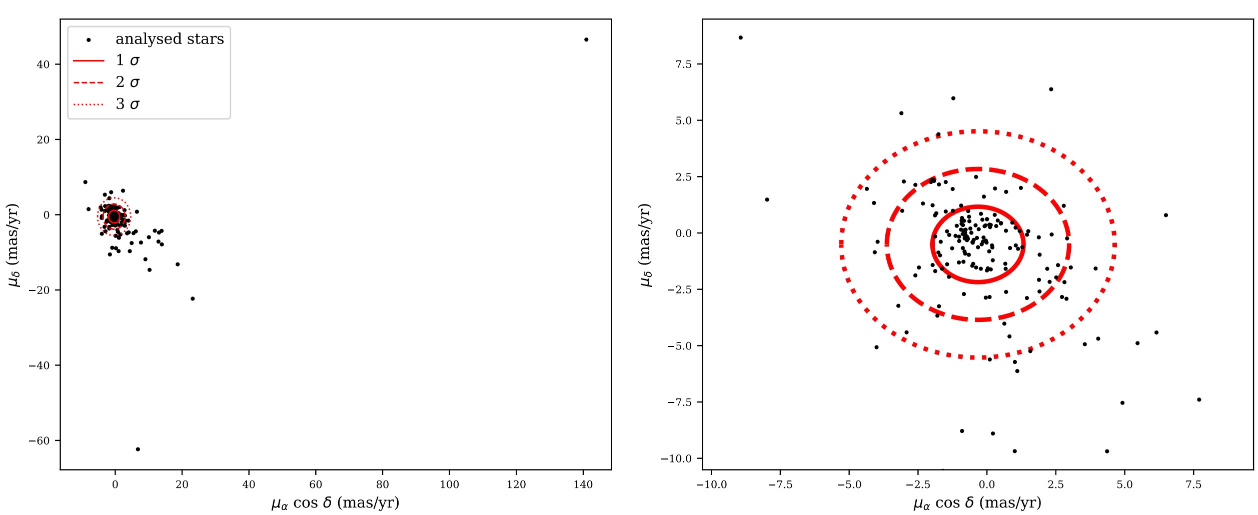

Figure 32: The proper motions of all analyzed stars including the proper motion of the cluster (red) extracted in figure 29. The right side is a zoom-in of the left side.

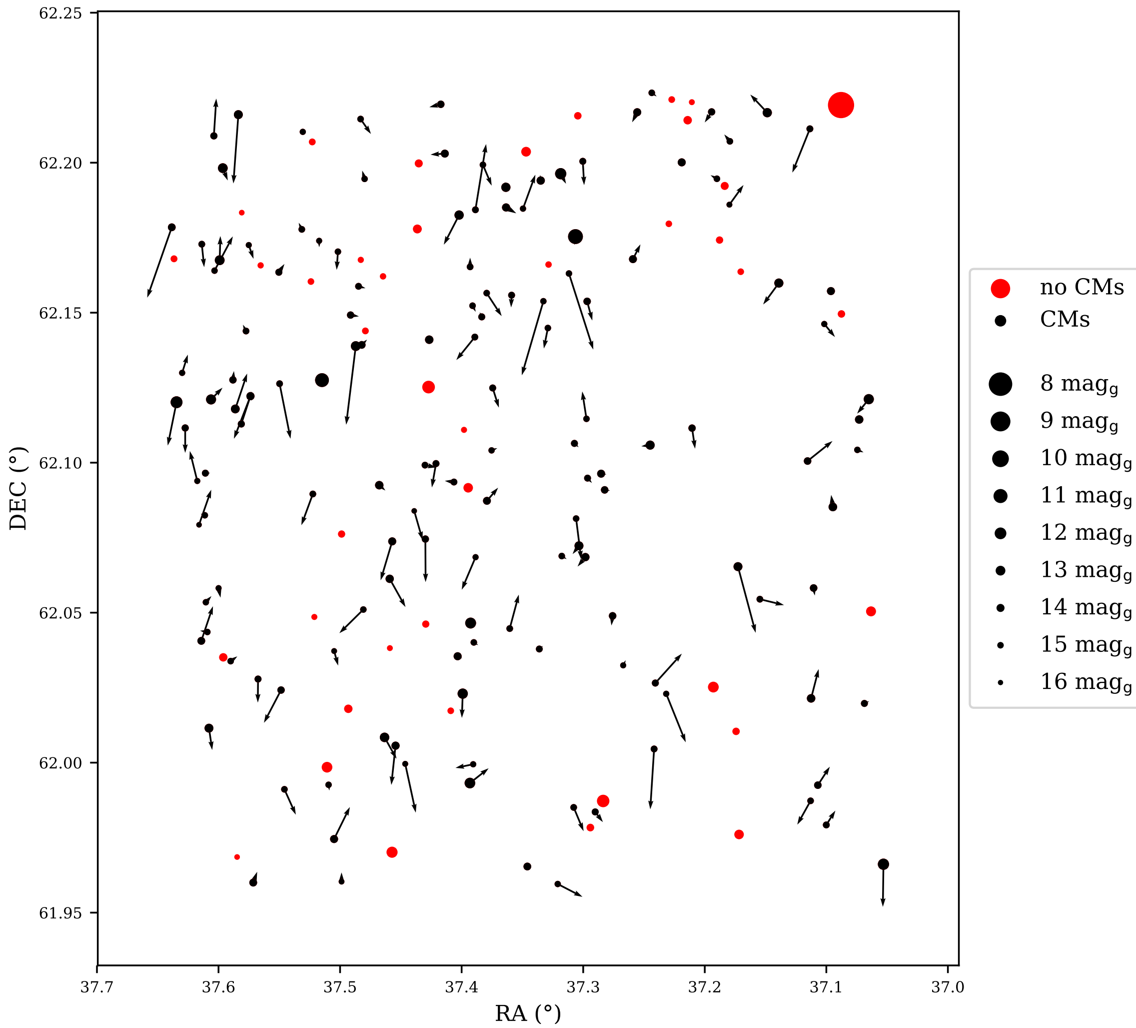

Figure 33: Similar to figure 28, however just including our cluster members (CMs).

In contrast M34 (25) we do not see, that those stars are moving as a group in one direction. We also see this very broad distribution in distances and proper motions in figure 29. So we cannot really confirm this cluster.

4.2.2.3 Stock 19 (C0001+557)

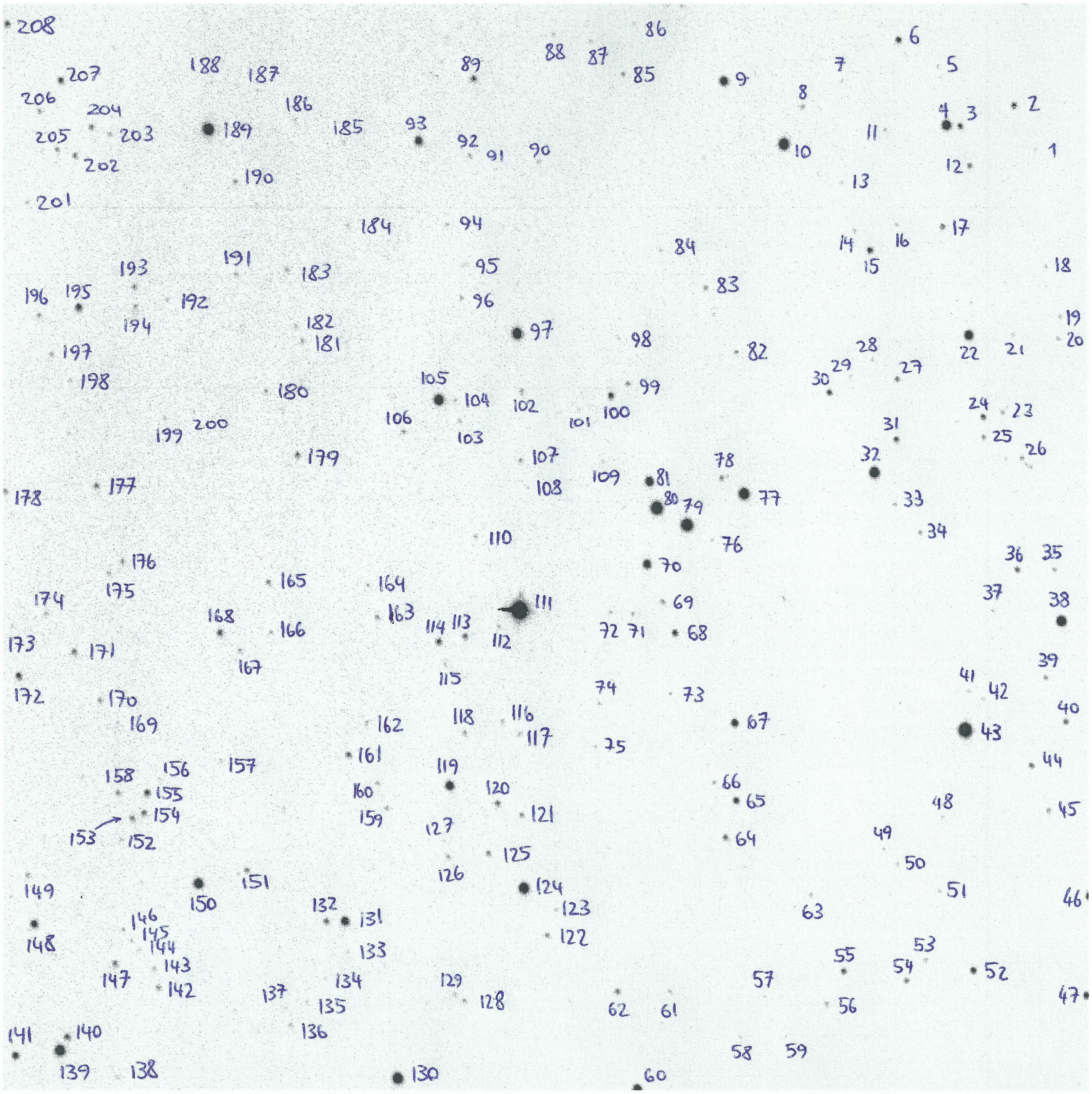

Figure 34: Our observation of Stock 19 in the red filter with an exposure time of 200 seconds. The numbers are in correspondence with those in image 35.

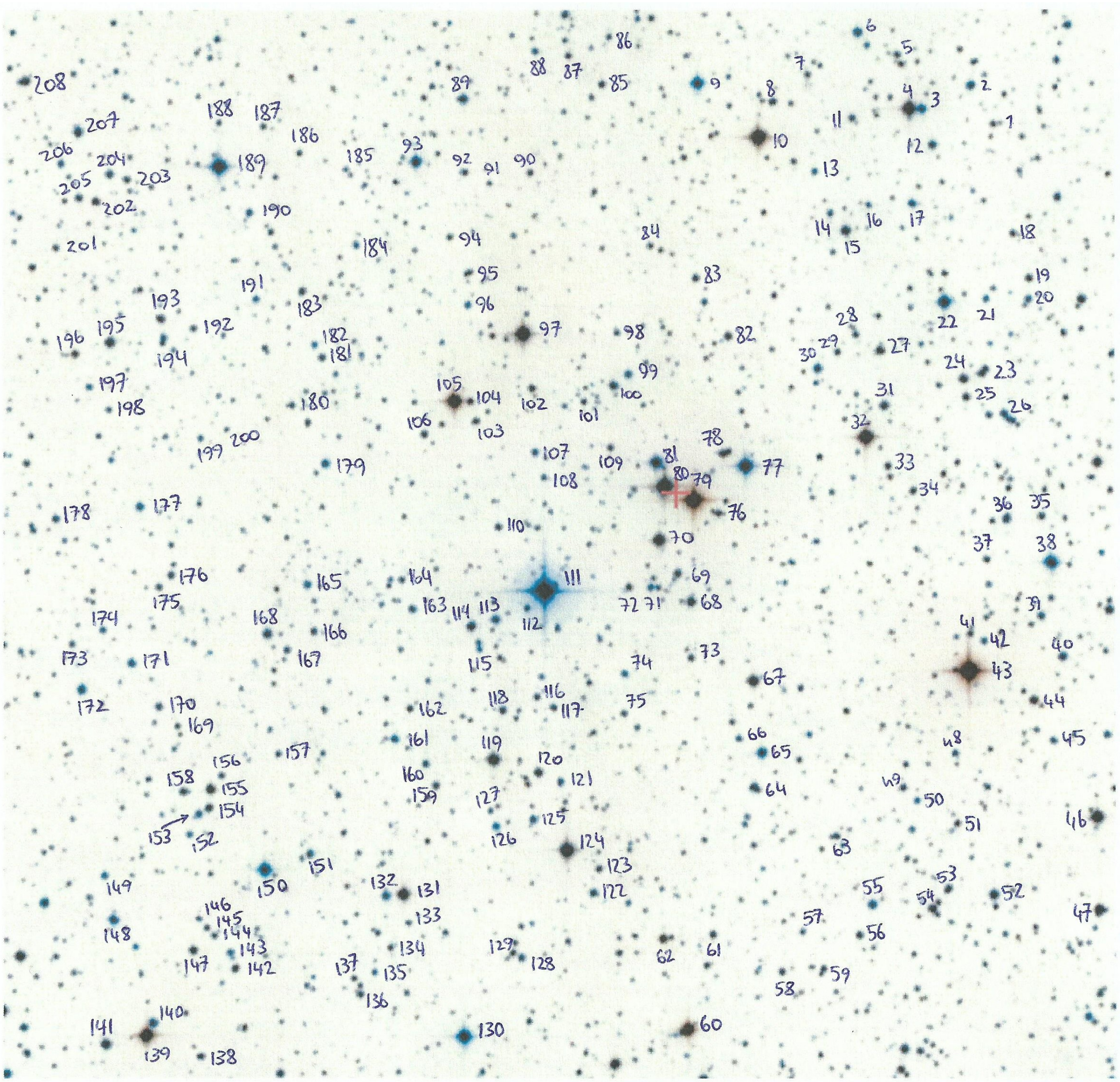

Figure 35: The negative of the observation of Stock 19 by the DSS2. This picture was extracted from *Aladin*. The numbers are in correspondence with those in image 34.

The only light source we observed -of the about 600 in total -without a Gaia DR2 entry is star 124 (in the lower middle of 34 and 35) known as TYC 3656-465-1. The specific reason that this star has no Gaia entry is unknown. It however has a 2MASS entry. The stars magnitude is at about 11 (visual).

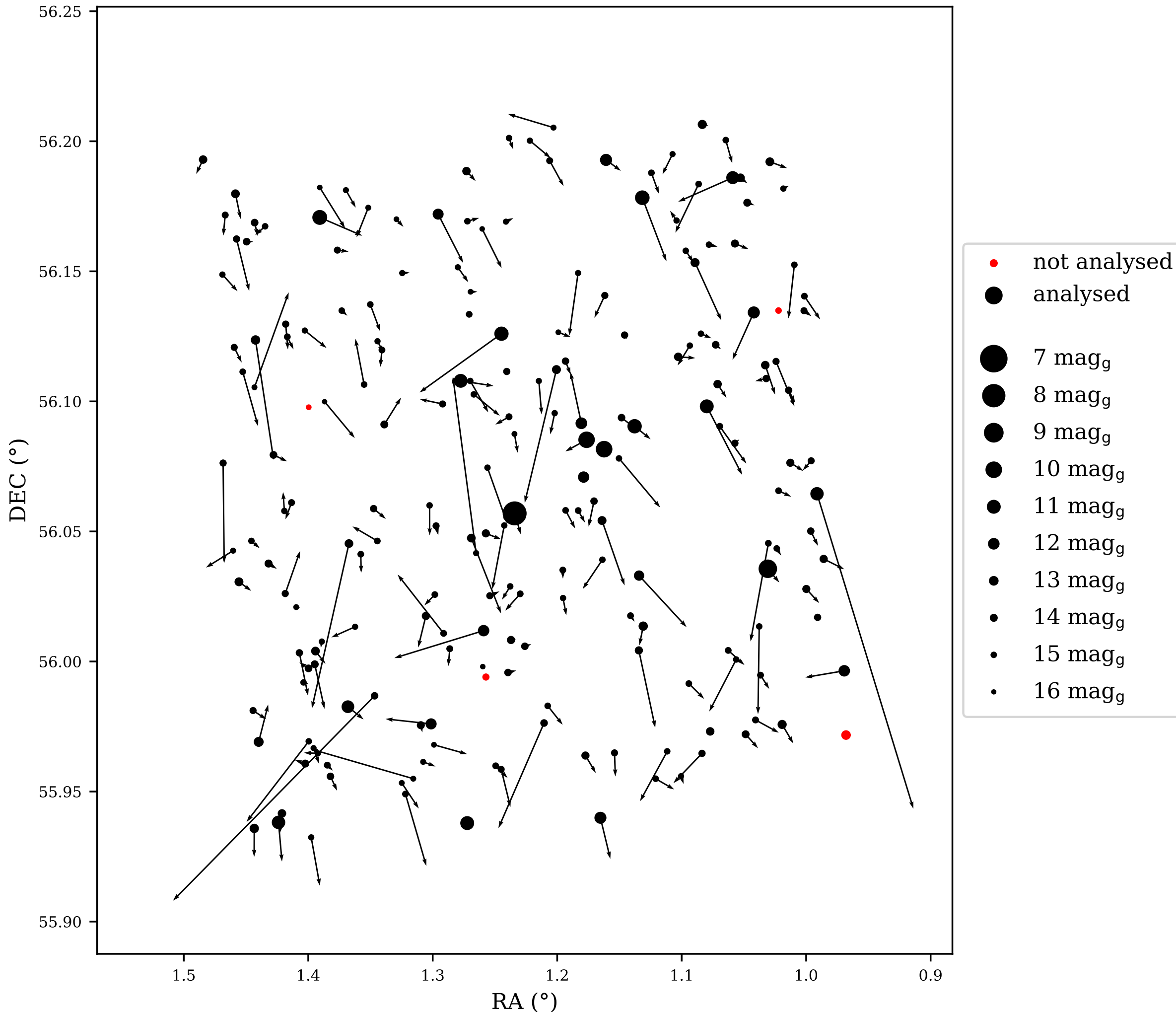

Figure 36: Every point is an extracted source. The size corresponds to the Gaia magnitude. The arrows illustrate the direction of the proper motion. A star was for example not analyzed if the proper motions were missing.

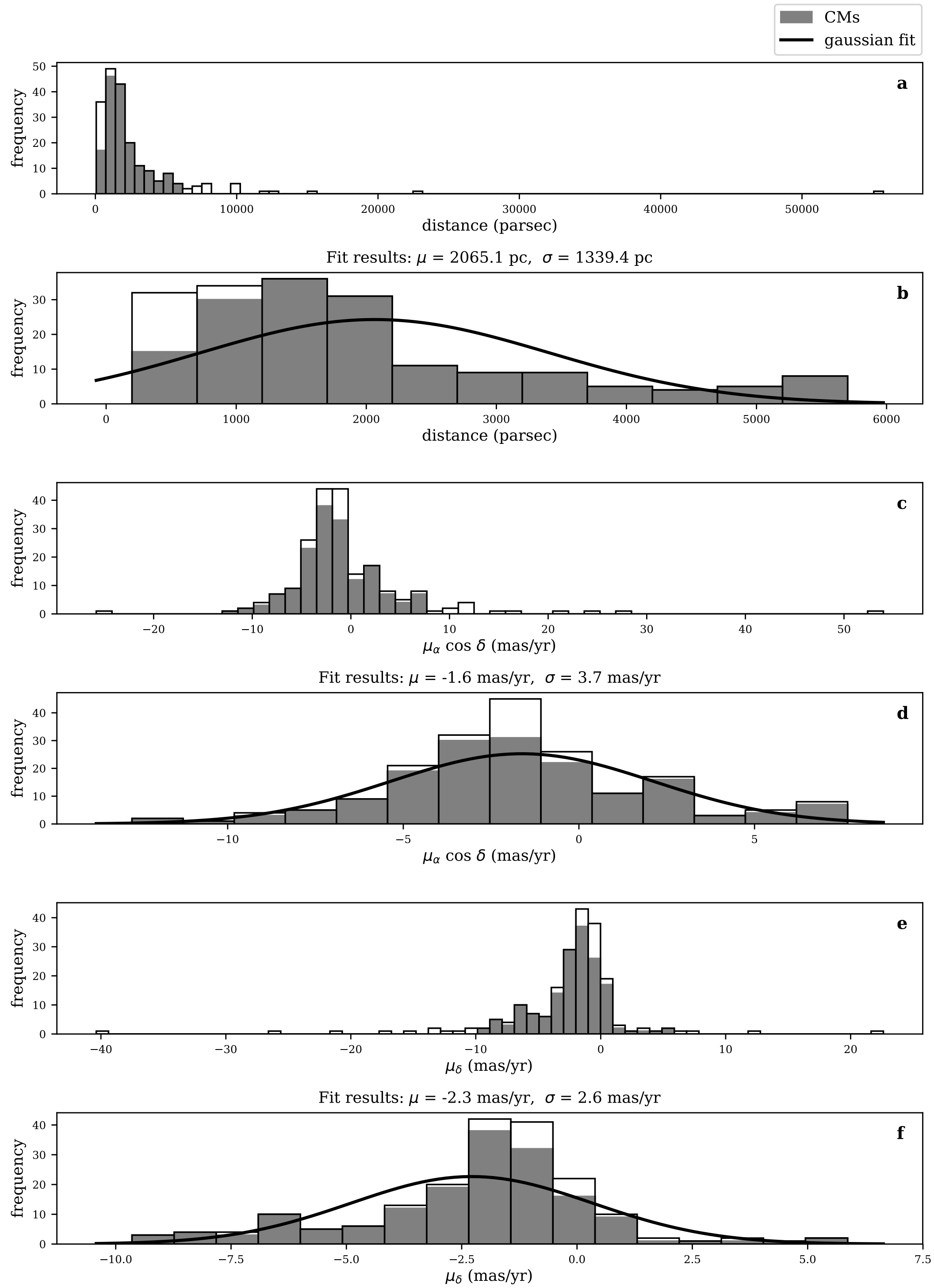

Figure 37: Histogram of the analysed stars. In order to determine the Cluster members (CMs) an iterative sigma clipping procedure was applied (see point 8 in section 4.2.2). **a, c, e**: The distances and proper motions for all stars and the CMs (in gray). **b, d, f**: This zoom-in also includes a gaussian fit of the CMs. Above those plots the mean and standard deviation of this gaussian.

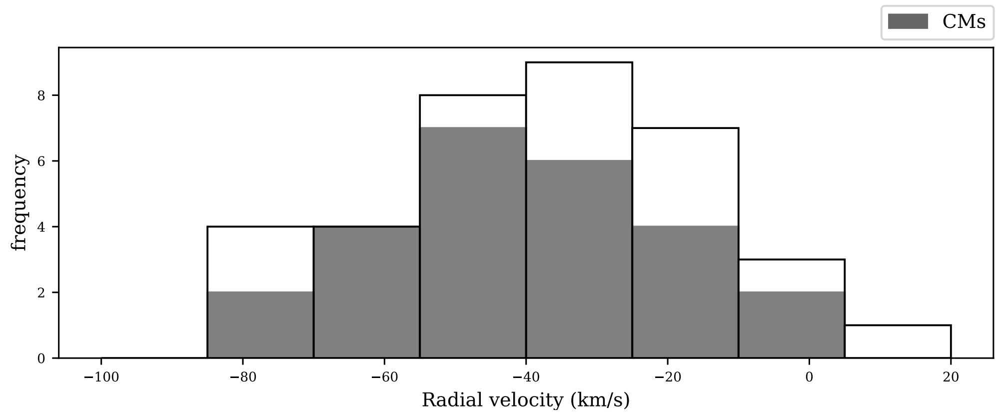

Figure 38: A histogram of the radial velocities. In gray our cluster members determined with figure 37.

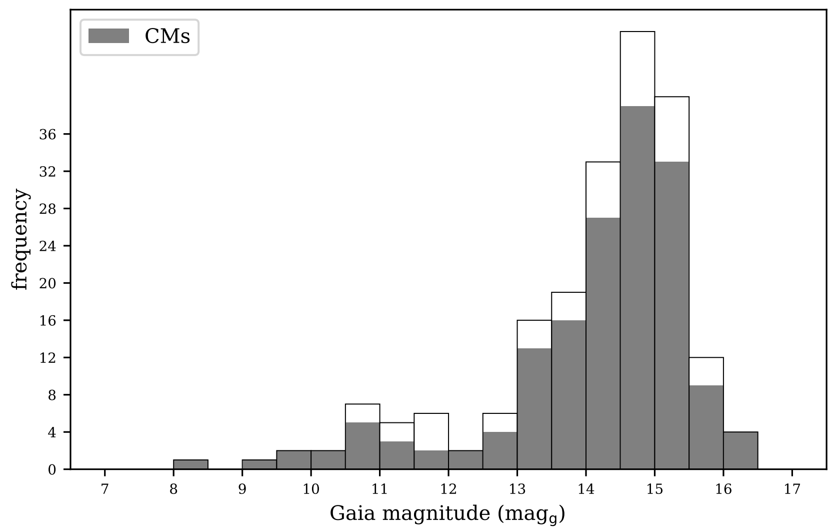

Figure 39: The distribution of Gaia magnitudes of the analyzed stars.

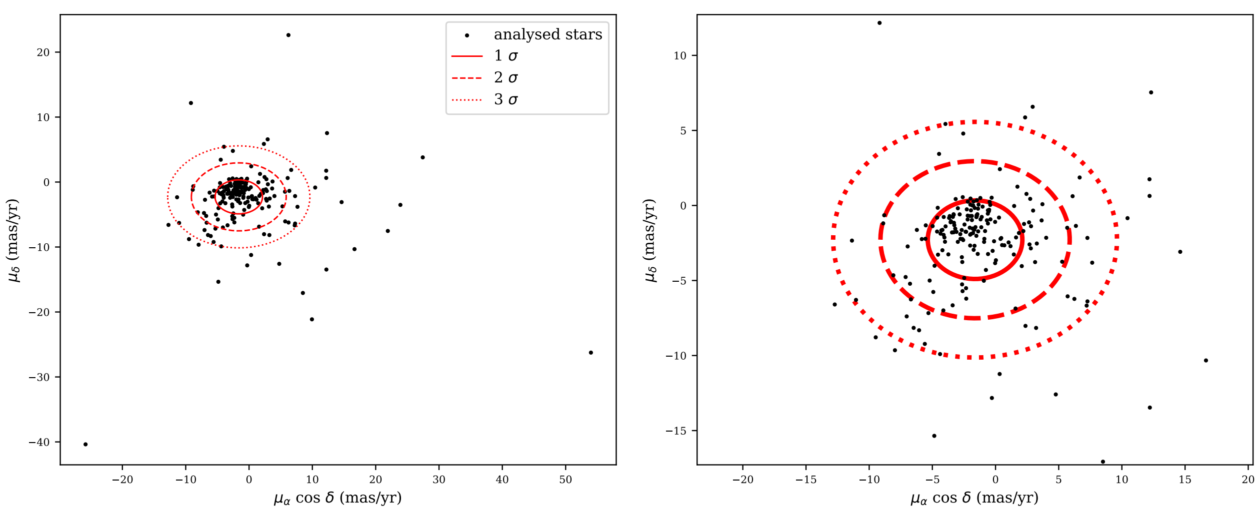

Figure 40: The proper motions of all analyzed stars including the proper motion of the cluster (red) extracted in figure 37. The right side is a zoom-in of the left side.

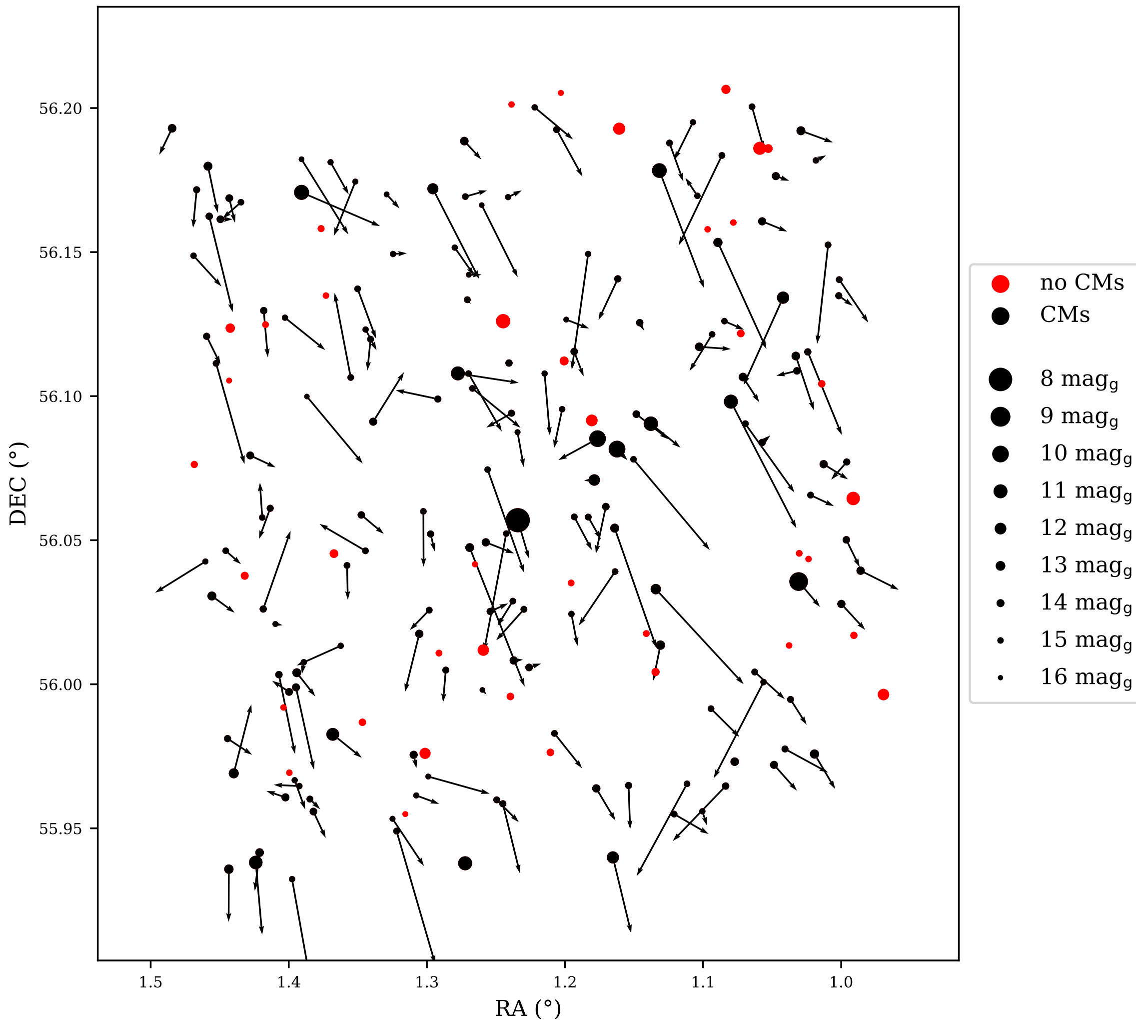

Figure 41: Similar to figure 36 yet just including our cluster members (CMs).

Similar to 33, but in contrast to figure 25 we do not see, that those stars are moving as a group in one direction. We also see this very broad distribution in distances and proper motions in figure 37. So we cannot really confirm this cluster.

To conclude, it proves to be rather difficult to tell whether the imaged objects actually can be classified as galactic open clusters. It might be interesting to look at the color of the suspected cluster members but we do not have color information for a sufficient amount of stars in the images as extracting sources from the images is not trivial, especially in the Johnson B filter. Furthermore, Gaia data has to be studied very thoroughly [illegible]ften times measured properties are wrong in a very obvious way, for example negative parallaxes can be found for several stars.

4.3 Imaging using a "lucky imager"

Lucky imaging is a technique used to counteract the negative influence of the turbulence in the air of the Earth's atmosphere. During long exposures the movement of the atmosphere smears out the imaged object which results in sub optimal images. Therefore the idea is to reduce exposure time to a minimum by basically taking a video of the object one wants to image. From the video one can select the frame or frames which show the least amount of turbulence in the atmosphere. This technique is therefore only nicely applicable for setups and sources which do not require long exposure times.

In practice the selection of high quality frames is not done manually but with an automated software algorithm like the one used by Autostakkert [Kra19], which we use for generating the images taken with the lucky imaging camera. Software like this automatically stacks single frames from a video which have a high quality according to an algorithm which looks at, for example, the FWHM of stars or the surface structures of the moon. For stacking, the images are aligned using the brightest pixels as reference before being combined. Afterwards it is possible to apply artificial sharpening via a convolution.

The influence of this sharpening convolution can be seen in figure 42 and the overall improvement which can be achieved using lucky imaging is shown in figure 43. The videos from which these images are generated are taken with the 60cm telescope and the lucky imaging camera on December 13$^{\text{th}}$ while waiting for the comet 46P/Wirtanen to appear above the horizon. As already mentioned in the section about imaging this comet, the seeing was not great that night however the lucky images of the moon are of an impressively high quality given the setup and location.

Figure 42: Comparison of a stacked image generated from the best 27% of frames of a 1000 frames movie of the Moon (upper image) using the Autostakkert software [Kra19] and a sharpened version of the same stacked image (lower image). An automatic convolution is applied to the stacked image in order to obtain the sharpened version.

Figure 43: Comparison of an arbitrarily chosen frame of a video of a different part of the Moon (upper image) and the final sharpened version produced from the same video by stacking the top 25% of frames and sharpening. This was also done using Autostakkert [Kra19]. The improvement can easily be seen when comparing both images.

5 Spectroscopy

In this section of our report, we describe the methods of spectroscopy using the Lhires III spectrograph. Subsection 5.1 gives a summary of observational methods including a short overview of the inner workings of a Littrow-Spectrograph and the means of preparation in order to reduce the taken spectra. In subsection 5.2 we report on how to reduce and extract a spectrum from a CCD image using IRAF. Continuing in subsection 5.3 we show how to map CCD pixel number to a wavelength scale in order to calibrate the spectrum and how to normalize the continuum. Finishing up in 5.4 we will discuss observed spectra from two well known sources (Vega -α Lyrae & Deneb -α Cygni) concerning problems that our method of observation may show.

5.1 Observational Methods & Preparation

As documented in [TC06] Lhires III (Littrow High REsolution Spectrograph) is a spectrograph in Littrow configuration meaning it has an optical path and general structure as in figure 44. Rendering this special kind of setup for a spectrograph, both compact and affordable, the Littrow configuration is defined by having the same optical element -a 200mm lens -be both the collimator, parallelizing the beam, and the imaging lens at once. The diffraction grating (300 lines per mm) allows for expected spectral dispersions of 1.493 Å per pixel. In the vicinity of the H Alpha line in the red part of the spectrum, the resolving power $\frac{\Delta\lambda}{\lambda}$ is approximately 1300. A spreadsheet [TC06] with simulated results, assuming a telescope aperture of $\mathrm{D} = 60\,\mathrm{cm}$ and a focal ratio $\frac{\mathrm{F}}{\mathrm{D}} = 8$, defines the limiting magnitude in a one hour ($\frac{\mathrm{S}}{\mathrm{N}} = 100$) exposure to be $\mathrm{m} = 11.3$, when simulated with a target star of type B0V.

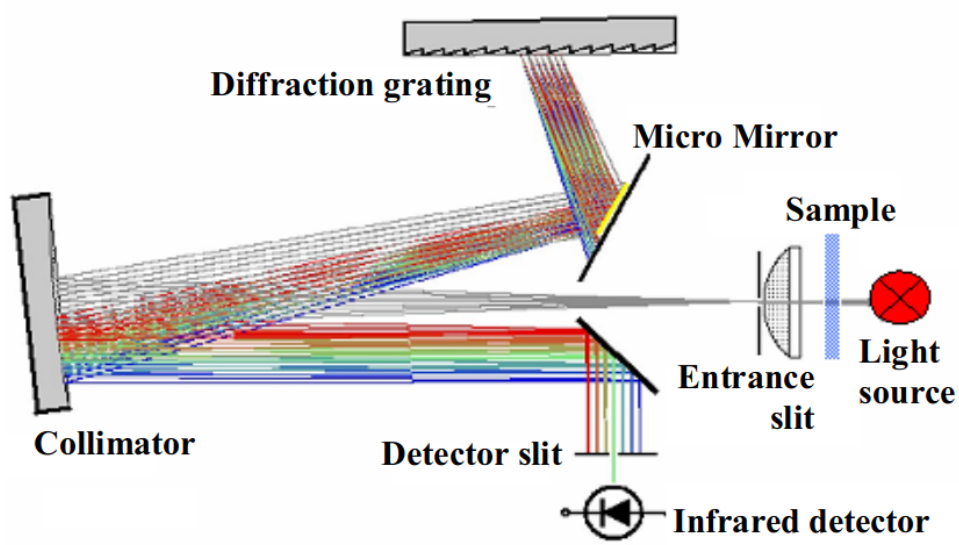

Figure 44: Here one can see the general structure and optical path of a spectrograph in Littrow configuration, which is the configuration of Lhires. Image taken from [SOG04]

Let us now look at preparation steps to take in order to observe real spectra with this tool. First, since the observation of spectra in this fashion uses CCD imaging, we need to take several bias, dark and flat images to later reduce the images as described in section 5.2. Furthermore, calibration images of a neon reference lamp have to be taken in order to do the wavelength calibration (subsection 5.3). One such image of the emission lines of neon and other residual elements can be seen in figure 45. The tricky part in taking this image is exposing long enough to have good signal to noise values in the weak emission lines (rightmost part of the image), while not over exposing the strong lines in the center. An exposure time of $t = 10\,\mathrm{s}$ proved favorable in our case. Once done with taking several of these line calibration images one can start to search for an object on the sky to observe and center it in the middle of the field of view using an imaging camera. Coming to the tricky part of the quest, we now need to focus the image of the object on the entrance slit of the spectrograph. Once this is accomplished an image of the object, such as the spectrum of the star Vega (α Lyrae) with an exposure time of $t = 200\,\mathrm{s}$, can be taken -see figure 46.

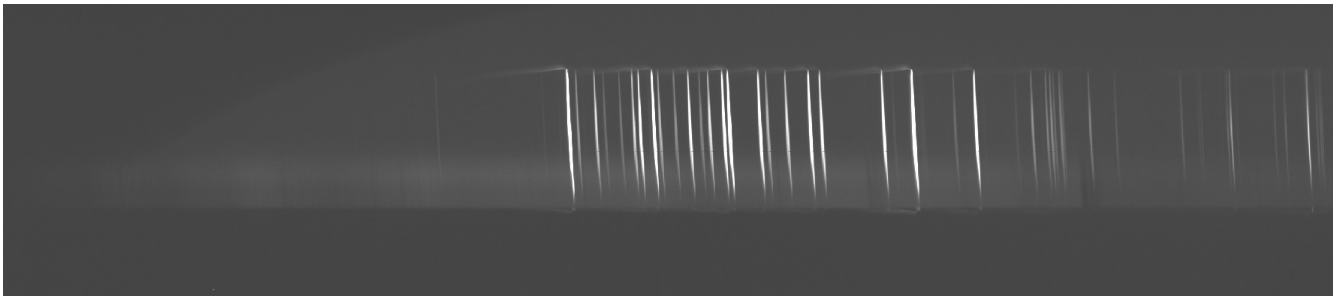

Figure 45: This figure shows a CCD image of the neon calibration lamp. It's easy to see that there are insufficiently many lines in the blue wavelength regime (leftmost part). Still, it is possible to find at least some weak lines of residual elements such as quicksilver.

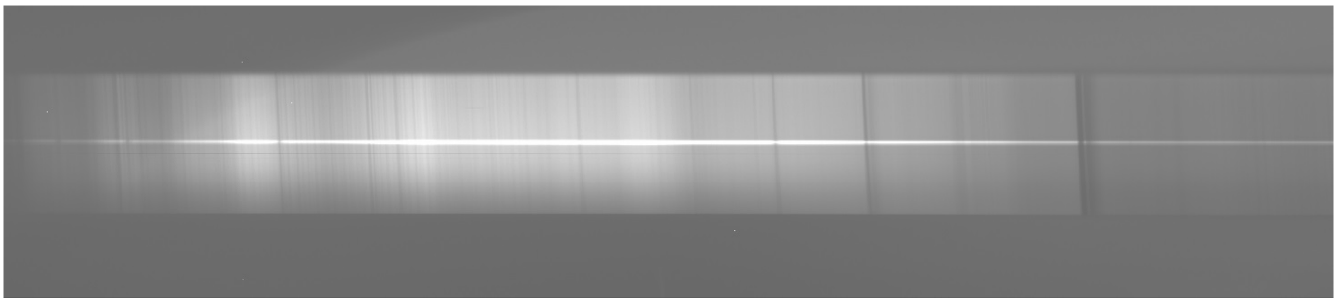

Figure 46: This figure shows the CCD-Image of the spectrum of the star "Vega" -α Lyrae. The image was taken with an exposure time of $t = 200$s. Already, one can clearly see structures such as Hydrogen Balmer lines and water absorption regions.

5.2 Data Reduction & Spectrum Extraction

As the description of each individual command in IRAF concerning the reduction of the spectrum would certainly exceed the volume of this report I want to instead just refer to the excellent instructions given in chapter 4 of [Lar11], which the following procedures are based upon.

The first step to take in extracting the spectrum is finding the correct aperture of the spectrum on the CCD image. One may, perhaps, erroneously think that the whole illuminated part of the image in figure 46 is the spectrum.

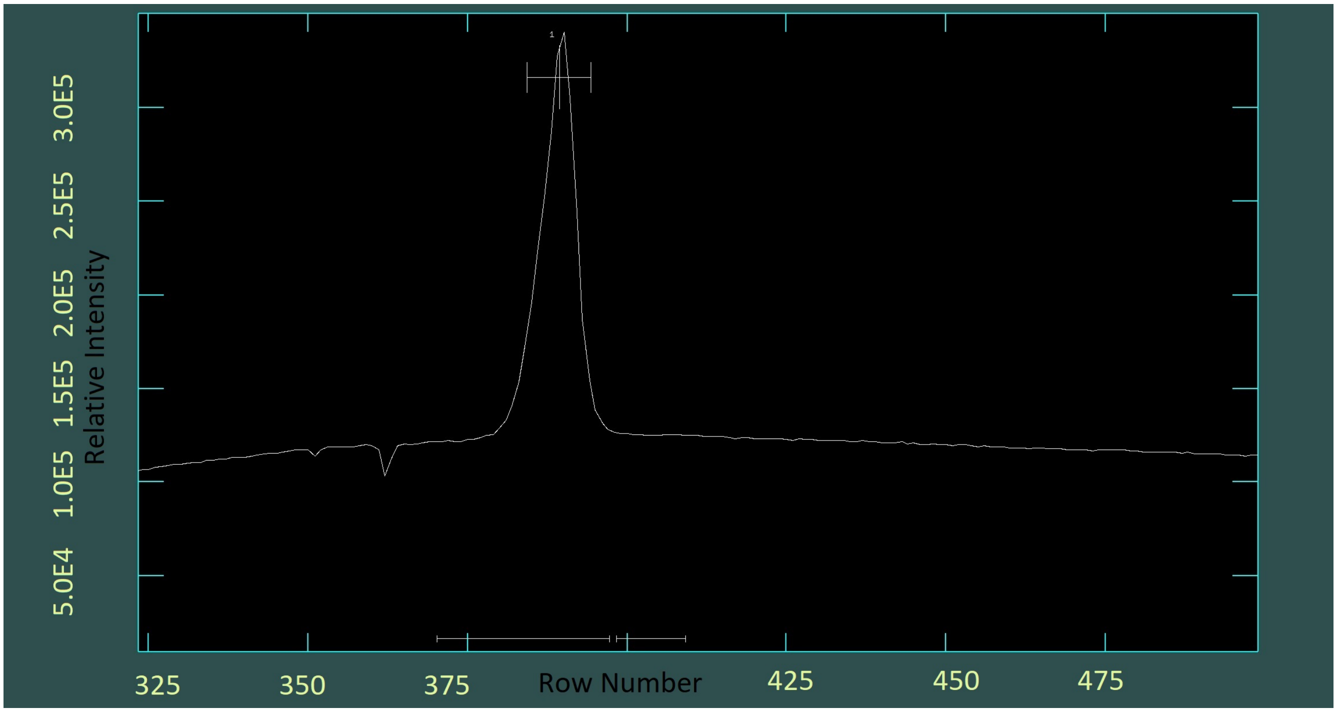

Figure 47: This figure shows a plot of measured instrumental intensity as a function of the CCD row number. This configuration is used to choose the correct aperture on the chip using the command "apall".

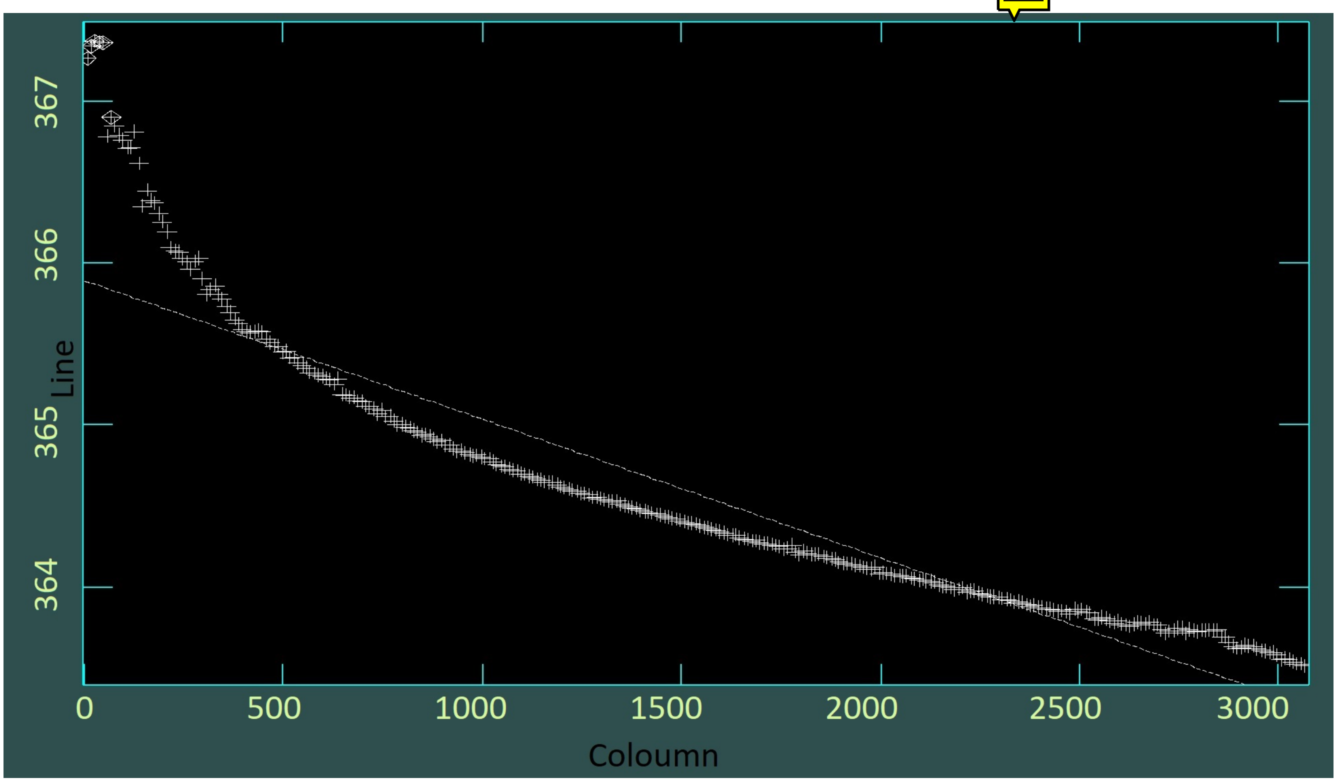

Figure 48: This figure shows a plot of the distribution of the aperture on the chip (Row aperture position as a function of CCD column number). One can see, that it has a nonlinear component, which has to be fit by a polynomial to extract the spectrum.

However, only the brightest most central part of the image is the objects signal, everything else is sky background, stray light and the sort. Using the command „apall“ in IRAF we can allocate the correct aperture, that is, the correct rows of the CCD image, and correct for the background. Figures 47 and 48 show parts of this procedure. In the former one, one can see the process of finding the aperture as a function of row number and the background level (ca. a factor of three apart). In the peak of the intensity curve, one can see the manually defined aperture, that tells the program in which rows the spectrum is to be found. In the second figure 48 one can see the process of fitting the spectrum („Lines“-Axis) as a function of the column pixel value. This has to be done as the bright line in figure 46 is not absolutely horizontal, but skewed up and down. Correcting with a Legendre polynomial of order 3 or 4 suffices and produces a spectrum as the one in figure 49.

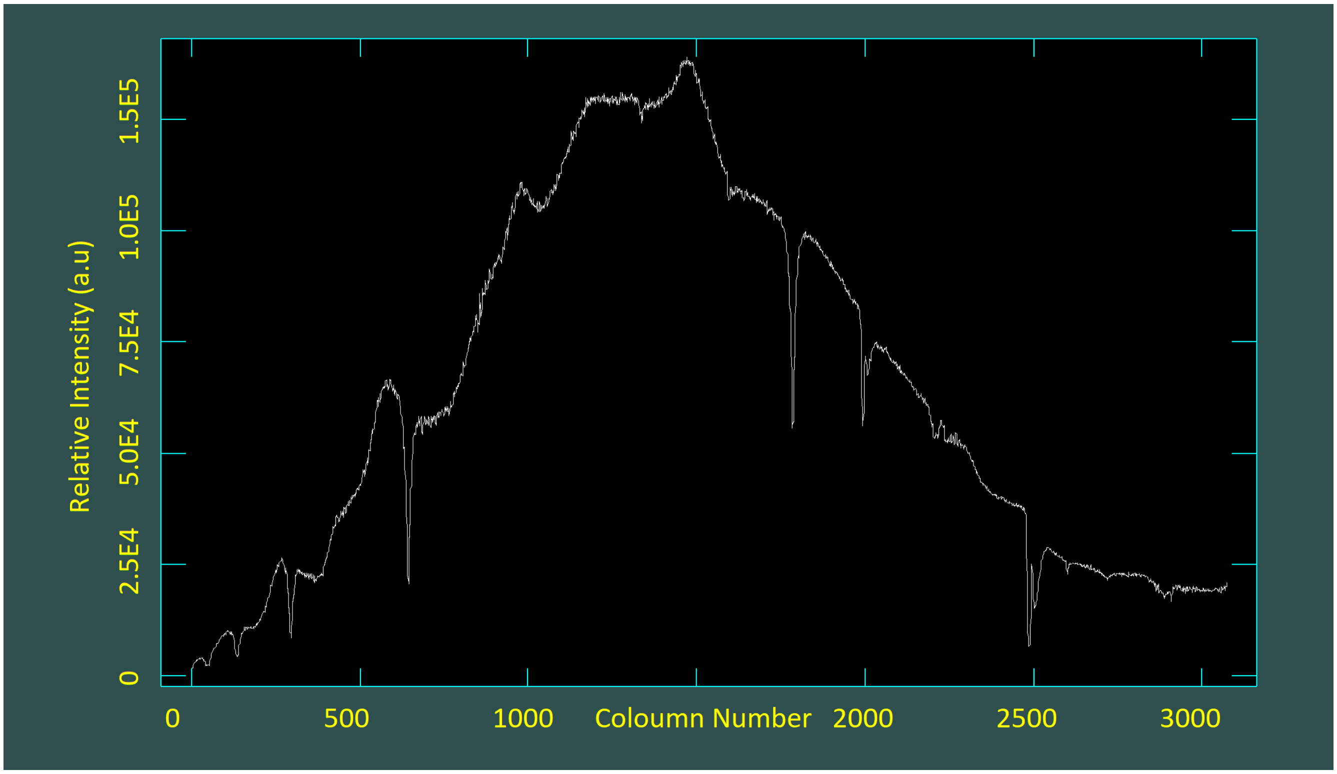

Figure 49: Here you can see the non flux-calibrated spectrum of Vega as mapped on the pixel values of the chip. An image like this is the result of using the „apall“command as documented in 5.2.

As can be seen clearly, the spectrum still has imprint of the response of the CCD chip in it and is a function not of wavelength but of the column pixel value. We explain how to calibrate and normalize it in the following section 5.3.

5.3 Wavelength Calibration & Continuum Normalization

As before, we again use „apall“ with slightly modified parameters to extract a spectrum of the calibration lamp image 45. Proceeding with the IRAF command „identify“ , it opens up an image similar to figure 50, which shows the individual lines of the n lamp to map the pixel values to a preferred wavelength solution. It is now on the user to mark the lines and assign them their correct wavelength -a task which is greatly simplified using the resources of line lists for common calibration lamps: [Gar07] & [Cer00]

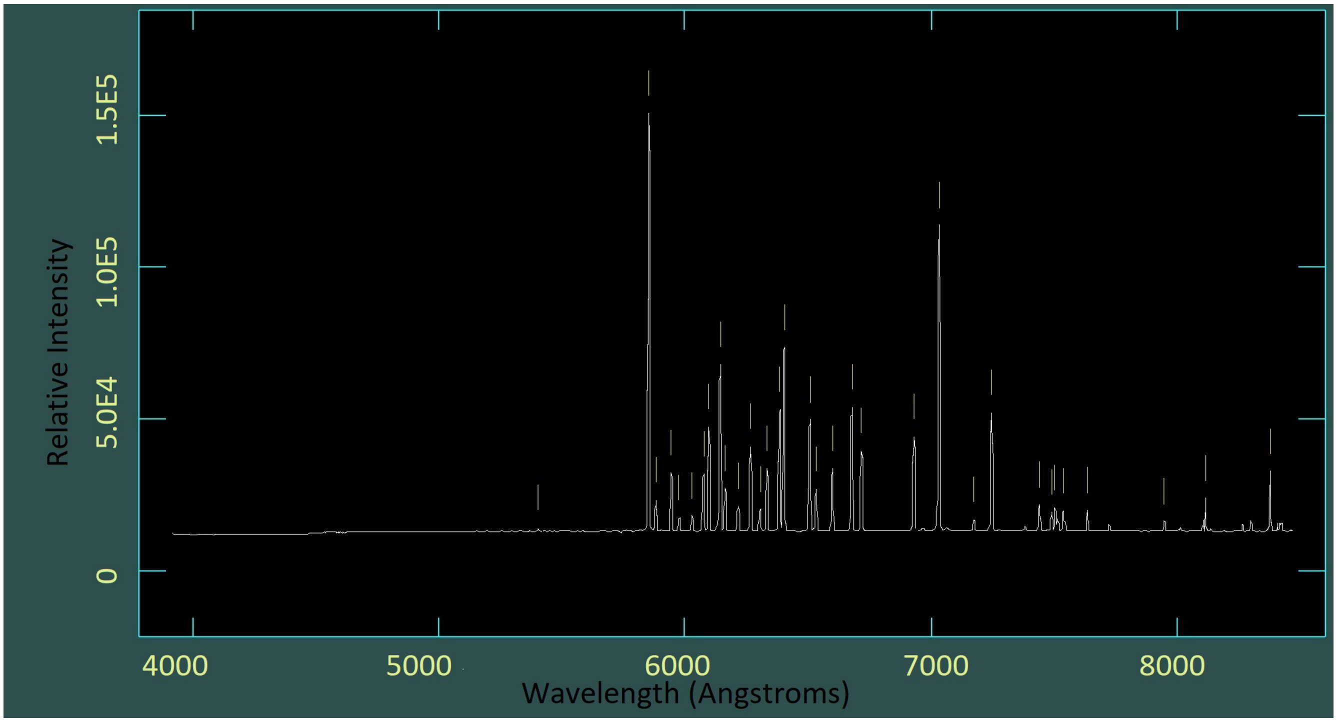

Figure 50: This graph shows the intensity distribution of the calibration lamp light as a function of wavelength. It is used to map the pixel number on the CCD to a wavelength regime.

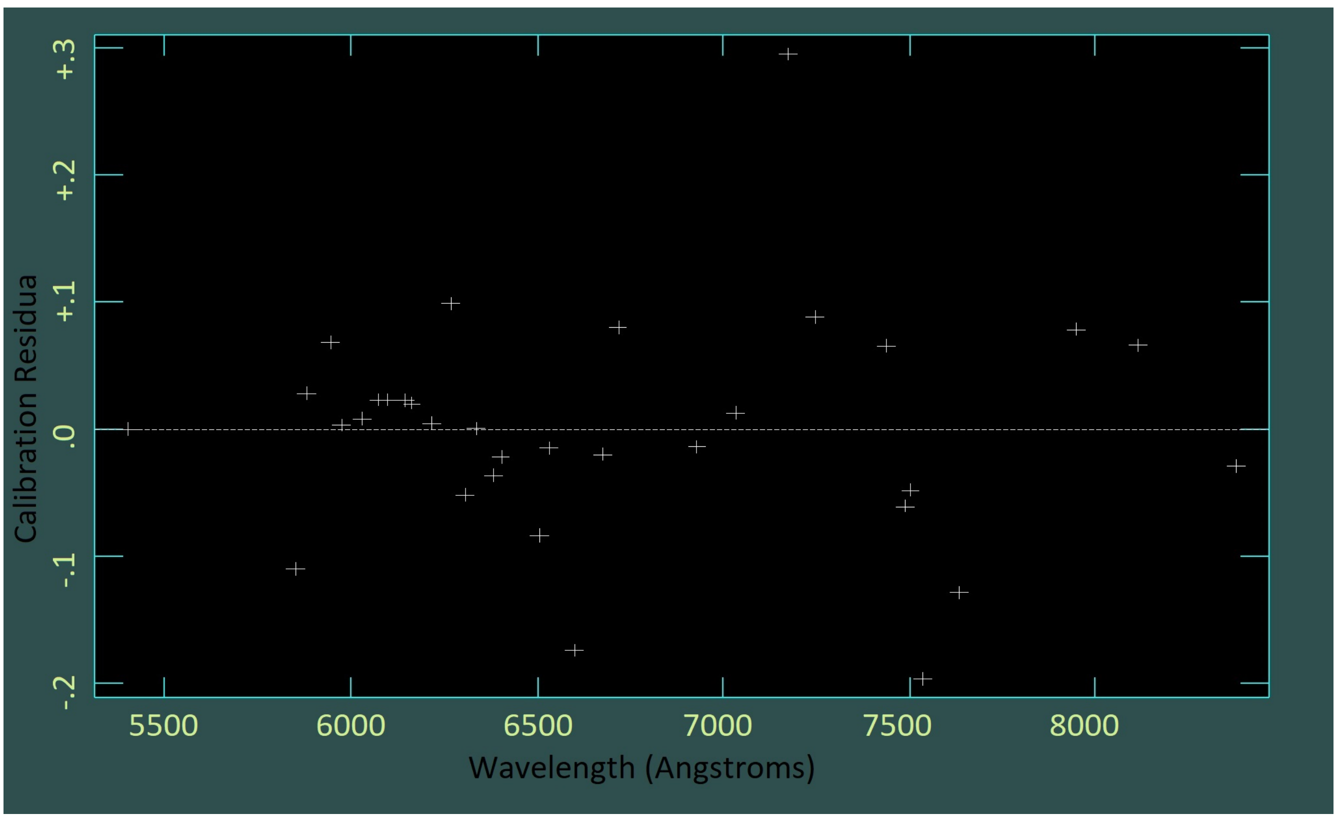

Figure 51: This graph shows the residua (in Angstroms) of the fit to the calibration spectrum as a function of wavelength.

Finding and identifying all the lines allows us to again fit a polynomial like a Legendre or a Chebychev to the CCD pixel-wavelength function. The result is an image like figure 51, showing the residuals of the fitting process with a RMS-scatter of about 0.3 Å. The solution can now be applied to the uncalibrated spectrum (figure 49) using the „dispcor“ command. Viewing it now with „splot“ will show the spectrum as a function of wavelength.

For quantitative analysis of spectra, it is sometimes convenient to normalize the spectrum with the continuum. This can be done using the command „continuum“ in order to fit a high order polynomial to the spectrum (see figure 52). Keyword parameters can be used to tell the program at what sigma level it is supposed to sort out non-continuum points -i.e. the lines. IRAF will then iteratively fit the spectrum to normalize to the now defined continuum level. The output spectrum of the wavelength calibrated and continuum normalized spectrum can be seen in figure 53.

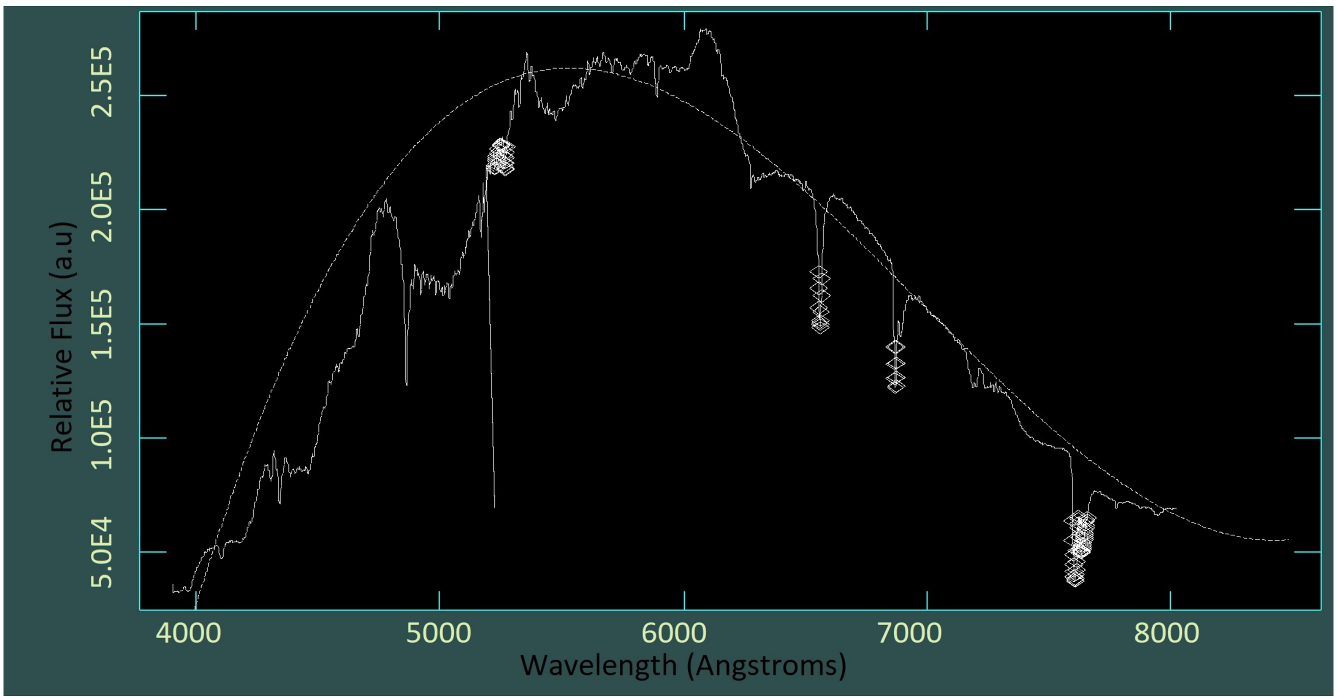

Figure 52: In this figure one can see the unnormalized, wavelength calibrated spectrum of Vega. The continuum must be fit by a high order spline to normalize the spectrum.

5.4 Discussion

Even though the extracted and processed spectrum of Vega, which can be seen in figure 53, certainly looks nice enough it is by no means perfect. The very first point of critique is that the fit of the polynomial in the process of wavelength calibration and normalization seems to leave ugly divergent tails on the left-and rightmost edge of the spectrum. Moreover, due to the way the optical image is mapped onto the CCD, the edges are skewed upwards, to higher intensities -as can be seen particularly well in the range below Hγ. Consequently, we cannot trust continuum levels in parts below Hβ or above the waterbands in the red, leaving us with a useable wavelength range of ca. 4700 Å $< \lambda <$ 7800 Å.

Another weak point in the procedure is the huge wavelength shift introduced by the calibration lamp. The light of the neon lamp is not, as ought to be, collimated with the same focal ratio of the telescope ($\frac{F}{D} = 8$) and guided towards the slit with a mirror. Rather, the lamp just shines through the slit with an unknown focal ratio, introducing wavelength dependent blues hifts into the spectrum. The effect was measured to be about $\Delta\lambda_{H\alpha} = 3.3$ Å in the vicinity of Hα and to staggering $\Delta\lambda_{H\beta} = 12.9$ Å at Hβ. This obviously hinders any type of research on radial velocity shifts and greatly complicates the process of identifying small metal lines.

Since we observed two objects, we can compare this rather obvious A0 V Vega archetype spectrum to our Deneb spectrum (see figure 54). We immediately see vast differences in the morphology and strength of the lines -the supergiant nature of Deneb enhances the strong metal lines and its stellar wind greatly diminishes the Balmer lines [Kau+96] as can be seen in figure 55. Nevertheless, one can still recognize problems for wavelength values outside the aforementioned interval of 4700 Å $< \lambda <$ 7800 Å.

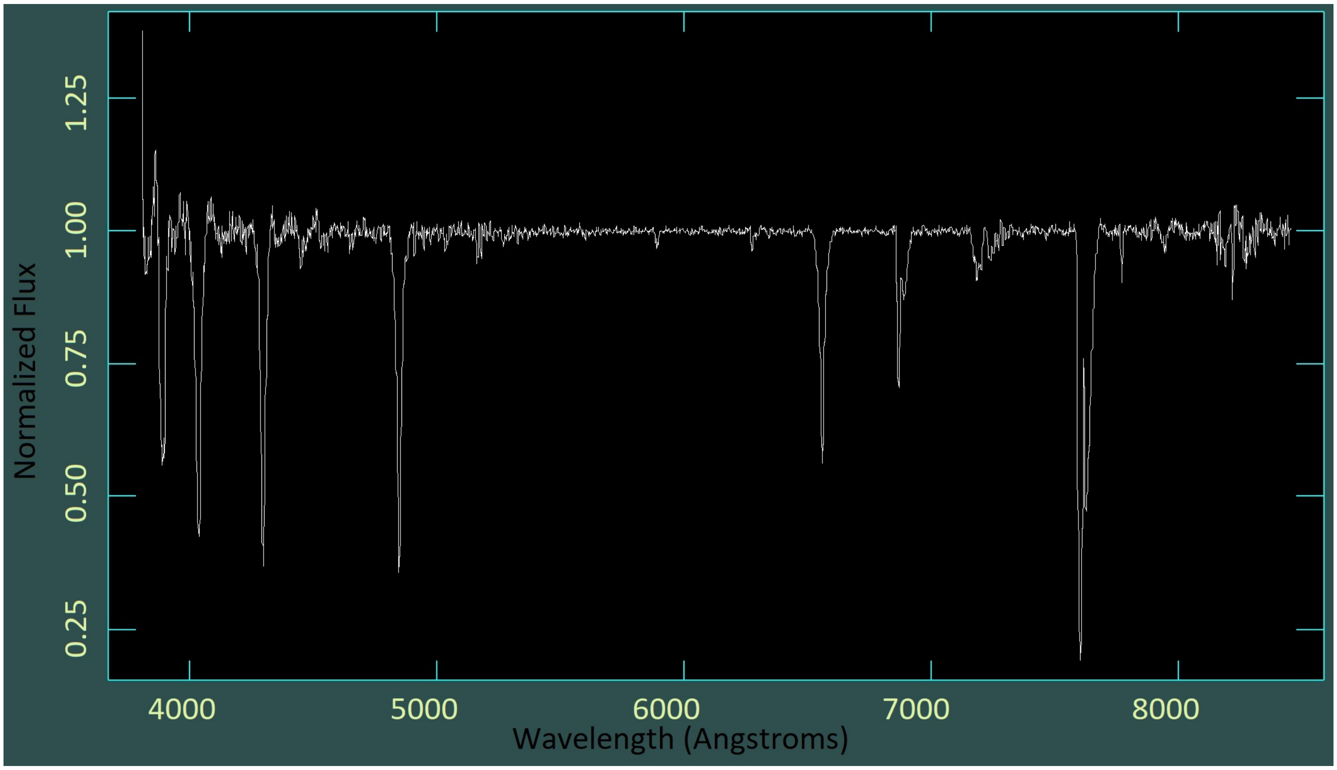

Figure 53: This figure shows the final, normalized and wavelength calibrated spectrum of Vega.

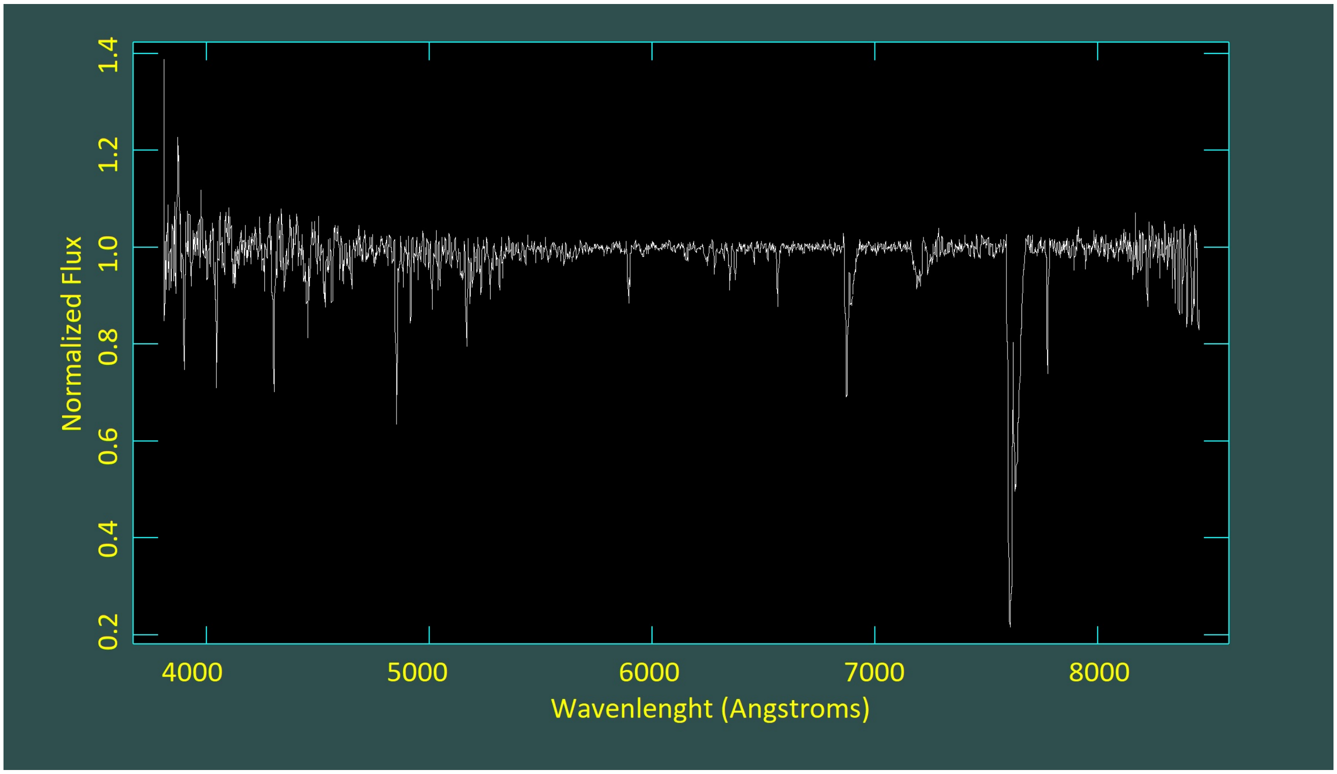

Figure 54: This figure shows the final, normalized and wavelength calibrated spectrum of Deneb. You can clearly see the difference to Vega, due to its supergiant nature.

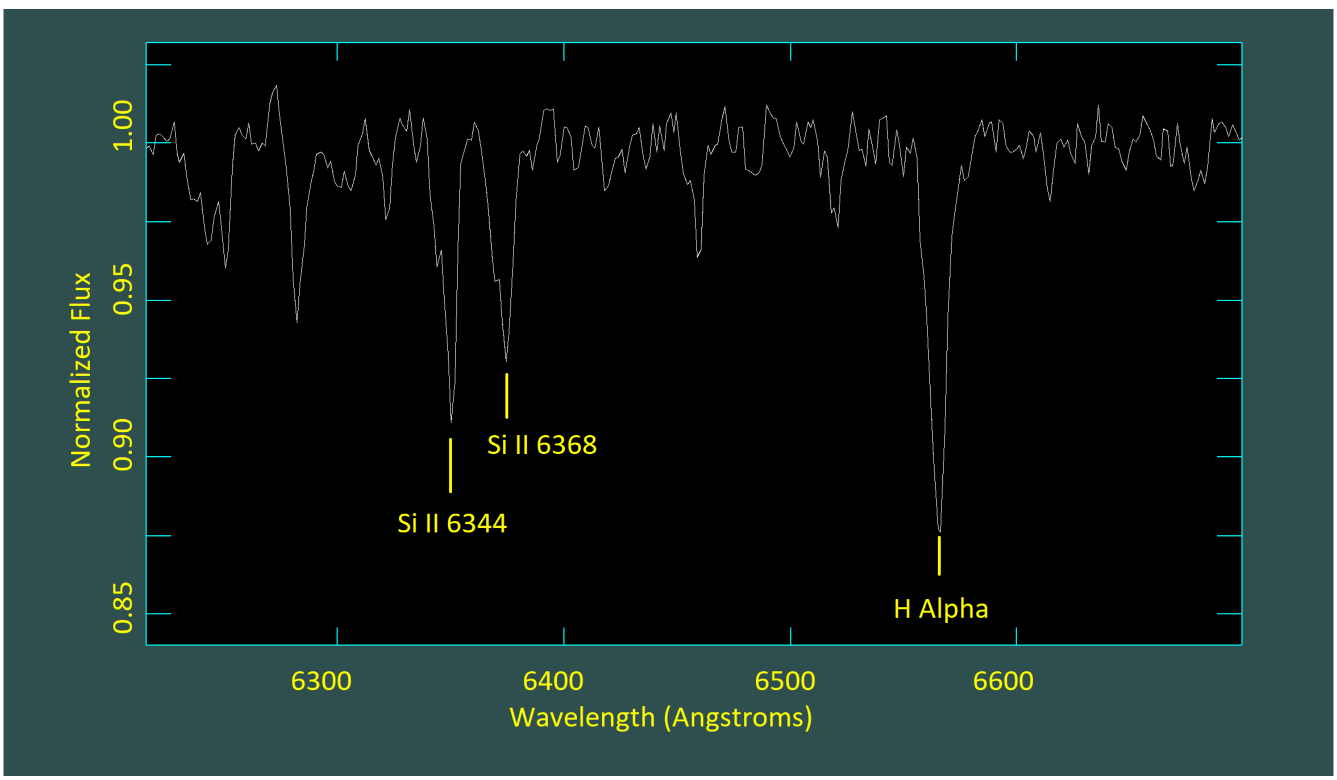

Figure 55: In this figure you can see Hα in direct comparison to two of the stronger Silicon II lines for the star Deneb -α Cygni.

6 Acknowledgements

This research has made use of the programming language Python[3].
This research made use of Astropy,[4] a community-developed core Python package for Astronomy [Ast+13; Ast+18].
This research made use of SciPy [JOP+01].
This research made use of NumPy [VCV11].
This research made use of matplotlib, a Python library for publication quality graphics [Hun07].
This research made use of ccdproc [Cra+15].
This research made use of data provided by Astrometry.net. [Lan+10]
This research made use of SExtractor [BA96].
This research has made use of "Aladin sky atlas" developed at CDS, Strasbourg Observatory, France.
This research has made use of the VizieR catalogue access tool, CDS, Strasbourg, France.
This research has made use of the SIMBAD database, operated at CDS, Strasbourg, France.
This work has made use of data from the European Space Agency (ESA) mission *Gaia* (`https://www.cosmos.esa.int/gaia`), processed by the *Gaia* Data Processing and Analysis Consortium (DPAC, `https://www.cosmos.esa.int/web/gaia/dpac/consortium`). Funding for the DPAC has been provided by national institutions, in particular the institutions participating in the *Gaia* Multilateral Agreement.
This research has made use of NASA's Astrophysics Data System.
This research has made use of the Minor Planet & Comet Ephemeris Service (IAU Minor Planet Center).
This research made use of ds9, a tool for data visualization supported by the Chandra X-ray Science Center (CXC) and the High Energy Astrophysics Science Archive Center (HEASARC) with support from the JWST Mission office at the Space Telescope Science Institute for 3D visualization[JM03].
IRAF is distributed by the National Optical Astronomy Observatory, which is operated by the Association of Universities for Research in Astronomy (AURA) under cooperative agreement with the National Science Foundation [Tod93].
The authors are grateful to Thomas Steindl, BSc. for providing the cooperative writing environment in Overleaf.

[3] `https://www.python.org`
[4] `http://www.astropy.org`

7 References

[Ast+13] Astropy Collaboration et al. "Astropy: A community Python package for astronomy". In: *Astronomy and Astrophysics* 558, A33 (Oct. 2013), A33. DOI: 10.1051/0004-6361/201322068.

[Ast+18] Astropy Collaboration et al. "The Astropy Project: Building an Open-science Project and Status of the v2.0 Core Package". In: *Astronomical Journal* 156, 123 (Sept. 2018), p. 123. DOI: 10.3847/1538-3881/aabc4f.

[BA96] E. Bertin and S. Arnouts. "SExtractor: Software for source extraction." In: *Astronomy and Astrophysics, Supplement* 117 (June 1996), pp. 393–404. DOI: 10.1051/aas:1996164.

[BF14] T. Boch and P. Fernique. "Aladin Lite: Embed your Sky in the Browser". In: *Astronomical Data Analysis Software and Systems XXIII*. Ed. by N. Manset and P. Forshay. Vol. 485. Astronomical Society of the Pacific Conference Series. May 2014, p. 277.

[Can+18] T. Cantat-Gaudin et al. "A Gaia DR2 view of the open cluster population in the Milky Way". In: *Astronomy and Astrophysics* 618, A93 (Oct. 2018), A93. DOI: 10.1051/0004-6361/201833476.

[Cer00] Unknown author of the Cerro Tololo Inter-American Observatory. *Calibration Lamp Emission Line Identifier Plots*. http://www.ctio.noao.edu/noao/content/Reference-Spectra. 2000.

[Cra+15] M. W. Craig et al. *ccdproc: CCD data reduction software*. Oct. 2015.

[Gai+16] Gaia Collaboration et al. "The Gaia mission". In: *Astronomy and Astrophysics* 595, A1 (Nov. 2016), A1. DOI: 10.1051/0004-6361/201629272.

[Gai+18] Gaia Collaboration et al. "Gaia Data Release 2. Summary of the contents and survey properties". In: *Astronomy and Astrophysics* 616, A1 (Aug. 2018), A1. DOI: 10.1051/0004-6361/201833051.

[Gar07] O. Garde. *Ne Ar Lamp Relco*. http://www.spectro-aras.com/forum/viewtopic.php?f=8&t=1673. 2007.

[Gin+18] A. Ginsburg et al. *astropy/astroquery: v0.3.7 release*. Jan. 2018. DOI: 10.5281/zenodo.1160627. URL: https://doi.org/10.5281/zenodo.1160627.

[Hun07] J. D. Hunter. "Matplotlib: A 2D graphics environment". In: *Computing In Science & Engineering* 9.3 (2007), pp. 90–95.

[JM03] W. A. Joye and E. Mandel. "New Features of SAOImage DS9". In: *Astronomical Data Analysis Software and Systems XII*. Ed. by H. E. Payne, R. I. Jedrzejewski, and R. N. Hook. Vol. 295. Astronomical Society of the Pacific Conference Series. 2003, p. 489.

[JOP+01] E. Jones, T. Oliphant, P. Peterson, et al. *SciPy: Open source scientific tools for Python*. http://www.scipy.org/. 2001.

[Kau+96] A. Kaufer et al. "Long-term spectroscopic monitoring of BA-type supergiants. II. High-velocity absorptions in βOri and HD96919." In: *Astronomy and Astrophysics* 314 (Oct. 1996), pp. 599–608.

[Kra19] E. Kraaikamp. *Autostakkert*. https://www.autostakkert.com. 2019.

[Lan+10] D. Lang et al. "Astrometry.net: Blind astrometric calibration of arbitrary astronomical images". In: *Astronomical Journal* 137 (2010), pp. 1782–2800. DOI: 10.1088/0004-6256/139/5/1782.

[Lar11] S. Larsen. *IRAF notes for Observational Astrophysics I*. http://www.astro.ru.nl/~slarsen/teaching/OA1UU/OA1_1112/notes/iraf.pdf. 2011.

[SOG04] R. Saupe, T. Otto, and T. Gessner. *Micro Mirror Spectrometer*. https://www.zfm.tu-chemnitz.de/download/pdf/annual_report_2004/81-82.pdf. 2004.

[TC06] O. Thizy and F. Cochard. *Lhires User Guide*. https://observatori.uv.es/images/stories/instrum/lhires.pdf. 2006.

[Tod93] D. Tody. "IRAF in the Nineties". In: *Astronomical Data Analysis Software and Systems II*. Ed. by R. J. Hanisch, R. J. V. Brissenden, and J. Barnes. Vol. 52. Astronomical Society of the Pacific Conference Series. Jan. 1993, p. 173.

[VCV11] S. Van Der Walt, S. C. Colbert, and G. Varoquaux. "The NumPy array: a structure for efficient numerical computation". In: *Computing in Science & Engineering* 13.2 (2011), pp. 22–30.

[Wie18] Wiener Arbeitsgemeinschaft für Astronomie. *Minor Planet Ephemeris Service Query Results*. https://www.waa.at/hotspots/kometen/46p/MinorPlanetEphemerisServiceQueryResults.htm. 2018.

A *Gaia* data on the extracted sources of the three clusters

This appendix contains the various properties determined by *Gaia* for every star we had a look at during the cluster analysis. Those properties are the Gaia Source ID, the position of the star in right ascension (RA) and declination (Dec), the proper motions in those directions, the parallax, the radial velocity (RV) and finally the Gaia magnitude (mag_g). Notice that the designation cluster member (CM) only means that those stars were still standing after the iterative sigma clipping procedure explained in point 8 of section 4.2.2.

A.1 M34

Table 2: *Gaia Source IDs* and various other properties of our identified cluster members (CMs) of M34.

Gaia Source ID	RA in °	Dec in °	pm RA in mas year^{-1}	pm Dec in mas year^{-1}	parallax in mas	RV in km s^{-1}	mag_g
337 189 979 669 777 024	40.560 156 620 192 65	42.866 452 267 306 37	0.739 395 730 654 888 2	−6.154 489 489 256 771	1.938 407 243 361 282 5	-	9.307 584
337 189 640 368 700 416	40.523 544 902 157 12	42.850 723 072 351 62	0.725 955 401 905 549 9	−5.645 853 506 012 63	2.044 822 813 443 019	−2.037 735 079 575 139	12.382 146
337 189 842 231 829 632	40.510 634 382 718 65	42.864 296 541 598 64	0.436 167 722 230 425 44	−5.896 082 347 078 511	1.924 732 216 318 750 4	-	14.904 77
337 167 370 961 929 600	40.415 415 299 733 65	42.879 196 854 009 94	0.254 418 544 335 190 5	−5.864 582 756 421 505	1.932 006 242 203 607 3	-	10.461 576
337 167 066 020 594 304	40.461 806 317 506 195	42.860 537 383 525 475	1.169 969 730 341 958 3	−5.176 383 334 479 912	1.831 602 589 699 686 4	-	11.428 344
337 167 169 099 820 416	40.402 558 307 081 33	42.838 886 463 631 43	0.484 392 496 618 440 5	−5.738 499 444 959 825	1.955 059 183 085 298 8	-	14.139 617
337 166 134 011 354 624	40.439 667 203 441 665	42.816 789 706 029 695	0.594 007 096 127 192 8	−5.564 160 297 113 032	1.995 245 287 858 631	-	12.453 591
337 165 584 255 547 008	40.394 255 385 327 05	42.764 400 180 584 495	0.887 280 349 120 208 6	−5.665 184 255 192 452	2.076 067 479 934 679 7	-	12.870 287
337 165 966 508 978 688	40.501 780 797 906 93	42.814 829 684 632 166	0.817 162 752 394 959 6	−5.927 451 998 411 301	1.960 701 912 401 062 5	−3.046 613 509 163 048 4	12.660 326
337 165 829 070 036 608	40.486 431 216 094 45	42.789 786 836 334 045	0.690 704 044 179 403 7	−5.999 321 387 172 316 6	2.131 796 813 153 491	-	8.516 829 5
337 165 932 149 250 176	40.493 507 975 699 65	42.791 819 767 992 75	0.533 884 032 404 142 5	−5.963 456 686 579 961	2.268 362 012 723 940 3	-	8.460 669 5
337 165 481 176 331 008	40.452 021 675 117 9	42.770 580 914 265 63	0.885 200 924 381 093 9	−5.814 526 473 818 964	1.901 388 366 364 632 7	-	8.993 172
337 165 652 975 852 160	40.434 071 291 331 95	42.768 749 985 996 7	0.961 058 296 742 523 6	−5.925 723 851 358 306	1.948 569 404 701 82	-	14.258 711
337 165 657 269 539 712	40.422 423 245 026 74	42.771 628 394 171 4	0.617 718 506 452 388 5	−5.891 677 037 969 887	1.829 108 616 449 149 5	-	10.450 06
337 154 215 478 462 720	40.528 637 307 557 16	42.796 246 782 316 43	0.450 667 147 967 702 7	−5.844 071 073 895 666	2.018 797 453 476 119	−6.775 649 112 057 755	12.339 784
337 154 146 758 992 000	40.524 082 950 285 155	42.781 550 988 511 505	1.089 296 048 418 367 8	−5.704 047 060 783 228	2.065 232 055 476 835	-	14.215 683
337 154 073 743 193 088	40.493 321 436 616 185	42.767 534 894 552 3	1.482 878 730 048 042	−5.150 604 393 558 284	1.989 484 607 867 795 2	−3.835 527 515 804 791 7	11.836 37
337 153 631 361 117 952	40.467 792 198 724 38	42.743 733 947 529 314	0.599 172 052 268 363	−5.438 646 992 335 187	2.044 676 312 352 882	2.899 372 171 590 462 3	12.088 861
337 165 378 097 895 424	40.459 628 725 817 4	42.743 759 082 518 31	0.804 495 755 260 186 8	−5.320 720 510 826 125	1.863 227 891 224 478 4	-	15.580 971
337 165 275 017 903 744	40.447 479 164 657 94	42.727 407 490 170 606	1.082 173 593 788 214 6	−5.579 545 573 535 113	2.033 293 259 278 873	-	13.007 686
337 153 493 924 213 888	40.446 153 708 341 69	42.715 672 192 885 17	0.494 462 924 492 538 7	−5.768 111 642 453 199	1.903 403 206 058 742 7	-	11.191 233
337 153 493 923 993 344	40.441 410 005 513 54	42.713 892 401 750 8	0.263 586 115 725 484 2	−5.197 446 720 714 103	1.884 843 879 900 080 8	−6.849 702 181 248 542	13.050 076
337 163 698 766 294 784	40.389 318 966 514 445	42.703 264 909 066 704	0.284 602 749 343 680 9	−5.799 523 609 196 647	1.944 359 728 540 265 4	-	13.758 88
337 164 038 067 322 368	40.408 917 861 140 15	42.734 536 561 887 61	0.796 225 797 306 451	−5.842 996 816 921 702	2.014 389 685 366 987 6	-	13.870 821
337 163 630 046 824 064	40.396 895 221 450 18	42.684 000 957 966 28	−0.270 615 308 461 274 13	−5.510 149 274 309 205	1.918 464 865 981 777 3	-	14.347 987
337 151 840 360 210 688	40.410 278 194 940 865	42.651 205 192 313 32	0.583 861 185 627 686 1	−5.450 557 394 393 163	1.957 125 109 598 076	-	13.409 018 5
337 151 604 138 401 024	40.450 136 456 046 486	42.651 038 470 478 65	0.634 279 834 720 241 2	−5.829 300 886 054 024	1.969 388 786 275 078 5	2.848 651 469 893 596 3	12.782 405
337 151 707 217 611 520	40.454 103 891 459 08	42.666 575 737 153 07	0.917 701 982 288 696 5	−5.523 858 239 428 492	1.936 196 997 069 861 8	-	15.540 309
337 152 153 894 211 712	40.534 124 483 064 616	42.644 990 741 794 885	1.145 834 095 134 047 5	−6.380 607 345 140 575	2.033 013 636 054 482 4	-	12.983 199
337 153 184 686 353 280	40.498 175 486 747 904	42.683 848 131 375 015	0.853 575 853 046 069 8	−6.026 107 206 494 212 5	2.094 009 363 115 346	-	13.050 89
337 153 322 125 297 408	40.524 071 294 619 475	42.707 391 500 815 94	1.289 110 111 699 257 8	−6.295 267 290 866 99	2.051 538 450 306 046 5	-	8.324 035
337 152 561 914 712 320	40.536 292 461 368 9	42.696 352 347 986 23	0.608 802 189 863 764 3	−5.967 805 810 838 485	1.995 181 198 718 711 4	-	13.258 907
337 154 112 399 259 008	40.526 694 463 145 44	42.765 751 851 238 58	0.633 977 699 439 908 7	−5.235 412 928 089 799	1.741 598 568 077 592 7	-	10.701 713
337 153 837 521 355 520	40.542 102 227 926 57	42.753 108 380 541 09	0.669 141 437 374 558 1	−6.066 205 258 380 643	1.982 635 233 108 220 4	-	11.145 508
337 153 837 521 356 928	40.554 020 978 993 17	42.747 064 699 778 01	1.684 631 068 673 182 7	−5.060 649 618 842 151	2.019 136 898 561 415 5	-	9.923 235
337 152 978 527 902 592	40.548 787 318 591 586	42.730 044 513 970 67	0.715 537 518 453 482 7	−5.804 636 930 853 455	1.947 190 923 303 089 7	-	15.277 863
337 153 081 607 118 080	40.553 981 226 215 69	42.727 507 875 170 79	0.463 148 934 602 912 73	−5.598 180 808 135 995	1.926 317 126 273 732	-	13.453 57
337 177 408 301 862 784	40.550 556 271 304 81	42.786 347 388 559 89	0.739 677 745 292 719 5	−6.611 657 320 779 389	1.871 956 690 218 415 5	-	10.018 776
337 177 373 942 124 672	40.578 840 745 610 54	42.780 191 107 621 924	0.049 007 112 846 099 38	−5.589 021 568 652 715	1.923 739 499 940 524 4	−12.153 871 992 040 925	12.394 317
337 176 446 229 194 752	40.613 605 604 569 92	42.758 043 969 556 02	0.920 672 193 155 825 9	−5.576 426 781 767 088	2.103 658 758 511 036 5	-	9.312 699
337 176 240 070 775 424	40.609 566 045 856 084	42.728 225 065 829 92	0.995 407 189 608 773 3	−5.803 889 628 510 524	1.913 570 865 989 791 9	-	14.568 987
337 176 377 509 719 424	40.644 045 877 277 755	42.747 429 789 641 906	0.677 449 411 970 651 3	−5.915 372 315 333 506 5	1.996 323 150 043 784 1	-	11.435 862
337 149 783 072 247 424	40.606 743 521 964 84	42.685 765 773 507 64	1.107 160 750 218 566 7	−5.508 277 771 568 149 5	1.749 789 172 787 868 5	-	15.169 638
337 149 748 712 509 440	40.625 818 170 029 23	42.679 467 574 687 244	0.888 885 571 314 279 1	−5.245 501 349 967 203	1.800 623 709 165 568 8	-	13.996 222 5

Continued on the next page...

... Continuation of table 2

Gaia Source ID	RA in °	Dec in °	pm RA in mas year^{-1}	pm Dec in mas year^{-1}	parallax in mas	RV in km s^{-1}	mag$_g$
337 172 975 895 643 648	40.676 876 402 720 38	42.675 372 851 844 78	1.919 991 011 118 470 8	−6.044 220 444 570 486	2.019 692 176 213 879	-	12.707 199
337 172 112 606 444 672	40.693 406 330 497 37	42.653 122 074 173 2	1.023 516 084 868 097 3	−5.559 333 581 365 037	1.929 072 865 558 062 2	-	14.776 998 5
337 172 323 060 610 944	40.699 276 740 227 55	42.680 048 554 149 714	0.404 394 752 034 781 04	−5.819 833 619 884 735	2.217 197 193 999 348	-	10.604 108
337 173 147 694 323 968	40.679 430 486 894	42.704 900 254 204 65	0.808 246 799 034 313 8	−5.333 587 676 089 643	1.986 206 460 494 971	−7.444 378 533 430 068 5	12.729 845
337 173 078 974 848 000	40.688 739 247 841 04	42.700 065 697 348 13	0.556 381 726 335 606 8	−5.666 300 029 605 214	1.853 119 177 781 451 3	-	11.320 46
337 172 288 701 093 632	40.727 596 574 583 615	42.686 297 049 844 98	−0.004 286 697 942 583 739	−5.353 667 579 584 009	1.977 282 335 945 593 5	-	13.179 166
337 173 525 651 437 568	40.714 100 054 570 5	42.724 618 918 124	0.672 530 276 393 533 7	−5.749 229 498 064 526	1.954 990 811 211 538 4	−11.160 974 407 918 337	11.738 579
337 173 113 334 580 224	40.694 735 182 813 73	42.720 492 485 585 93	0.580 996 580 935 483 6	−6.063 249 597 623 127	1.993 794 920 322 502	-	12.714 427
337 173 663 090 374 272	40.729 518 484 111 04	42.764 003 555 753 28	0.587 205 798 865 879 4	−5.402 197 828 836 687	1.732 274 418 009 529 7	-	15.489 165
337 174 006 687 749 504	40.698 907 935 548 27	42.795 236 903 470 08	1.075 773 164 214 039 6	−5.253 086 137 415 607	1.932 483 921 827 235 8	-	14.715 499
337 175 415 437 021 824	40.714 042 338 028 015	42.797 903 824 231 916	1.528 657 246 047 473 9	−6.057 273 645 688 289	2.100 927 495 906 063	−7.859 604 387 920 974 5	12.808 669
337 175 346 717 538 304	40.748 125 567 496 51	42.806 529 975 121 14	0.869 827 634 903 324 7	−5.823 097 112 888 048	1.950 803 298 357 265 8	-	15.170 338
337 178 439 093 990 656	40.690 624 543 851 64	42.820 276 285 784 21	0.713 429 448 604 907 5	−5.811 441 717 115 686	2.039 457 426 712 511 6	-	8.249 465
337 178 503 517 166 208	40.686 554 075 001 99	42.824 053 700 743 1	0.554 317 343 080 403 4	−5.903 971 156 570 471	1.962 823 343 567 971	-	10.288 737
337 177 167 783 677 056	40.634 522 678 761 414	42.818 295 293 351 32	0.854 825 657 960 350 1	−5.166 972 569 436 737	1.916 517 789 304 898	-	14.659 524
337 177 236 503 146 624	40.662 752 494 592 71	42.829 714 895 607 27	0.504 414 359 943 645 7	−5.756 880 183 210 535	1.946 246 045 003 934 3	-	11.383 089
337 178 851 410 839 040	40.689 426 691 988 51	42.868 194 751 403 92	0.600 267 248 076 736 1	−5.940 050 554 841 671 5	2.069 995 472 474 133 6	-	15.107 468
337 177 545 740 806 656	40.571 826 733 080 69	42.805 158 436 295 07	0.577 415 348 340 983 8	−5.323 366 280 125 767	2.002 398 370 825 723	-	15.437 962

End of table 2

Table 3: *Gaia Source IDs* and various other properties of the non CMs of M34.

Gaia Source ID	RA in °	Dec in °	pm RA in mas year^{-1}	pm Dec in mas year^{-1}	parallax in mas	RV in km s^{-1}	mag$_g$
337 190 014 029 514 240	40.568 643 038 763 035	42.880 030 305 931 75	1.891 615 877 530 138	−6.908 371 439 220 168 5	1.869 347 883 176 732	-	11.408 614
337 190 018 325 811 456	40.560 857 739 052 25	42.880 513 287 708 57	18.208 609 356 398 096	−8.275 058 259 113 575	1.924 172 859 655 434 4	-	10.440 701
337 177 850 682 133 760	40.558 993 854 523 78	42.856 104 239 324 63	10.365 034 554 325 19	−44.825 567 462 733 28	4.053 474 274 831 12	-	11.961 855
337 177 820 618 702 848	40.547 178 383 614 51	42.843 432 710 247 18	−0.422 456 089 709 135 84	−5.052 818 501 366 556	1.919 717 966 258 668 5	-	14.192 156
337 189 571 649 224 832	40.543 981 896 256 81	42.843 711 510 930 76	−1.632 539 359 520 071 2	−2.974 980 333 792 293 8	0.886 409 023 843 461 7	-	13.523 145
337 177 820 618 707 712	40.544 156 631 765 36	42.832 262 259 189 22	−1.231 050 228 743 901	−15.449 699 124 827 006	1.847 405 197 428 325 7	16.070 793 757 977 84	9.352 79
337 177 717 539 493 504	40.539 160 795 459 324	42.828 512 318 290 39	1.523 732 416 889 501 7	−7.594 154 656 395 988	1.964 570 308 163 394 7	−8.463 086 144 243 011	13.085 924
337 189 567 352 918 400	40.529 004 055 232 57	42.844 032 277 230 53	8.769 373 690 167 743	−1.899 041 825 809 509 6	0.672 654 314 957 49	-	15.308 662
337 189 743 447 917 696	40.501 523 690 218 22	42.850 045 059 760 14	0.816 774 099 372 208 6	−2.403 695 979 042 039 4	0.447 691 487 172 962 5	-	14.424 773
337 190 568 081 631 488	40.476 780 090 286 19	42.877 872 402 241 96	−0.535 487 629 450 575 7	0.005 719 654 123 160 532	0.126 760 650 818 209 95	-	14.729 764
337 190 568 081 630 464	40.479 186 695 930 174	42.881 462 532 899 63	−1.090 701 682 522 503 8	−4.386 283 519 693 217	1.935 412 334 949 745 8	-	14.163 465 5
337 190 563 785 327 232	40.472 178 810 119 85	42.888 216 491 561 75	0.095 455 862 506 745 43	−7.441 484 649 462 692	1.628 769 860 911 832 4	-	13.585 251
337 190 666 871 477 760	40.494 566 573 266 77	42.891 433 630 383 37	1.958 572 265 505 529 5	−1.464 760 847 813 521 2	0.425 802 919 809 792 73	-	13.687 228
337 190 632 505 871 744	40.464 837 754 960 45	42.900 082 869 726 69	3.561 453 500 418 704	−4.438 087 685 888 384	0.067 485 755 433 379 47	-	14.551 223
337 190 636 801 101 312	40.463 326 976 589 81	42.903 397 297 299 8	−0.189 363 122 739 326 7	−0.203 128 058 103 846 93	0.212 627 387 388 217 76	-	14.147 348
337 167 203 459 553 280	40.418 684 241 083 72	42.853 134 502 145 04	2.576 149 404 397 658 5	−2.616 127 130 674 132 5	0.334 272 905 103 709 55	-	15.039 844 5
337 167 031 660 864 640	40.447 579 435 468 45	42.835 827 556 767 52	0.833 052 816 173 764 3	−1.722 446 956 568 825 4	0.063 567 935 996 442	-	13.317 151
337 166 172 667 408 512	40.452 003 373 157 07	42.825 978 344 836 17	1.074 979 639 279 556 8	−6.261 624 394 431 292	1.531 771 283 472 772 1	-	15.646 473
337 166 172 667 412 096	40.452 170 752 858 15	42.818 037 843 827 1	1.170 165 577 315 153 6	−6.059 190 115 183 131 6	1.630 968 741 878 428 7	−8.447 432 611 213 78	12.651 826
337 166 207 027 147 136	40.464 521 396 057 44	42.822 807 252 642 91	0.296 724 762 066 931 55	−3.296 794 688 407 811	0.529 075 643 240 450 8	-	14.590 059
337 166 516 264 801 920	40.411 116 033 974 9	42.810 330 498 355 04	−0.224 060 760 370 734 2	−1.334 171 102 669 080 3	0.763 071 294 670 159 6	-	14.693 654
337 166 378 825 857 664	40.403 188 602 760 56	42.788 298 204 437 055	−0.536 866 651 256 801 9	−0.066 320 421 071 250 91	0.568 736 537 121 580 8	-	14.462 487
337 165 897 789 510 528	40.481 001 886 229 52	42.797 711 939 598 89	6.278 356 976 177 427	−5.592 599 911 051 21	1.117 522 555 424 917 3	-	14.988 136
337 165 893 493 188 096	40.477 827 346 042 33	42.795 610 892 521 38	−1.710 366 037 591 834 6	−7.162 481 671 487 452	1.822 668 727 318 403	-	12.191 734
337 165 897 789 512 064	40.469 282 234 114 08	42.796 633 146 247 12	−2.963 316 028 526 600 5	2.433 059 123 830 400 2	2.319 287 905 566 082	-	13.353 833
337 177 614 460 287 360	40.538 541 791 343 8	42.802 104 767 797 83	−0.874 995 670 895 036 2	1.989 286 789 922 742 7	0.198 761 200 481 063 44	-	14.428 499
337 177 614 460 290 048	40.536 198 444 217 824	42.797 591 986 670 01	25.915 446 442 631 84	−19.195 090 984 957 8	2.093 982 921 387 401 5	-	14.432 119
337 154 181 118 730 752	40.512 327 982 001 715	42.783 400 931 394 58	2.458 800 436 596 817	−5.463 641 581 255 786	0.952 977 104 930 405 2	-	11.759 975
337 154 078 039 521 536	40.505 819 394 656 7	42.767 751 812 065 87	2.262 131 317 038 218 5	1.788 140 002 331 802 1	0.499 514 849 752 806 74	-	15.133 781
337 165 416 753 189 760	40.457 201 616 094 3	42.759 223 811 612 54	−0.029 990 736 974 957 688	−4.103 438 711 171 192	0.694 715 546 935 065 8	-	15.517 716
337 165 382 393 453 056	40.463 920 999 513 206	42.749 725 728 665 23	−1.740 193 443 497 734 9	−1.510 395 575 112 597	0.807 841 354 148 356 6	-	14.307 448
337 152 012 158 896 256	40.438 215 922 360 98	42.704 548 151 816 79	1.429 098 266 773 643	−4.094 473 838 366 905	0.473 531 787 289 097 06	-	13.534 069
337 163 733 124 237 824	40.416 635 982 269 82	42.705 639 884 937 1	−0.890 240 217 737 340 6	−1.194 314 449 455 193 8	0.474 828 577 000 183 94	−48.333 433 772 105 95	10.945 272
337 163 698 766 295 808	40.403 219 855 338 51	42.698 171 558 709 22	−0.651 610 646 653 461 5	0.013 422 948 947 457 991	0.207 299 205 570 306 04	-	14.887 019

Continued on the next page...

... Continuation of table 3

Gaia Source ID	RA in °	Dec in °	pm RA in mas year^{-1}	pm Dec in mas year^{-1}	parallax in mas	RV in km s^{-1}	mag$_g$
337 163 698 766 295 936	40.392 771 287 877 49	42.699 966 355 739 73	12.854 683 313 281 015	−15.673 526 308 595 122	1.963 731 275 142 137	9.547 993 889 840 242	12.942 654
337 164 003 707 585 920	40.390 136 619 718 36	42.712 992 787 709 65	0.906 042 445 145 229 1	1.189 998 533 135 62	0.585 792 970 637 887 2	−100.598 899 264 514 05	12.010 015 5
337 164 008 003 935 744	40.397 444 795 418 714	42.717 001 458 163 864	0.838 646 868 751 051 2	−1.257 153 235 966 833 1	0.753 960 941 460 004 3	-	14.713 009
337 151 913 376 040 704	40.433 301 174 841 26	42.675 416 427 603 516	32.494 231 509 302 07	−20.654 881 941 575 326	2.612 487 926 570 7	-	15.098 282
337 151 810 296 828 288	40.433 845 996 571 64	42.665 290 819 055 43	−3.623 693 380 076 282	−6.805 293 720 857 303	0.476 480 731 572 948 85	-	13.556 066 5
337 151 638 498 142 464	40.460 302 164 028 725	42.641 733 862 081 04	0.808 289 097 512 615 6	0.243 922 773 120 426 12	0.126 346 827 838 352 88	−22.701 868 442 658 192	12.104 058
337 151 702 921 857 536	40.453 485 771 331 835	42.659 245 372 909 815	−1.175 311 200 495 449 8	−8.867 513 428 279 274	0.923 902 622 309 876 6	-	15.483 531
337 152 119 534 475 136	40.525 733 148 969 59	42.640 822 075 504 246	−0.131 262 606 854 892 4	−0.264 748 004 933 989 87	0.922 737 547 658 384 1	-	14.177 278
337 152 394 412 380 032	40.495 180 395 813 39	42.654 841 990 495 36	0.079 941 084 144 523 61	−7.788 359 179 023 116	2.111 049 133 111 59	-	11.411 084
337 153 150 326 620 928	40.491 046 997 776 78	42.667 320 542 596 61	9.812 237 064 764 222	−10.951 549 409 429 34	0.728 535 618 031 561 5	-	14.748 391
337 153 146 030 266 752	40.476 811 207 198 566	42.673 272 628 204 764	−3.386 473 587 305 866 7	−0.283 852 166 851 661 37	0.651 916 097 493 621 4	−40.062 969 783 452 46	10.858 964
337 153 219 046 094 464	40.467 566 537 379 52	42.680 160 353 085 53	−2.713 850 842 356 629 7	1.272 940 905 770 661	0.267 652 001 728 534 7	-	14.315 986
337 151 943 439 422 208	40.449 528 229 119 24	42.688 456 975 272 366	−6.590 576 470 770 74	−5.361 986 030 186 525	3.168 466 053 596 28	−5.263 572 128 685 727	12.064 829
337 152 424 475 762 432	40.511 477 086 752 18	42.664 805 723 813 54	0.962 781 409 751 907 8	0.805 616 302 373 44	0.158 349 237 508 558	-	13.721 717
337 152 531 851 323 776	40.522 281 314 194 27	42.681 973 845 486 915	1.819 555 047 342 798 8	−4.524 408 484 790 626 5	0.764 486 642 724 767 6	-	13.972 701
337 152 566 211 055 104	40.527 492 081 958 606	42.703 221 765 299 18	10.010 780 297 977 643	−3.750 526 803 718 105 7	1.614 343 178 877 620 4	−25.149 324 251 484 515	12.334 158
337 152 566 211 055 744	40.528 487 718 041 58	42.699 512 901 926 91	−1.161 505 004 919 060 7	−8.252 336 386 990 86	0.041 214 738 495 882 405	-	14.035 502
337 152 944 168 176 640	40.539 092 355 916 28	42.701 509 160 223 01	−0.275 436 457 161 870 8	−6.332 968 106 686 197	1.140 411 547 240 025 4	-	13.307 088
337 153 425 204 519 040	40.466 765 079 776 91	42.701 854 608 469 525	−2.349 446 784 813 878 7	−2.267 765 375 664 665 4	0.516 459 459 270 782 7	-	15.027 414
337 153 356 485 035 904	40.487 316 668 040 19	42.714 760 877 154 234	−2.668 180 058 125 345	−4.175 250 784 704 525 5	0.635 223 578 942 060 5	-	15.194 497
337 153 459 564 251 520	40.469 414 250 019 91	42.717 606 371 750 485	−0.009 317 636 245 252 447	−1.345 612 247 252 567 1	0.565 445 428 199 070 3	-	13.307 842
337 153 974 960 313 344	40.507 381 459 809 935	42.748 309 209 489 11	1.097 759 314 475 132 5	−5.399 768 738 190 967	0.018 877 809 751 093 988	-	9.705 938
337 152 978 527 905 664	40.552 753 980 818 97	42.722 010 611 795 085	5.025 511 725 953 956	−3.430 596 679 565 698	1.575 262 037 271 805 4	-	14.532 167
337 177 404 005 543 552	40.556 082 557 507	42.777 929 528 053 27	−0.634 922 891 350 227 6	−6.896 554 613 147 542	1.994 047 388 748 816 6	-	8.802 774
337 176 618 028 304 128	40.587 047 316 362 664	42.778 452 695 933 254	3.281 087 445 114 992 3	5.378 396 789 809 352 5	0.660 486 735 775 035 1	-	15.343 011
337 176 583 668 152 448	40.578 076 473 018 626	42.752 602 096 825 59	−14.469 173 288 568 886	−4.723 337 709 320 459	1.141 018 154 453 999 2	-	14.2539
337 153 115 966 851 328	40.570 885 771 760 76	42.743 305 394 717 14	0.344 792 627 232 105 9	0.165 287 339 581 147 72	0.128 465 887 876 608 84	-	15.104 812
337 176 652 387 618 432	40.613 929 552 910 45	42.773 621 947 475 014	3.807 536 533 903 570 5	−2.512 789 371 814 035 3	0.421 446 900 383 708 25	-	15.020 187
337 176 648 091 300 736	40.615 602 772 524 08	42.771 128 518 409 01	1.779 300 621 933 569 9	−3.196 644 204 431 346 6	2.211 238 738 644 222 5	−5.861 064 583 705 145	12.233 851
337 152 841 089 175 168	40.586 892 664 547 47	42.727 285 153 121 8	4.364 011 896 976 907	−5.657 522 322 395 081 5	1.723 309 579 079 134 4	-	14.963 131
337 153 012 887 641 600	40.575 741 000 432 92	42.722 590 947 223 246	3.648 730 402 590 688 4	−0.082 751 876 061 038 51	0.511 556 339 008 783 1	-	15.586 887
337 152 806 729 441 664	40.583 453 419 695 27	42.710 209 343 877 03	3.208 513 155 443 68	3.775 240 303 742 949	0.434 625 192 161 139 65	-	15.386 777
337 176 377 509 721 088	40.627 863 443 521 235	42.745 391 981 772 87	−2.257 237 795 683 673 6	−0.655 039 213 477 913 9	1.030 531 029 018 729 5	-	13.696 852
337 173 422 572 224 768	40.649 321 339 126 79	42.731 894 895 777	6.126 565 050 330 507	−4.099 837 917 100 839	0.734 589 199 057 291 7	-	14.523 602
337 173 353 852 753 280	40.657 819 135 167 3	42.713 644 680 754 17	1.402 062 479 172 231 8	−5.658 434 006 759 149	1.626 248 307 799 207 8	7.274 973 739 410 365	12.238 515
337 173 216 413 805 312	40.639 043 891 768 15	42.700 306 375 626 1	7.730 319 628 874 697	−3.419 323 562 968 564 5	1.218 767 578 990 771 3	-	12.699 638
337 149 817 431 979 264	40.623 721 008 861 49	42.699 076 810 268 735	8.077 069 075 937 382	−0.847 009 246 633 132 7	0.453 145 715 891 723 9	-	14.533 483 5
337 149 817 431 981 568	40.624 472 952 939 605	42.692 658 168 537 94	−1.532 096 482 541 773 8	−5.312 416 618 103 242	0.497 657 853 027 273 8	-	14.6883
337 173 005 959 042 432	40.650 435 649 989 53	42.682 899 774 428 28	−5.326 512 617 787 249	−10.394 966 165 192 5	3.287 244 169 819 352 6	-	13.408 147
337 172 941 535 906 432	40.663 951 291 452 25	42.675 806 796 420 68	10.153 068 631 085 798	−3.844 076 306 471 521	1.041 016 449 894 113 5	-	15.474 223
337 172 219 981 401 856	40.678 669 647 334 175	42.670 565 011 231 42	11.480 714 087 513 544	−2.322 532 006 166 505 3	0.992 642 720 155 599 7	-	14.426 065
337 172 219 981 402 496	40.686 059 942 243 22	42.666 263 314 533 76	13.190 673 669 025 632	−1.489 452 496 063 169 2	0.615 334 484 826 334 8	-	15.378 628
337 171 945 103 720 832	40.709 320 909 430 92	42.649 550 899 260 72	2.157 212 561 233 839 8	−5.573 445 380 936 603	0.961 306 788 308 075 8	-	15.403 963
337 171 910 743 987 968	40.699 241 473 330 82	42.629 222 528 086 84	−4.687 139 942 815 532 5	−4.452 799 007 957 906	0.454 024 500 593 631 64	-	14.044 898
337 171 876 382 612 992	40.725 024 007 102 81	42.627 202 703 654 454	−0.595 557 657 902 063 6	−5.303 340 370 991 808	3.485 020 299 624 389 8	-	14.453 591
337 124 936 685 069 824	40.739 089 021 713 04	42.628 089 379 488 56	2.251 121 378 693 128	−6.643 932 968 123 716	0.988 094 011 523 038 3	-	13.003 897
337 149 302 035 925 248	40.623 865 194 748 426	42.632 497 643 553 364	−3.034 837 267 215 700 2	1.007 753 079 109 067 4	0.538 510 420 769 228 4	-	14.922 718
337 172 975 895 640 064	40.682 827 540 386 52	42.683 489 178 348 18	−0.940 725 211 059 784 6	−5.327 662 481 002 997	0.474 559 090 777 159 63	-	15.120 518
337 173 078 974 851 584	40.687 893 909 058	42.690 130 858 649 1	−4.149 081 178 025 11	−1.148 714 445 507 816	0.899 428 468 271 649 5	-	15.087 069
337 173 078 974 849 664	40.679 000 897 751 244	42.697 010 358 942 69	−0.067 604 379 988 257 97	−3.222 765 804 734 665 5	0.293 685 595 562 314 7	-	14.939 399
337 172 662 361 656 320	40.732 545 944 459 915	42.703 485 851 332 67	0.696 525 880 249 608 4	−5.703 902 604 627 259	2.726 379 780 433 308 3	-	13.188 314
337 173 525 651 433 344	40.724 296 664 007 845	42.735 040 493 675 214	−0.038 149 530 702 731 75	0.893 812 974 806 265 2	0.669 845 932 113 559 6	-	14.865 163
337 173 525 651 432 832	40.710 238 077 992 72	42.739 335 700 756 72	3.617 639 258 606 113	1.442 554 853 789 114 4	0.563 782 313 126 090 8	-	15.342 305
337 173 800 529 335 680	40.688 509 913 077 18	42.753 677 898 166 636	−3.055 194 086 597 596	1.119 999 244 397 628 5	0.276 442 159 264 903 45	-	14.808 578
337 173 697 450 114 176	40.715 334 858 811 55	42.763 426 270 338 215	1.205 349 322 718 641 6	−4.255 771 662 771 290 5	0.545 094 759 881 290 4	-	14.654 981
337 172 907 176 365 824	40.744 186 383 479 33	42.754 246 123 133 186	0.355 110 027 116 853 47	−5.510 998 028 834 294	1.146 488 832 669 106	-	13.339 802
337 176 824 184 478 080	40.667 593 943 190 7	42.772 859 372 728 04	2.980 207 825 593 849	−2.356 409 639 388 3	2.605 643 099 204 77	-	16.321 571
337 176 789 826 567 424	40.658 976 854 164 42	42.774 935 056 241 326	−1.450 098 837 063 278	−4.349 405 564 171 699	0.322 838 757 900 687 5	-	13.389 842
337 176 785 531 080 576	40.648 879 584 267 675	42.773 784 736 463 234	−2.456 515 241 297 611	−5.199 039 275 262 662	0.794 327 719 745 658 3	-	15.278 083

Continued on the next page...

... Continuation of table 3

Gaia Source ID	RA in °	Dec in °	pm RA in mas year^{-1}	pm Dec in mas year^{-1}	parallax in mas	RV in km s^{-1}	mag$_g$
337 176 892 905 777 536	40.654 629 219 705 505	42.789 141 921 384 456	3.023 794 165 388 12	−2.827 126 819 229 911	0.538 941 008 008 598 7	-	15.356 74
337 176 824 186 301 440	40.669 323 476 909 04	42.783 751 977 441	9.844 649 957 673 896	−3.028 601 285 794 936 7	1.007 291 929 194 731	-	13.021 440 5
337 173 903 608 540 800	40.701 423 751 554 096	42.775 807 842 155 18	−4.382 155 032 721 712	−1.156 753 776 593 925 8	1.069 954 818 914 993	-	15.305 799 5
337 174 006 687 747 968	40.700 831 184 634 694	42.802 428 072 043 14	4.548 895 808 315 484	−1.805 333 407 002 320 4	0.928 354 509 169 190 3	-	14.878 363
337 175 552 875 965 824	40.734 154 353 981 6	42.818 896 580 990 08	3.334 752 435 956 733 3	−4.060 684 031 554 751	1.320 121 808 098 419 2	-	10.910 192 5
337 176 995 984 984 960	40.666 415 583 379 94	42.812 310 323 193 34	0.727 596 907 133 575 6	−2.226 797 272 626 575	0.117 256 829 872 240 73	-	15.367 575
337 178 537 876 901 888	40.686 967 553 714 42	42.845 444 289 752 02	−10.448 965 166 813 554	−4.231 609 227 071 345	1.764 682 635 723 64	0.792 233 998 566 295 8	12.443 459
337 175 552 875 962 368	40.742 252 666 058 6	42.829 455 296 527 605	−1.039 167 893 017 890 3	−4.046 642 394 929 059	0.137 211 125 144 264 87	-	15.333 184
337 175 651 659 849 856	40.739 145 236 840 386	42.843 098 848 961 48	3.004 953 495 721 158 3	0.443 521 750 849 152 13	0.313 495 315 701 694 4	-	15.447 381
337 176 033 912 291 456	40.743 155 292 623 43	42.861 408 830 714 05	5.197 904 996 260 194	−2.696 711 868 947 409 7	1.116 951 831 802 067 7	-	15.766 297
337 176 063 976 748 160	40.764 762 842 947 86	42.865 163 566 043 81	−6.767 446 599 861 426	0.288 154 246 180 505 95	0.547 914 204 768 574 3	-	15.573 445
337 176 068 272 026 368	40.751 749 895 273 306	42.873 539 544 852 62	−0.987 402 744 520 114 2	1.535 121 907 140 295 5	0.302 006 173 223 612 84	-	13.558 908
337 176 171 351 238 656	40.762 327 795 918 75	42.882 691 063 387 846	8.522 841 479 776 073	−8.962 709 293 234 742	0.666 910 062 654 688 9	-	14.693 163
337 178 679 612 144 128	40.718 039 807 657 526	42.876 993 842 322 335	5.111 323 567 521 993 5	−1.909 427 381 097 748 7	0.609 098 147 140 837 7	-	15.165 317
337 178 640 957 119 744	40.712 162 837 051 19	42.861 873 259 803 72	−1.376 260 729 589 378	−4.893 774 657 407 928	0.477 485 336 085 717 8	-	15.589 704
337 178 847 115 567 360	40.692 888 524 856 7	42.873 246 600 959 5	0.904 907 526 859 771 8	−3.012 505 698 910 894 5	0.715 637 825 105 309 7	-	15.734 483
337 178 920 130 314 112	40.681 011 657 224 24	42.875 020 707 166 86	1.014 561 238 601 884 5	−5.394 835 041 040 148	1.607 698 676 510 360 2	-	15.303 944
337 179 538 605 845 248	40.644 563 144 366 94	42.865 726 612 870 68	5.826 669 231 474 886	2.940 124 308 852 497	1.694 037 459 881 151	-	15.791 277
337 179 607 325 083 520	40.633 515 138 258 15	42.878 708 058 594 434	12.832 123 158 237 71	−11.575 253 839 673 069	1.828 424 824 611 640 6	-	15.630 863
337 178 026 777 124 736	40.627 475 196 213 56	42.854 532 282 075 176	−2.168 047 737 749 24	−13.361 983 941 618 607	2.065 014 405 017 068 5	-	14.419 366
337 178 091 200 302 592	40.609 768 846 393 2	42.854 877 133 036 22	−1.903 839 305 804 981 4	−1.264 092 462 714 629 5	0.897 988 280 807 620 9	-	13.869 157
337 178 022 481 798 912	40.631 982 307 514 185	42.845 423 748 124 944	1.783 817 248 103 865 7	−4.225 430 926 554 358	0.492 932 597 048 052 53	-	14.751 718
337 177 923 697 917 696	40.613 676 729 929 82	42.830 357 034 025 695	−1.133 006 577 468 503 6	−6.359 869 383 232 998	2.155 204 697 261 435	−11.434 148 695 445 685	12.773 405
337 177 889 338 184 576	40.607 328 002 064 58	42.818 256 460 966 19	5.098 253 506 406 833 5	−0.113 662 250 096 207 73	0.583 958 641 735 465 9	-	15.114 154
337 177 889 338 182 400	40.602 190 847 081 98	42.826 033 956 696 506	47.577 604 294 580 01	−12.968 748 736 758 583	7.943 163 916 194 72	75.141 769 308 162 13	11.668 056 5
337 177 958 057 657 344	40.594 939 127 922 11	42.830 729 365 369 71	11.542 549 957 120 602	−1.167 048 763 979 790 4	0.668 958 831 766 832 8	-	14.655 812
337 178 159 920 736 128	40.581 660 675 216 945	42.837 756 489 315 07	−15.458 603 907 470 483	4.528 702 861 070 498 5	1.281 364 849 947 915	-	15.496 715
337 177 541 445 409 664	40.573 576 474 888 56	42.817 706 058 010 86	−21.930 049 551 230 535	8.185 023 363 608 38	3.184 671 524 178 139	-	15.023 482
337 177 545 740 805 504	40.564 244 625 829 026	42.809 197 907 969 484	0.933 807 709 733 924 5	−0.084 914 763 516 453 34	0.067 026 248 788 582 82	-	14.853 158
337 177 472 725 904 512	40.581 342 035 198 425	42.802 606 402 680 54	−1.276 656 706 567 116	−4.635 393 936 772 511	4.620 959 643 164 303	-	15.613 037

End of table 3

Table 4: *Gaia Source IDs* and various other properties of the stars in M34, which were not analysed.

Gaia Source ID	RA in °	Dec in °	pm RA in mas year^{-1}	pm Dec in mas year^{-1}	parallax in mas	RV in km s^{-1}	mag$_g$
337 166 000 868 718 592	40.491 157 024 236 2	42.813 424 936 491 565	0.688 270 414 893 407 3	−5.518 749 761 209 667	1.990 994 230 872 524 1	−7.632 652 103 149 402	12.611 690 5
337 153 695 786 800 256	40.529 807 194 328 235	42.721 976 408 258 23	-	-	-	-	15.358 773
337 172 254 341 137 280	40.704 593 798 855 356	42.670 659 374 550 02	0.944 046 358 927 410 4	−5.595 341 301 100 831	1.851 937 665 871 220 6	-	15.504 933
337 176 549 308 410 752	40.592 284 147 967 36	42.760 133 704 042 34	1.785 834 139 558 16	−5.367 981 222 900 212	2.051 609 833 659 635 6	-	8.872 074
337 173 147 694 322 944	40.680 493 117 471 74	42.709 361 578 612 86	-	-	-	-	14.382 927
337 172 460 499 782 912	40.741 153 682 158 22	42.696 268 356 439 65	-	-	-	-	15.616 076
337 152 875 448 699 392	40.554 729 654 052 366	42.699 192 337 924 345	1.620 398 868 360 720 2	−6.763 332 025 267 104	2.177 706 364 268 440 4	-	8.394 316
337 153 253 405 824 384	40.485 363 466 640 166	42.705 209 042 358 14	−1.714 541 151 958 267 4	0.290 984 368 924 165 46	−0.128 109 771 210 527 36	-	16.068 165
337 153 597 003 194 624	40.490 335 610 331 82	42.737 899 414 648 49	2.468 564 781 240 94	1.279 481 667 000 684 3	1.127 993 996 817 530 5	−32.195 545 665 155 66	12.776 587 5
337 165 794 710 535 040	40.465 774 628 229 09	42.772 235 291 723 4	−0.509 662 747 897 215 3	−9.037 531 477 765 214	−0.478 559 385 994 397 9	-	14.180 278

End of table 4

A.2 Teutsch 55

Table 5: *Gaia Source IDs* and various other properties of our identified cluster members (CMs) of Teutsch 55.

Gaia Source ID	RA in °	Dec in °	pm RA in mas year^{-1}	pm Dec in mas year^{-1}	parallax in mas	RV in km s^{-1}	mag$_g$
513 620 643 419 170 048	37.113 536 059 243	62.211 291 656 056 15	3.548 173 790 218 282	−2.919 730 110 428 931 7	0.560 448 234 080 396 9	-	14.677 266
513 620 471 620 472 576	37.148 588 284 777 354	62.216 677 934 876 486	3.413 909 530 743 849	1.205 364 151 366 741 7	0.563 848 237 051 379 4	−41.184 037 856 886 52	12.918 45
513 620 402 900 999 680	37.179 351 957 376 994	62.207 121 987 553 58	1.135 449 820 880 218 8	0.459 731 735 259 108 65	0.247 242 660 732 283 5	-	14.972 388
513 620 505 980 209 280	37.194 366 158 982 46	62.216 931 879 436 6	1.381 771 538 910 987 5	−0.702 913 359 301 840 6	1.378 145 563 809 635 8	-	14.334 359
513 620 162 382 821 376	37.243 605 909 504 13	62.223 296 347 555 93	−0.981 732 053 879 037 1	−0.241 550 574 540 253 64	0.385 198 737 339 788 65	-	14.983 799
513 620 093 663 346 560	37.255 566 555 407 53	62.216 821 319 117 96	1.025 612 525 657 923 6	−0.668 985 792 124 676 3	0.197 087 506 840 994 52	−40.199 721 739 495 004	13.725 58
513 619 750 065 972 608	37.218 946 479 562 72	62.200 111 817 672 08	−0.152 515 780 917 928 86	−0.201 669 165 984 136 26	0.452 772 935 269 613 15	-	13.737 646
513 619 646 986 761 600	37.190 013 129 533 014	62.194 641 883 602 88	1.295 394 506 341 459	0.236 706 176 487 989	1.429 967 639 487 094 8	-	14.999 822
513 619 612 627 027 200	37.179 731 259 495 13	62.186 012 651 648 944	−2.907 901 410 342 505	1.307 661 056 087 667 4	0.790 115 400 492 001 9	-	15.717 331
513 618 100 798 551 680	37.139 062 693 284 45	62.159 875 341 802 12	3.295 393 406 304 653 7	−1.426 587 634 000 171	1.274 792 040 110 764 9	-	13.003 155
513 618 822 353 389 184	37.096 228 875 186 11	62.157 202 076 602 18	−0.381 266 178 736 410 67	0.168 411 919 773 708 29	0.401 747 596 079 856 8	-	13.754 608
513 618 719 273 849 216	37.101 689 405 633 48	62.146 228 567 677 75	−2.276 040 264 442 366	−0.866 855 235 955 869 1	0.842 105 296 734 532 4	-	15.382 743
513 619 372 108 862 720	37.259 087 046 468 14	62.167 852 507 906 666	−1.567 135 728 010 213 8	0.984 222 472 038 828 7	0.476 562 651 651 685 4	-	13.799 037
513 619 887 504 920 576	37.300 329 613 829 98	62.200 461 639 994 02	−0.274 828 264 954 479 65	−1.587 565 887 009 551 7	0.933 871 276 088 717	-	14.622 742
513 619 814 486 284 416	37.318 511 013 390 85	62.196 330 549 444 2	−1.087 927 321 327 253	−0.671 040 121 234 659 2	0.231 991 593 614 360 34	−15.471 294 252 799 433	11.842 687
513 616 898 207 875 200	37.334 944 894 841 83	62.194 044 218 094 81	0.112 962 125 105 986 85	0.370 630 108 136 081 7	0.459 219 539 455 903 8	-	13.573 714
513 616 898 207 683 584	37.363 622 118 704 335	62.191 799 678 339 42	0.172 822 187 793 275 68	0.355 766 491 134 707 26	0.446 494 235 356 334 6	-	12.931 595
513 616 829 488 210 688	37.363 451 964 641 27	62.185 076 916 397 826	−2.099 991 903 306 712 7	−0.390 183 433 982 211 5	0.312 725 875 109 749 03	−82.536 002 156 342 18	13.658 681
513 616 898 207 688 576	37.349 525 429 795 91	62.184 689 452 947 69	−2.549 006 915 976 381	2.260 224 901 005 824 6	0.397 630 432 647 347 1	-	15.313 266
513 616 932 567 425 024	37.388 657 786 465 91	62.184 305 975 877 05	−2.203 972 342 932 563 5	4.381 008 215 008 512	0.642 084 093 168 559	-	14.753 162
513 616 726 408 994 944	37.402 083 905 428 77	62.182 538 971 917 99	3.157 058 203 013 271 2	−1.973 332 335 699 820 5	1.160 187 759 892 005 8	-	12.894 406
513 616 966 927 154 560	37.413 825 320 580 166	62.203 029 057 754 335	2.904 806 981 952 326	−0.067 808 227 237 981 84	1.633 807 934 053 826 5	-	13.779 806
513 992 278 352 841 600	37.417 145 984 919 17	62.219 473 853 553 5	2.300 363 052 746 053	−0.193 037 030 534 349 62	0.551 083 007 109 126	-	14.210 414
513 616 928 269 018 368	37.382 490 418 720 906	62.199 294 048 368 47	−1.792 491 082 283 854 7	−1.389 201 701 131 198 1	0.318 049 474 832 447 44	-	15.045 88
513 992 140 913 887 360	37.483 118 679 284 57	62.214 553 022 450 69	−2.087 568 849 106 312	−0.994 108 532 554 317 4	0.199 854 569 096 885	-	14.938 597
513 992 037 834 676 096	37.479 825 562 127 004	62.194 601 679 286 436	0.487 664 001 131 671 63	0.553 441 987 563 540 2	0.387 473 512 963 325 2	-	15.136 193
513 991 419 359 381 376	37.530 680 474 790 03	62.210 283 618 676 33	−0.694 292 113 758 247 6	0.007 863 089 793 305 963	0.470 289 916 152 691 45	-	15.356 837
513 991 762 957 004 416	37.583 676 877 569 66	62.216 019 379 124 44	1.002 182 114 369 861 3	−4.590 222 976 717 125	0.987 252 025 227 617 1	-	13.115 083
513 991 556 798 575 616	37.603 819 358 994 45	62.208 939 925 565 32	−0.486 448 927 875 351 43	2.486 378 193 451 83	0.585 342 952 929 367 9	-	14.421 945
513 991 522 438 846 080	37.596 462 467 877 78	62.198 186 176 387 41	−1.008 954 017 351 389	−0.822 594 562 518 891 7	0.711 815 448 048 823 7	-	12.625 072
513 991 041 402 525 952	37.575 108 902 589 21	62.172 538 584 730 4	−0.997 693 125 779 938 2	−0.916 747 305 431 536 8	0.332 121 516 084 534	-	15.505 297
513 991 007 042 793 856	37.550 364 731 626 146	62.163 484 139 243 77	−1.171 048 981 053 791 6	0.549 451 692 654 599 3	0.294 596 492 567 620 94	-	14.542 803
513 979 320 431 655 168	37.599 031 607 157 62	62.167 495 016 915 37	−0.140 443 513 969 699 45	1.611 678 649 211 424	0.213 007 546 973 086 66	−30.693 728 161 365 456	12.594 542 5
513 979 324 731 745 408	37.603 281 553 065 464	62.164 011 403 433 385	−3.841 030 079 583 298	2.284 172 769 330 611	0.805 990 387 871 085 2	-	15.157 68
513 979 702 688 856 704	37.638 442 545 049 34	62.178 465 557 592 446	5.084 882 340 163 663	−4.691 169 367 625 989	1.491 209 549 027 331 8	-	13.948 023
513 979 324 731 738 624	37.613 757 780 351 44	62.172 833 687 266 95	−0.496 962 024 538 518 6	−1.532 189 497 438 277	0.702 882 582 864 507 1	-	14.755 655
513 991 213 200 956 800	37.531 475 423 983 83	62.177 775 944 693 55	0.642 201 298 673 070 7	0.438 959 163 661 190 7	0.214 908 994 419 057 5	-	14.893 354
513 991 208 901 147 648	37.517 212 248 068 51	62.173 961 616 690 03	−0.016 720 899 728 731 28	−0.425 368 424 241 942 43	0.216 749 290 030 132 55	-	15.507 906
513 991 178 841 219 200	37.501 766 670 582 38	62.170 326 496 624 18	0.267 392 753 807 201 8	−1.211 158 491 742 586 2	0.179 258 792 496 965 86	-	15.078 706
513 615 867 415 543 552	37.484 815 586 431 65	62.158 792 286 850 534	−1.456 967 178 133 610 2	−0.127 388 673 387 761 16	0.528 373 344 223 743	-	14.757 354
513 615 867 415 546 624	37.491 368 180 958 38	62.149 207 715 441 996	−1.765 424 444 641 090 5	−0.087 556 292 836 326 4	0.254 235 203 698 704 9	-	14.360 904
513 615 833 055 812 864	37.482 178 617 524 48	62.139 260 940 421 76	−1.130 765 972 406 667 9	0.350 297 497 117 476 1	0.430 890 973 663 840 44	-	14.007 084
513 615 622 598 206 336	37.487 107 328 966 66	62.138 866 224 788 13	2.046 387 117 017 762 8	−5.243 442 379 655 662	0.651 544 856 267 101 5	−28.599 057 585 506 64	12.616 636
513 615 558 173 884 544	37.514 874 031 777 91	62.127 516 363 096 95	−1.021 514 097 343 409	−0.244 539 166 365 321 58	0.455 499 204 656 317 27	-	10.772 052
513 979 187 292 805 760	37.577 373 103 318 514	62.143 882 506 865 395	0.658 297 921 942 324 1	0.421 957 678 747 727 7	0.283 181 593 006 797 5	-	14.850 387
513 603 841 507 296 768	37.549 753 711 390 8	62.126 332 347 191 266	−2.361 612 065 334 143 5	−3.670 125 168 426 938 7	0.839 519 970 670 945 6	-	14.832 096
513 979 152 933 080 192	37.573 708 411 093 31	62.122 180 541 724 1	3.590 040 820 845 916	−2.840 580 500 028 687	0.886 648 050 759 599 6	-	13.640 244
513 979 084 213 598 720	37.588 140 594 654 12	62.127 598 836 744	−0.215 525 517 398 376 58	0.589 367 500 822 726 8	0.343 418 802 620 573 06	-	14.283 874
513 979 084 213 601 792	37.606 138 416 025 47	62.121 082 893 854 02	−2.486 355 056 651 257 6	0.780 808 637 511 681 8	1.285 365 596 572 330 7	-	12.457 915
513 979 015 494 118 784	37.629 909 645 345 42	62.129 941 730 296 49	−1.225 733 898 935 944 8	1.214 740 685 779 209 4	0.442 141 782 414 592 3	-	15.350 099
513 978 912 414 908 416	37.634 520 079 940 35	62.120 144 694 443 89	1.914 944 309 205 047 5	−2.888 426 544 914 209 2	0.838 019 093 622 829 8	−21.765 960 403 242 91	11.545 884
513 978 912 414 914 560	37.627 403 469 840 516	62.111 570 696 327 28	0.000 313 587 137 145 465 7	−1.661 288 894 861 327 6	0.472 120 431 874 087 86	-	14.425 41
513 979 084 213 604 992	37.586 196 419 448 59	62.117 908 957 575 37	−2.577 014 035 525 158 5	2.359 705 979 849 042	0.230 026 667 338 395 75	−36.114 985 810 582 326	13.211 61
513 603 772 787 821 056	37.581 240 711 474 01	62.112 908 528 547 8	−2.313 274 050 005 937 4	2.154 128 884 158 348	0.277 549 148 903 553 9	-	14.493 714
513 603 566 629 392 128	37.610 810 436 933 23	62.096 502 972 219 55	−1.067 294 828 665 748 2	0.008 249 855 624 353 496	0.420 647 124 074 516 15	-	14.602 252

Continued on the next page...

... Continuation of table 5

Gaia Source ID	RA in °	Dec in °	pm RA in mas year^{-1}	pm Dec in mas year^{-1}	parallax in mas	RV in km s^{-1}	mag$_g$
513 603 497 909 917 952	37.611 239 325 054 31	62.082 463 149 020 09	0.942 156 749 118 161 9	0.099 756 264 049 379 57	0.210 719 040 085 272 12	-	15.129 133
513 603 497 909 915 776	37.617 462 346 977 66	62.093 897 196 056 83	1.664 946 340 290 292 9	1.999 418 723 155 321 3	0.290 989 429 184 943 36	-	15.485 07
513 603 497 909 918 720	37.616 023 544 804 925	62.079 296 326 106 58	−2.750 078 805 029 190 7	2.335 420 342 774 25	0.328 816 730 351 886 63	-	16.158 36
513 603 356 171 236 864	37.599 944 311 237 174	62.058 176 057 317 866	−0.453 101 870 766 207 17	−0.632 966 299 849 660 6	0.555 500 578 880 939 4	-	15.521 87
513 602 604 556 727 168	37.610 417 163 192 835	62.053 473 219 888 296	−1.293 758 404 049 083 7	0.408 122 762 947 982 05	0.217 513 994 763 646 5	-	15.180 038
513 602 604 556 729 856	37.609 172 685 415 466	62.043 558 304 405 85	1.687 059 147 403 777 3	0.086 659 763 121 567 02	0.178 161 246 344 301 86	-	15.128 802
513 602 600 256 983 168	37.614 160 610 699 98	62.040 603 774 330 17	−2.732 382 815 809 592 6	2.308 357 206 712 99	0.397 111 161 798 920 1	-	13.900 522
513 602 570 196 995 840	37.590 016 599 900 785	62.033 840 700 787 46	−1.568 323 721 757 44	0.317 108 410 111 391 57	0.956 515 098 070 663 3	-	15.022 539
513 602 192 239 875 712	37.567 488 321 568 256	62.027 872 635 784 38	0.050 130 275 575 424 82	−1.569 747 700 017 993 4	0.473 633 803 850 291 97	-	14.600 714
513 602 913 794 383 360	37.548 547 603 201 26	62.024 202 304 110 2	4.069 374 786 255 989	−2.182 709 062 388 933	0.468 096 073 494 152 9	-	14.241 188
513 602 119 220 208 384	37.607 846 435 422 32	62.011 498 389 384 9	−0.778 858 915 191 787 2	−1.455 495 211 418 637 2	0.477 048 587 253 533 33	−25.257 827 707 897 363	13.167 582
513 601 745 563 300 096	37.571 439 352 243 495	61.960 016 630 509 31	−1.009 224 060 266 901 1	0.719 768 923 159 679 6	0.446 398 071 050 602 14	-	13.901 739
513 602 020 441 196 416	37.545 788 075 823 61	61.991 117 080 420 66	−2.815 509 818 212 601 3	−1.692 646 825 793 81	0.871 133 680 600 616 9	-	14.964 732
513 602 776 355 441 024	37.509 466 932 658 51	61.992 624 453 725 6	−0.211 094 919 550 931 51	−0.383 404 720 691 667 03	0.419 573 643 279 483 54	-	15.139 373
513 600 508 612 716 032	37.504 929 681 920 295	61.974 534 229 024 76	−3.966 708 573 012 838 6	2.134 007 844 870 52	0.418 644 303 775 487 06	−46.507 677 965 078 75	13.757 518
513 600 508 612 723 200	37.498 779 199 281 1	61.960 341 552 396 16	0.007 243 663 759 142 982	0.611 774 111 254 394 2	0.231 841 246 833 782 8	-	15.831 093
513 601 367 606 164 864	37.463 410 769 151 15	62.008 427 010 500 14	−2.898 279 674 990 696 3	−1.422 655 433 838 886 8	0.387 114 377 223 549 97	−62.615 574 359 278 65	12.785 621
513 601 573 764 596 096	37.454 371 839 667 33	62.005 661 699 489 47	1.024 465 415 981 462 8	−2.616 093 931 794 474	1.013 898 929 323 739 5	-	13.637 57
513 601 539 400 829 568	37.446 412 841 852 88	61.999 601 230 740 96	−2.584 829 091 460 240 3	−3.252 442 252 976 745 6	0.318 696 277 998 061 9	-	15.676 939
513 601 505 044 977 920	37.390 499 185 119 36	61.999 461 394 006 96	4.322 352 299 207 1	−0.240 962 027 334 774 87	0.597 137 688 372 300 1	-	15.359 557
513 601 466 386 006 016	37.393 190 613 403	61.993 196 917 042 52	−4.600 389 707 482 861 5	0.984 539 290 128 756 8	0.746 076 458 303 641 1	−57.925 497 667 465 756	12.153 213
513 601 058 368 394 752	37.345 953 487 587 28	61.965 379 557 355 78	0.172 376 371 758 719 45	0.258 996 391 895 374 77	0.180 234 069 432 733 65	−38.280 782 987 117 52	13.953 483
513 612 706 319 704 320	37.320 958 813 728 296	61.959 547 639 867 04	−6.329 665 598 131 617	−0.856 006 038 847 922 3	2.022 678 925 818 554 7	-	15.227 361
513 612 775 039 173 760	37.290 115 887 956 41	61.983 579 813 038 176	−1.911 793 792 303 502 7	−0.679 236 147 053 982 4	0.247 339 220 305 967 75	-	14.575 618
513 612 878 118 387 456	37.307 825 372 195 18	61.985 081 212 096 58	−2.459 286 965 852 467	−1.584 118 508 155 052	0.331 360 301 233 542 4	-	14.852 546
513 613 359 154 704 128	37.399 111 893 770 15	62.023 007 368 460 05	0.202 442 006 100 083 67	−1.616 225 408 459 427 4	0.634 552 778 462 510 3	-	12.337 074
513 613 530 953 392 896	37.336 109 146 084 006	62.037 886 908 966 506	−0.858 279 352 334 994 9	0.197 947 713 609 662 57	0.463 919 453 979 847 63	-	14.703 156
513 613 427 874 173 440	37.360 448 270 756 606	62.044 703 650 855 844	−2.118 417 105 349 963	2.260 289 803 687 509 6	0.911 330 217 244 899 3	-	14.836 292
513 613 457 934 694 272	37.392 608 382 646 63	62.046 538 373 631 5	−1.222 205 139 186 021 4	0.113 905 566 653 412 1	0.472 163 006 158 363 76	-	12.029 709
513 613 462 233 912 576	37.389 985 817 255 59	62.040 085 701 565 14	−1.014 623 705 722 096 4	−0.180 907 119 623 874 37	0.462 308 643 944 763 23	-	15.033 817
513 613 393 514 437 120	37.403 290 440 096 38	62.035 471 678 987 946	−1.081 377 628 067 923	−0.130 464 667 218 481 74	0.412 390 175 425 789 6	-	13.736 413
513 602 982 513 857 024	37.504 877 605 544 39	62.037 207 908 679 484	−0.938 454 775 330 293 1	−0.969 414 976 755 954 7	0.431 008 349 745 782 5	-	15.813 707
513 603 188 672 284 544	37.480 849 071 393 15	62.051 044 322 389 025	5.552 347 306 021 817	−1.576 872 302 291 065 8	1.206 906 552 550 484 3	-	15.058 381
513 603 257 391 604 352	37.459 178 620 737 69	62.061 286 506 376 51	−3.619 532 650 331 654	−1.881 809 211 896 032 3	1.488 872 152 014 741	-	13.548 839
513 615 145 861 079 808	37.388 540 149 881 955	62.068 496 240 873 216	3.148 712 965 225 291	−2.169 686 474 728 941	0.603 033 342 892 225 1	-	15.432 465
513 614 974 062 383 360	37.429 845 946 173 984	62.074 541 334 416 72	−0.056 633 567 293 129 516	−2.870 505 101 013 477 2	0.900 283 597 422 872 3	-	14.351 376
513 615 008 422 120 832	37.457 104 570 989 1	62.073 769 737 507 05	2.628 373 153 535 576 5	−2.597 011 997 630 9	0.348 812 580 655 471 44	-	13.732 299
513 603 704 068 348 800	37.522 398 274 030 29	62.089 561 913 206 14	2.562 455 815 498 812 4	−2.080 020 098 132 782 5	0.964 804 769 040 795 3	-	14.843 324
513 615 042 781 850 112	37.467 767 414 067 836	62.092 495 313 473 115	−1.363 468 512 111 605 7	−0.355 313 713 370 526 5	0.413 741 663 992 255 26	−58.234 780 709 031 84	13.449 687
513 615 077 141 594 880	37.439 006 652 539 53	62.083 922 687 269 634	−1.879 728 837 507 090 9	−1.944 359 963 759 930 3	1.175 736 640 010 962 1	-	16.173 405
513 615 317 659 755 776	37.430 146 858 579 896	62.099 184 271 890 98	−2.529 729 463 672 908 6	−0.154 574 839 068 608 47	0.474 846 180 597 622 57	-	14.829 65
513 615 283 300 017 536	37.421 097 760 443 99	62.099 697 461 248 04	0.914 228 126 788 902 8	−1.590 286 511 764 209 5	0.652 917 125 235 249 9	-	14.619 179
513 615 283 300 021 760	37.406 327 593 852 474	62.093 546 442 265 61	2.028 717 061 517 163	0.079 001 390 789 858 82	0.669 601 809 030 733 9	-	14.731 992
513 615 180 220 811 264	37.379 189 500 620 036	62.087 286 163 737 86	−2.499 856 350 722 880 4	0.873 973 698 636 660 6	1.012 629 770 332 027	-	13.846 761
513 615 248 940 279 936	37.375 377 830 430 374	62.104 096 146 456 04	−1.261 114 838 146 748 5	0.146 777 016 532 113 4	0.220 239 054 365 316 24	-	15.249 423
513 616 107 933 729 664	37.374 455 259 679 08	62.124 901 356 765 66	−1.338 274 553 973 382	−1.308 773 430 561 984 3	0.267 395 361 394 317 13	-	14.625 939
513 615 798 696 076 544	37.426 665 856 394 38	62.140 994 686 518 13	−0.472 315 443 578 106 23	−0.219 850 321 952 290 48	0.363 482 699 290 609 2	-	13.446 878
513 616 520 250 583 680	37.389 145 150 236 16	62.141 874 888 715 74	3.946 459 265 170 237	−1.530 379 900 530 991	1.108 642 644 515 251 3	-	14.752 252
513 616 588 970 057 344	37.383 460 621 607 36	62.148 603 159 749 165	0.433 544 070 406 980 9	0.307 119 724 968 514 86	0.345 784 106 192 186 9	-	14.583 09
513 616 520 250 578 944	37.391 021 844 115 58	62.152 323 918 843 6	−0.675 384 836 379 849 8	−0.405 729 128 244 492 7	0.394 972 076 738 611 4	-	15.006 449
513 616 588 970 054 272	37.379 396 292 341 53	62.156 531 371 773 56	−3.161 606 157 808 927 6	−1.532 679 189 336 176 9	0.720 015 300 521 725 8	-	14.997 65
513 616 623 329 788 928	37.393 034 588 545 34	62.165 284 881 882 926	−0.000 730 161 251 179 029	0.611 719 812 229 295 5	0.279 586 394 621 479 8	-	14.827 627
513 616 588 970 055 552	37.358 902 213 926 75	62.155 830 669 209 905	0.103 835 384 390 418 62	−0.815 324 489 028 774 3	0.608 036 269 252 822 3	-	14.661 725
513 616 417 171 365 632	37.332 752 831 931 47	62.153 825 266 057 154	4.560 027 343 300 623	−4.937 618 562 334 583	0.515 560 393 221 374 1	-	15.213 013
513 616 382 811 631 488	37.329 059 003 633 155	62.144 887 741 018 124	0.861 933 703 919 892 2	−1.366 145 547 796 740 6	1.096 026 312 114 202 9	-	15.042 995
513 616 451 531 105 920	37.296 762 339 307 43	62.153 773 709 113 62	−1.092 771 936 820 280 4	−1.277 266 756 543 209 9	0.403 897 362 565 390 27	-	14.172 926
513 616 485 890 839 552	37.311 723 265 061 62	62.163 062 487 629 04	−5.105 233 378 157 144	−5.070 334 728 429 227	1.799 469 270 437 379 6	-	15.098 961
513 619 440 828 334 464	37.306 357 038 794 275	62.175 366 424 877 17	0.231 587 793 153 763 7	−0.553 322 235 143 479 2	0.361 709 806 401 287 36	−43.532 490 198 800 105	10.401 895
513 617 654 121 970 176	37.210 453 245 540 74	62.111 516 750 796 63	−0.665 571 860 611 077 1	−1.370 519 205 709 037 8	0.366 117 157 438 872 63	-	14.268 944

Continued on the next page...

... Continuation of table 5

Gaia Source ID	RA in °	Dec in °	pm RA in mas year^{-1}	pm Dec in mas year^{-1}	parallax in mas	RV in km s^{-1}	mag$_g$
513 614 802 263 686 912	37.244 920 321 220 82	62.105 851 695 035 24	1.944 222 942 779 263	−0.076 354 151 394 562 18	0.501 139 156 450 460 6	−33.144 556 988 984 63	13.014 843
513 616 245 372 852 736	37.297 308 229 283 93	62.114 622 027 68	0.924 090 752 098 575	1.824 721 915 148 191 3	0.716 441 185 703 539 1	-	15.084 039
513 616 039 214 263 808	37.307 218 659 684 21	62.106 428 738 950 044	−0.920 381 576 069 520 4	−0.255 006 956 661 777 03	0.449 003 275 209 188 6	-	14.588 244
513 614 561 745 676 160	37.285 255 131 847 435	62.096 330 013 491 354	−1.164 459 331 902 247 8	−0.050 037 582 634 613 775	0.422 422 097 251 889 8	-	13.766 996
513 614 561 745 520 896	37.296 426 532 052 18	62.094 847 101 965 28	−0.978 482 005 770 152 7	−0.320 836 677 049 167 2	0.395 840 372 237 684 37	-	14.667 604
513 614 527 385 939 584	37.282 354 969 639 236	62.090 926 568 758 29	−1.194 222 590 655 752 9	−0.047 423 724 975 555 83	0.468 345 506 468 207 44	-	14.169 106
513 614 458 666 310 784	37.305 833 984 271 51	62.081 363 334 036 49	−1.143 276 284 374 766 6	−2.710 860 371 813 691	0.535 215 364 608 207 8	-	15.024 524
513 614 458 666 314 624	37.303 477 557 020 85	62.072 296 800 368 77	1.443 937 384 605 720 2	−0.551 985 613 062 108 4	0.876 316 650 892 656 2	-	13.109 868
513 614 458 666 316 800	37.298 195 393 285 845	62.068 521 871 933 136	1.781 834 532 442 761 1	−0.629 055 294 594 263 6	0.300 281 578 184 541 4	−32.312 821 254 160 88	13.597 972
513 613 702 752 071 168	37.317 634 508 804 545	62.068 876 506 417 55	−1.112 077 425 357 417 5	−0.201 772 442 656 578 57	0.412 091 732 570 786 63	-	15.007 875
513 613 908 910 524 288	37.240 667 383 682 33	62.026 543 119 936 804	−6.290 827 831 304 392	1.957 369 208 366 024 1	0.852 069 820 773 213 7	-	14.542 943
513 613 904 611 707 648	37.231 727 781 935	62.022 951 534 940 93	−4.656 076 732 743 249	−3.232 569 852 524 908 2	0.614 271 095 038 879	-	15.363 523 5
513 613 049 917 218 560	37.241 676 803 026 145	62.004 566 600 857 03	0.933 926 449 802 123 6	−4.023 136 355 885 061	1.039 389 587 085 181 7	-	14.714 533
513 607 655 438 172 544	37.053 011 385 604 75	61.966 139 284 082 49	0.149 750 891 065 832 73	−2.841 867 604 695 064 4	1.333 695 008 090 204	-	11.849 045
513 607 999 035 549 056	37.100 034 931 437 094	61.979 243 200 640 21	−2.271 821 132 724 072 3	0.952 649 440 831 037 4	0.343 098 585 811 665 8	-	14.689 989
513 608 033 395 284 480	37.112 948 267 808 875	61.987 282 807 648 825	3.294 935 756 915 684	−1.589 508 492 920 964	1.055 497 941 658 470 7	-	14.922 136
513 608 033 395 282 304	37.106 989 261 792 81	61.992 500 284 470 85	−2.951 958 483 735 033 7	1.228 878 478 622 850 4	0.548 190 124 168 958 3	−89.987 886 385 691 17	14.135 737
513 608 205 193 962 752	37.112 534 177 295 63	62.021 431 464 280 8	−1.804 277 172 491 743	1.950 640 991 471 429 3	1.027 923 994 870 948 9	-	13.419 964
513 611 052 753 420 160	37.068 678 436 172 09	62.019 738 950 215 945	−1.122 542 744 169 411 6	0.145 663 894 935 591 37	0.306 044 912 455 261 7	-	14.600 695
513 617 134 427 177 216	37.110 454 672 206 66	62.058 218 283 303 63	−0.264 478 107 977 583 53	−0.501 827 462 591 459 6	1.037 790 019 112 535 8	-	14.121 49
513 614 149 428 684 288	37.154 665 294 472 79	62.054 488 700 476 746	−5.565 507 213 539 718	−0.390 969 042 847 660 76	0.788 976 058 020 340 9	-	14.817 942
513 614 252 507 894 016	37.172 693 496 113 44	62.065 346 784 169 85	−4.047 343 519 852 394	−4.410 897 946 995 186	2.424 713 385 179 602 6	-	13.1225
513 613 938 971 458 176	37.267 116 383 440 13	62.032 436 570 475 305	−0.590 129 455 289 511 3	0.340 523 700 307 201	0.255 847 432 416 528 74	-	15.535 659
513 614 321 227 373 184	37.275 812 904 635 03	62.048 931 289 181 99	0.277 498 648 410 291 5	−0.641 443 319 517 694 1	1.852 391 077 793 674 3	-	14.130 234
513 617 379 244 080 640	37.094 627 494 239 234	62.085 241 342 839 296	0.386 147 941 874 659 73	0.803 658 722 950 163 6	0.341 461 403 704 317 9	−58.356 932 194 167 98	13.321 979
513 617 482 323 287 552	37.115 435 778 870 314	62.100 548 596 922 75	−5.507 275 271 007 262	1.330 838 100 893 134 7	1.704 605 916 268 933 3	-	14.122 297
513 617 447 963 853 184	37.074 470 010 429 95	62.104 271 058 837 74	−1.355 031 246 763 696	−0.165 348 403 279 028 3	0.442 605 482 336 335 1	-	15.128 893
513 618 306 957 312 512	37.072 983 031 123 6	62.114 389 594 513 74	−0.114 875 685 179 351 33	0.300 389 933 838 576 4	0.243 431 875 455 874 52	−71.463 601 160 922 05	13.459 733
513 618 306 957 002 368	37.065 081 092 907 3	62.121 168 190 989 24	2.524 385 564 490 021 5	−0.964 136 304 307 803 6	1.181 696 754 009 745 2	-	12.388 103

End of table 5

Table 6: *Gaia Source IDs* and various other properties of the non CMs of Teutsch 55.

Gaia Source ID	RA in °	Dec in °	pm RA in mas year^{-1}	pm Dec in mas year^{-1}	parallax in mas	RV in km s^{-1}	mag$_g$
513 619 234 669 893 120	37.087 904 868 998 39	62.219 212 482 679 24	172.278 601 990 088 87	46.545 915 886 405 3	16.650 070 803 297 115	−61.941 619 922 837 43	7.616 715
513 619 784 425 703 936	37.214 066 086 593 185	62.214 160 297 789 84	6.705 055 101 676 011	−4.891 560 237 371 672	0.822 638 988 786 519 1	-	13.428 595
513 620 540 339 946 112	37.210 631 716 234 87	62.220 175 861 134 194	−1.488 904 666 904 648 2	5.977 961 585 258 328	3.949 167 559 636 362 2	-	15.677 449
513 619 784 425 700 992	37.227 179 270 844 74	62.221 044 286 145 58	−0.046 582 049 521 459 39	−0.341 010 522 511 520 64	0.110 303 911 564 383	-	14.874 427
513 619 646 986 763 264	37.183 598 105 344 906	62.192 255 232 838 6	14.779 453 213 989 996	−4.257 249 060 643 067	1.137 561 127 280 257 5	−23.837 536 603 645 46	13.779 733
513 619 612 627 031 680	37.187 840 627 108 514	62.174 210 320 453 014	−0.858 956 310 124 010 6	0.972 627 884 069 943 2	0.011 062 142 802 277 193	-	14.307 193
513 618 135 158 287 360	37.170 402 694 839 04	62.163 655 430 848 07	−2.028 268 432 395 561 3	−10.557 935 514 224 695	1.262 821 924 615 92	-	14.956 237
513 618 787 993 324 288	37.087 569 915 287 496	62.149 578 688 049 395	−1.165 206 364 315 796 4	0.664 671 186 997 671	0.104 202 693 679 923 34	-	14.196 115 5
513 619 578 267 289 216	37.229 554 187 225 126	62.179 625 989 565 97	5.485 583 722 660 186	−9.688 299 434 943 012	2.441 703 819 980 382 7	-	15.004 44
513 619 917 573 669 120	37.304 430 998 843 68	62.215 634 930 066 756	−1.018 454 491 017 016 6	0.539 789 054 422 691 8	0.084 434 302 919 805 39	-	14.189 957
513 616 996 987 737 216	37.346 974 643 183 01	62.203 663 098 927 62	9.517 152 423 387 857	−7.396 112 309 854 291	2.127 453 456 677 739	−2.105 553 407 471 557 4	12.640 444
513 616 692 049 256 832	37.436 441 182 760 67	62.177 904 723 457 374	1.388 394 686 317 908 2	−6.127 699 721 085 118 5	1.110 461 536 961 1	-	13.150 287
513 992 067 894 589 056	37.435 279 315 437 43	62.199 762 493 833	2.887 749 353 203 747 5	6.378 749 694 283 717	0.936 264 480 856 408	-	13.750 717
513 991 384 999 644 672	37.522 886 249 352 23	62.206 925 054 982 925	0.361 422 826 920 525 63	1.973 660 579 129 113 7	0.157 010 517 590 555 04	-	14.730 757
513 991 075 762 257 792	37.580 882 975 402 13	62.183 346 445 249 36	8.151 503 795 643 01	0.789 864 163 871 142 1	0.904 849 455 761 373 9	-	15.984 069
513 991 041 402 529 664	37.565 346 609 702 175	62.165 768 274 608 02	−0.610 237 947 540 649 9	−0.305 802 382 540 604 54	0.056 318 728 440 216 716	-	15.324 029
513 990 972 682 789 376	37.523 976 250 622 3	62.160 382 531 320 27	−1.850 839 648 021 292 3	0.072 997 539 290 039 35	0.081 047 294 025 420 63	-	14.936 546
513 979 633 969 386 368	37.636 612 517 793 004	62.167 963 160 367 144	−0.652 647 248 483 583	−0.430 514 384 973 844 26	0.132 670 197 670 695 3	-	14.696 27
513 615 936 135 015 552	37.482 956 363 332 4	62.167 604 943 748 096	11.469 296 499 331 66	−11.835 295 824 167 81	0.817 171 470 555 154 6	-	15.378 632
513 615 936 135 019 776	37.464 654 287 697 56	62.162 107 486 061	7.848 398 072 207 136	−4.416 067 587 229 387	1.168 049 599 519 126	-	15.189 280 5
513 615 833 055 811 072	37.479 177 333 335 386	62.143 923 696 077 44	13.043 148 314 165 32	−5.983 215 831 121 425	0.882 119 336 715 022 4	-	14.770 611
513 602 565 896 806 656	37.596 083 150 529 89	62.035 107 002 726 4	14.688 734 879 726 141	−14.661 381 836 130 61	2.615 402 363 525 826 3	-	13.481 836
513 601 745 563 294 976	37.584 709 575 901 27	61.968 545 299 270 25	28.745 783 329 082 49	−13.187 629 104 921 63	1.502 066 293 857 419 4	-	16.022 63

Continued on the next page...

... Continuation of table 6

Gaia Source ID	RA in °	Dec in °	pm RA in mas year^{-1}	pm Dec in mas year^{-1}	parallax in mas	RV in km s^{-1}	mag$_g$
513 602 772 055 238 016	37.510 741 374 360 194	61.998 481 459 940 04	1.501 593 675 438 816 2	−9.683 983 269 226 365	1.454 825 703 183 744 6	−40.225 128 252 758 694	12.138 499
513 601 157 147 534 976	37.457 252 693 496 94	61.970 141 765 186 89	35.597 598 191 884 295	−22.313 862 609 512 9	3.861 371 094 797 364	16.969 851 928 349 86	11.923 601
513 602 840 774 713 984	37.493 229 728 080 73	62.017 955 470 330 61	7.163 366 310 666 6	−7.538 840 150 006 176	1.160 589 239 479 659 8	−11.340 180 353 970 004	13.458 588
513 612 775 039 175 808	37.294 108 139 107 33	61.978 361 678 995 55	−4.721 231 464 319 215	5.315 708 301 898 835	0.867 513 876 725 544 9	-	14.041 108
513 612 981 197 602 688	37.283 578 872 646 444	61.987 224 620 184 7	−13.458 532 377 237 939	8.669 714 664 904 891	1.397 939 459 751 253 3	−71.457 831 018 199 3	11.302 911
513 601 608 124 185 216	37.408 954 665 964 23	62.017 293 819 820 48	−0.071 178 373 301 426 87	0.334 798 798 475 007 7	0.117 386 609 192 028 02	-	14.921 617 5
513 614 870 983 181 696	37.429 526 574 185 23	62.046 193 804 447 554	−11.286 156 781 496 128	1.479 541 822 577 628	1.398 164 278 021 606 8	-	14.389 671
513 603 119 952 661 248	37.459 030 278 066 51	62.038 184 989 112 324	−1.288 513 386 012 278 2	−8.788 382 585 939 75	0.961 854 927 151 499 6	-	15.703 902
513 603 016 873 591 936	37.521 160 163 335 52	62.048 568 654 326 03	0.145 988 384 042 081 25	−5.614 001 248 558 347	1.100 809 277 524 233	-	15.545 251
513 603 291 751 491 072	37.498 760 789 569 36	62.076 211 047 646 21	−0.877 608 869 135 597 5	0.521 382 443 828 561	0.163 715 857 938 131 15	-	14.364 348
513 615 175 921 610 752	37.394 604 324 426 72	62.091 629 571 226 605	17.743 328 434 242 443	−4.740 283 047 425 629	1.958 774 958 087 971 4	7.705 791 638 882 642	12.764 158
513 615 352 019 490 432	37.398 039 595 684 85	62.110 940 875 427 545	0.289 181 866 347 844 26	−8.899 330 799 405 334	4.172 292 877 303 552	-	15.524 38
513 615 764 332 333 184	37.427 201 960 828 57	62.125 201 911 164 055	18.240 670 499 459 075	−4.303 323 771 876 052	8.805 691 633 886 939	−3.001 743 596 943 828	11.227 179
513 616 485 890 837 504	37.328 512 198 144 956	62.166 048 069 547 49	−0.275 819 390 804 765 9	0.849 441 706 260 312 6	0.165 056 324 485 505 25	-	15.108 696
513 613 870 251 555 328	37.192 950 233 362 346	62.025 194 440 752 11	18.687 663 725 275 6	−7.141 866 091 576 776	3.167 804 644 851 86	−11.438 819 450 355 751	12.077 888
513 607 964 675 796 864	37.174 247 843 239 93	62.010 430 334 470 634	1.489 291 140 279 515	−5.724 913 542 131 603	0.560 250 927 534 613 9	-	14.211 507
513 607 861 596 594 176	37.171 783 599 705 61	61.976 063 879 097 09	21.270 643 580 087 093	−7.888 690 705 166 464	0.563 525 575 490 264 2	−3.852 918 445 339 213	12.749 768
513 611 435 009 360 000	37.063 226 245 313 885	62.050 434 089 280 91	9.570 000 749 166 791	−62.341 850 111 585 586	2.696 715 254 860 562 6	−3.436 322 816 814 003 6	12.514 873

End of table 6

Table 7: *Gaia Source IDs* and various other properties of the stars in Teutsch 55, which were not analysed.

Gaia Source ID	RA in °	Dec in °	pm RA in mas year^{-1}	pm Dec in mas year^{-1}	parallax in mas	RV in km s^{-1}	mag$_g$
513 601 019 709 748 864	37.384 931 236 325 73	61.977 259 667 688 99	-	-	-	-	15.313 21
513 991 075 762 254 080	37.590 815 604 238 38	62.190 265 167 346 72	−0.330 988 655 576 135	−4.413 244 319 772 14	0.912 426 044 768 734	-	14.633 203 5
513 611 263 210 665 344	37.099 078 964 771 96	62.052 036 239 131 4	3.055 961 586 535 545 4	−1.168 007 157 965 656 8	0.607 588 579 074 425	-	15.310 316
513 617 100 066 960 640	37.138 491 822 658 5	62.056 720 449 601 02	-	-	-	-	13.193 157
513 601 779 923 030 400	37.581 125 011 100 504	61.978 678 649 998 905	-	-	-	-	15.000 754
513 617 482 323 290 496	37.115 393 161 347 356	62.094 529 771 253 264	−3.418 070 401 976 902 6	−4.306 282 895 872 227 5	0.453 725 233 390 073 6	−8.040 092 718 689 387	13.224 21
513 614 767 903 945 984	37.284 782 155 686 85	62.106 908 014 574 266	−1.024 273 085 012 09	−0.120 160 819 080 486 97	0.446 844 044 739 150 2	-	10.810 971

End of table 7

A.3 Stock 19

Table 8: *Gaia Source IDs* and various other properties of our identified cluster members (CMs) of Stock 19.

Gaia Source ID	RA in °	Dec in °	pm RA in mas $year^{-1}$	pm Dec in mas $year^{-1}$	parallax in mas	RV in km s^{-1}	mag_g
420 874 776 035 616 512	1.018 320 113 919 255 5	56.181 811 312 849 18	−1.582 362 329 716 556 5	0.350 101 020 579 013 6	0.607 974 326 874 460 1	-	15.214 654
420 875 188 352 476 160	1.029 155 724 872 352 9	56.192 120 744 471 75	−4.930 389 256 138 39	−0.809 957 011 157 161 9	0.472 587 481 085 868 6	−64.833 672 889 072 91	13.167 765
420 875 016 553 783 936	1.064 555 764 349 426 1	56.200 442 672 974 674	−1.840 784 084 319 933	−2.954 092 146 737 867	0.539 906 151 291 353 8	-	14.883 844
420 875 050 913 525 376	1.107 327 359 873 200 7	56.195 067 598 421 936	2.867 288 538 861 759	−2.595 794 495 317 197	0.482 893 090 432 099	-	15.409 718 5
420 874 290 700 505 600	1.124 311 732 455 892 9	56.187 852 748 030 15	−2.146 528 908 639 412 6	−2.669 680 965 398 71	0.576 531 290 809 128 6	-	14.795 434
420 874 294 999 283 584	1.131 642 186 814 906 7	56.178 298 481 929 914	−6.951 750 082 756 854	−8.156 042 193 009 334	1.952 591 007 530 505 7	-	10.446 197
420 874 947 834 311 168	1.086 359 430 792 023 5	56.183 548 281 580 81	6.680 169 542 555 629	−6.226 807 387 716 422 5	0.733 640 800 439 534 2	-	14.835 512
420 874 810 395 357 440	1.047 317 337 963 601	56.176 377 546 450 134	−2.087 884 524 038 072 3	−0.325 975 852 631 247 73	0.269 054 023 734 003 56	-	13.772 716 5
420 874 913 474 575 232	1.104 120 251 094 573 6	56.169 529 156 200 42	1.864 768 076 661 095 5	1.250 864 621 756 253 6	0.206 810 961 669 835 23	-	15.180 38
420 874 501 157 717 504	1.089 260 051 213 569 5	56.153 343 021 532 26	−7.618 101 544 239 403	−7.391 873 659 542 346	2.025 239 955 599 143	−3.338 954 076 972 712	12.998 795 5
420 874 569 877 191 040	1.057 220 602 021 324 4	56.160 679 759 270 03	−3.919 742 093 466 815	−0.707 782 432 424 211 5	0.183 277 391 453 341 1	-	13.708 995
420 874 707 316 144 256	1.009 467 101 081 216 6	56.152 508 341 161 386	1.716 865 331 696 694 2	−6.866 023 779 587 051	0.908 998 079 052 347 2	-	14.932 279
420 873 195 487 658 496	1.001 400 905 273 626 6	56.140 438 514 915 175	−4.579 794 703 258 754	−2.982 887 562 360 894	0.308 865 251 480 672	-	14.779 354
420 873 195 487 659 648	1.001 751 546 124 279 6	56.134 864 652 860 166	−2.194 792 048 330 754 6	−0.702 005 031 154 394 2	0.177 966 162 630 981 78	-	14.531 056
420 873 161 128 172 160	1.042 061 852 246 558 3	56.134 185 230 585 46	6.234 776 646 073 723	−6.055 575 866 091 416	0.807 264 998 316 158 6	−32.797 783 945 942 44	11.418 894
420 873 023 688 973 184	1.024 185 702 015 233 8	56.115 357 406 101 55	−5.427 840 615 614 58	−5.764 119 079 628 086	0.795 844 922 965 434 7	-	14.408 594
420 873 019 387 938 560	1.032 842 972 880 037	56.113 930 994 113 28	−2.901 199 592 593 101 3	−3.767 857 868 566 193 4	0.733 557 403 578 101 8	-	13.356 034
420 873 023 688 975 360	1.032 055 420 240 041 8	56.108 781 253 757 71	3.287 060 295 820 978 3	−0.339 484 253 462 202	0.876 790 421 328 734 7	-	14.187 485
420 874 363 718 770 048	1.084 546 087 567 375 6	56.126 033 628 911 47	−3.112 093 228 426 512	−0.592 532 455 632 363	0.298 022 637 881 795 7	-	15.111 009
420 874 363 718 771 840	1.093 431 987 340 719	56.121 447 857 490 37	3.589 800 049 155 812	−2.536 004 858 685 741	0.810 102 770 242 478	-	15.124 744
420 874 363 718 773 632	1.102 788 338 349 953 5	56.117 122 597 482 52	−5.036 556 523 554 23	−0.154 770 459 322 802 6	0.346 168 002 914 296 17	−77.565 119 895 779 02	13.373 176
420 872 920 609 763 200	1.071 132 302 096 009	56.106 627 881 755 44	−2.619 792 861 858 357	−1.747 755 047 058 013 9	0.531 218 974 971 232 9	-	13.420 071
420 872 748 811 076 224	1.079 850 022 515 746 4	56.098 089 452 823 66	−10.533 902 958 727 49	−8.786 020 697 280 769	1.860 287 969 983 058 1	-	10.702 864
420 872 778 869 755 776	1.069 420 506 872 017 5	56.090 410 463 567 57	−7.934 517 970 645 127	−4.769 047 891 392 751	0.806 724 813 806 830 8	-	14.690 775
420 872 783 170 817 280	1.057 273 583 951 572 1	56.083 897 865 550 98	−1.345 567 393 914 374 2	0.497 800 993 696 307 3	0.584 515 149 664 610 3	-	14.304 044
420 872 538 350 177 664	0.995 965 316 613 637	56.077 159 039 171 8	2.531 517 295 495 663 5	−1.231 877 686 427 950 4	0.616 965 218 211 554 1	-	14.481 853
420 872 542 652 648 320	1.012 711 339 984 913 3	56.076 395 931 500 166	−3.963 052 751 311 417	−1.050 819 704 856 109 2	0.251 256 106 601 049 7	-	13.632 519
420 872 473 933 176 192	1.022 157 524 581 579 5	56.065 649 398 723 92	−3.812 791 255 738 247	−0.761 383 992 950 489 4	0.773 627 757 230 943 9	-	14.781 374
420 866 632 777 656 704	0.996 282 080 706 300 5	56.050 130 576 674 85	−2.210 133 174 004 675 5	−1.898 998 833 357 455 2	0.175 424 044 671 103 5	-	14.184 538
420 866 594 115 318 400	0.985 934 649 995 436 5	56.039 428 310 097 76	−6.322 914 711 386 212	−1.325 267 233 357 118 5	0.223 526 924 643 796 78	-	13.550 409
420 866 564 058 188 672	1.030 795 874 155 018	56.035 643 306 397 37	−3.549 330 630 750 616 5	−1.760 163 371 103 346 2	5.024 448 810 544 65	-	9.266 619
420 866 495 338 712 576	0.999 865 914 370 411 3	56.027 871 262 788 46	−3.973 881 655 747 580 2	−1.798 237 387 647 841 2	0.366 109 422 566 108 1	-	13.649 393
420 866 220 460 819 072	1.062 593 482 845 515 2	56.004 261 345 369 41	−5.086 410 478 786 699	−1.877 144 231 504 990 7	0.533 869 510 998 138 6	-	14.747 762
420 866 220 460 820 480	1.056 202 453 441 953 8	56.000 764 223 522 96	8.448 434 128 935 43	−6.670 906 308 165 51	2.270 291 797 914 445	-	15.080 828
420 866 014 302 391 680	1.036 656 353 677 189 3	55.994 735 747 702 06	−2.739 272 284 411 144 6	−1.758 039 623 708 783 4	0.232 573 019 504 069 97	-	14.668 834
420 865 876 863 445 504	1.019 284 647 165 458 2	55.975 783 933 007 605	−3.551 896 111 205 479 7	−2.424 663 864 003 963 3	1.121 589 946 360 173 7	−45.274 840 632 148 454	12.959 934
420 865 979 942 662 016	1.040 682 110 020 290 3	55.977 529 069 147 17	−7.399 815 459 792 868	−1.629 351 265 869 453	0.625 725 997 346 490 5	-	14.612 854
420 865 773 784 235 392	1.048 635 102 218 347 3	55.972 019 849 078	−3.953 824 448 917 659	−1.786 460 297 748 111 4	0.395 720 065 972 484 66	-	13.781 613
420 865 739 424 500 096	1.077 087 178 891 868 8	55.973 123 014 946 914	−0.553 411 706 242 412 8	0.238 304 829 558 981 44	0.352 623 001 344 525 73	−80.133 239 996 772 2	13.372 68
420 865 705 064 765 696	1.083 660 675 260 715 4	55.964 670 329 051 36	9.169 980 487 550 585	−3.812 454 263 489 626	1.251 320 849 733 402 3	-	14.292 342
420 864 983 510 262 784	1.111 613 732 926 345 8	55.965 450 762 763 17	8.715 299 898 542 774	−6.391 457 017 973 752	1.424 041 049 304 676 2	-	15.014 255
420 864 983 510 269 568	1.120 921 353 261 5	55.954 926 423 672 156	−6.007 001 651 583 337	−1.375 685 352 029 249 4	1.048 190 743 910 494 3	-	14.920 389
420 865 700 763 485 696	1.100 509 380 934 194	55.955 913 043 580 935	−0.823 789 328 670 833 7	−0.992 364 128 837 478 7	0.454 933 983 140 168 2	-	15.345 004
420 864 708 632 374 784	1.165 278 998 765 513 4	55.939 909 687 135 554	−3.227 214 407 689 680 3	−5.258 831 545 714 107 5	1.028 066 413 286 467 6	-	11.463 161
420 865 327 107 652 352	1.153 955 515 326 876 8	55.964 867 409 529 24	−0.275 837 120 434 578 3	−3.025 905 707 759 971 4	0.555 147 191 899 851 8	-	14.474 897
420 865 120 949 224 704	1.177 321 685 294 408 4	55.963 841 094 726 18	−3.325 659 638 926 597 8	−2.225 788 296 846 972 4	0.527 707 861 110 410 3	-	13.604 035
420 866 151 741 352 704	1.094 250 623 327 171 6	55.991 516 736 609 6	−4.842 435 947 918 461	−1.959 997 150 738 419 5	1.565 514 686 345 833 6	-	14.871 621
420 871 408 781 519 232	1.130 887 666 212 090 8	56.013 584 446 258 946	1.202 222 750 494 244	−2.462 743 732 711 882	0.383 535 448 109 136 76	−51.301 336 250 042 7	12.851 732
420 871 541 916 442 880	1.134 227 760 699 530 4	56.033 020 791 591 795	−14.624 999 127 268 184	−6.597 481 529 217 386 5	1.139 574 326 399 098 5	−32.373 619 462 332 3	12.288 462
420 871 924 177 379 072	1.164 001 761 022 394 3	56.054 184 448 283 2	−6.873 306 757 980 366	−8.315 519 573 579 65	3.073 750 657 212 983 6	−66.096 383 617 119 73	13.092 379
420 871 718 018 945 024	1.170 424 801 220 666 6	56.061 649 365 175 15	1.638 168 902 661 266 7	−3.266 524 066 125 567	0.549 850 720 611 703 3	-	14.155 02
420 871 821 098 157 696	1.178 771 786 168 393 7	56.070 894 812 430 5	1.659 743 919 860 222 8	−0.034 504 087 980 696 33	1.340 703 541 205 465 8	-	11.757 168
420 871 718 019 163 904	1.183 127 697 596 585 9	56.058 029 573 315 615	−2.056 919 001 039 499 8	−1.539 332 789 151 259 8	0.224 931 402 133 047 33	-	14.808 091
420 871 821 098 164 608	1.193 252 408 989 401 7	56.058 095 321 179 66	−2.901 763 528 641 995	−2.306 531 742 840 093 5	0.665 818 971 477 494 7	-	14.840 058
420 871 511 860 522 624	1.163 689 357 400 571 3	56.039 116 115 475 23	6.039 758 169 290 529	−3.747 816 055 975 239	0.797 015 935 527 943 7	-	14.971 032

Continued on the next page...

... Continuation of table 8

Gaia Source ID	RA in °	Dec in °	pm RA in mas year^{-1}	pm Dec in mas year^{-1}	parallax in mas	RV in km s^{-1}	mag$_g$
420 871 305 702 102 144	1.195 322 286 846 601 6	56.024 395 297 306 61	−1.022 279 540 954 551 3	−2.222 352 200 967 482 5	0.897 206 036 452 068	-	15.180 55
420 872 027 256 582 656	1.150 377 084 619 900 2	56.078 080 706 430 7	−12.388 763 446 354 876	−6.292 686 620 844 353 5	1.184 696 004 155 420 2	-	15.045 71
420 872 130 335 792 256	1.137 813 672 088 432 6	56.090 435 801 484 2	−4.781 234 076 323 932	−1.660 754 711 491 672	0.403 594 842 393 457 8	−45.329 353 529 408 536	10.539 367
420 872 061 616 314 752	1.148 309 706 512 732 3	56.093 749 668 815 114	−5.150 851 465 110 145	−1.737 868 303 123 195 2	0.784 547 330 535 413 6	-	14.043 052
420 872 061 616 320 384	1.162 315 963 564 568 8	56.081 623 800 187 82	−1.696 178 613 767 385 3	−0.777 498 879 188 159 9	0.828 466 753 544 632 7	-	9.801 515
420 871 855 457 889 792	1.176 390 391 795 837 4	56.085 232 711 219 57	6.343 061 820 061 128	−1.486 738 530 316 826 8	0.987 387 585 906 695	−14.601 615 890 103 558	9.831 573 5
420 873 676 524 006 400	1.145 873 133 270 736	56.125 503 006 538 85	−0.668 373 194 877 879 6	−0.545 160 405 849 859	3.222 106 636 746 420 6	-	14.308 144
420 874 088 840 863 616	1.161 751 962 208 538 6	56.140 714 620 385 29	3.043 281 196 382 755 7	−2.858 936 857 286 350 3	0.528 057 650 773 682	-	14.388 99
420 873 917 042 170 496	1.183 220 406 881 135 6	56.149 339 942 809 3	2.573 041 380 812 353	−8.025 081 711 331 978	1.055 997 841 599 715 5	-	15.315 224
420 967 856 565 786 112	1.206 049 333 139 054 3	56.192 528 919 722 56	−3.984 169 921 347 579 6	−3.259 482 990 874 881	0.417 221 934 834 568 5	-	14.564 441
420 967 959 645 000 448	1.221 942 930 639 637 4	56.200 229 488 894 26	−5.903 132 780 329 849	−2.219 206 480 271 692	0.512 826 534 626 193 2	-	15.231 169
420 964 970 347 766 400	1.272 888 581 854 140 9	56.188 526 797 483 24	−2.624 618 892 008 903	−1.269 964 486 088 139	0.302 410 381 620 961 34	−50.784 580 283 334 53	13.393 201
420 964 901 628 291 584	1.241 195 612 466 222 7	56.169 090 088 791 65	−2.130 384 854 791 583	0.459 939 942 413 356 34	0.969 350 089 185 211	-	15.427 898
420 964 901 628 292 608	1.260 275 739 753 854	56.166 304 744 980 45	−5.619 873 207 265 435	−5.002 982 672 293 943	0.675 996 180 236 779 2	-	16.134 108
420 964 935 988 030 848	1.272 156 538 080 611 7	56.169 253 665 932 175	−3.396 811 558 609 149	0.428 310 183 316 859 55	0.456 599 880 869 716 65	-	14.930 487
420 964 759 890 587 648	1.295 656 937 383 475 2	56.171 985 729 005 17	−7.203 796 187 558 962	−6.258 097 548 889 124	0.595 747 319 007 339 9	−17.524 004 589 729 678	11.946 871
420 964 798 549 079 552	1.279 818 188 966 178 8	56.151 553 436 933 6	−3.021 684 698 946 243	−1.909 966 463 867 703	0.278 935 676 764 204 67	-	15.351 268
420 870 962 104 679 296	1.269 628 887 908 767 4	56.142 135 239 097 016	−1.995 319 596 604 515 2	0.002 390 584 679 652 298 3	0.621 488 441 892 964 1	-	15.873 859
420 870 962 104 682 112	1.270 712 035 759 38	56.133 470 715 793 29	−0.552 154 500 100 152 5	−0.287 023 974 706 723 53	0.189 787 665 154 966 12	-	14.807 27
420 873 882 682 440 960	1.199 070 924 444 154 4	56.126 567 421 662 166	−3.627 650 397 458 085	−0.617 835 615 252 435 1	0.448 295 138 864 623 74	-	15.825 01
420 873 504 725 321 856	1.193 328 221 035 746 5	56.115 474 348 388 55	−1.514 029 025 012 225	−1.725 919 050 173 979 8	0.198 804 539 712 294 75	-	14.178 903
420 873 436 005 849 344	1.214 740 671 672 228 9	56.107 845 200 200 42	−0.841 122 368 176 544 2	−4.297 567 722 875 516	0.796 194 170 979 286 2	-	15.369 040 5
420 870 859 025 472 768	1.240 536 902 053 645 9	56.111 494 426 542 805	−0.460 575 725 773 305 4	0.037 652 148 203 891 525	0.516 730 049 581 165 3	-	14.344 941
420 870 790 306 001 280	1.266 994 813 168 617 5	56.102 680 249 479 76	−7.708 462 983 975 238	−2.730 790 149 078 221 6	0.518 727 289 156 661	-	15.029 799
420 870 790 305 998 976	1.269 840 537 279 813 2	56.107 845 326 750 43	−5.335 402 927 451 414 5	−4.017 377 285 084 422 5	0.470 547 110 503 712 73	-	15.037 441
420 870 824 658 830 336	1.277 540 055 511 580 8	56.107 894 875 004 966	−9.739 978 665 600 656	−0.652 767 035 410 372 5	1.612 621 066 875 724	-	10.734 034
420 870 790 306 005 504	1.292 055 559 515 509 7	56.098 997 774 065 72	6.773 365 323 927 293	0.617 182 145 918 984 8	1.225 216 203 267 669 4	-	14.497 642 5
420 870 446 708 618 752	1.238 721 023 761 145	56.094 080 037 805 334	4.059 088 596 305 999	−0.996 230 370 630 927	0.598 082 588 564 979 2	-	14.578 852
420 870 446 708 621 696	1.234 345 903 184 672	56.087 486 499 168 12	−1.010 173 392 881 931 9	−2.427 791 532 765 186 7	0.477 561 335 808 482 3	-	15.677 135
420 873 294 265 833 856	1.202 037 481 392 710 6	56.095 466 921 295 3	1.319 458 883 693 117 1	−2.713 079 123 296 539	0.702 714 462 396 743 3	-	15.159 780 5
420 870 343 629 413 376	1.256 012 950 583 404 6	56.074 513 340 905 78	−5.969 310 422 960 193	−7.171 387 039 507 962	0.911 927 534 025 694 6	-	15.082 31
420 868 831 800 928 640	1.234 187 204 754 192	56.056 943 641 021 064	−1.886 949 195 878 608 4	−2.686 133 232 648 957 3	1.602 389 719 856 807 1	−15.629 061 551 957 21	8.013 69
420 868 831 800 930 560	1.242 528 139 603 279 2	56.052 293 716 014 14	3.651 305 129 283 262	−8.160 059 899 455 135	1.005 628 411 864 029 7	-	15.106 887
420 868 831 800 933 632	1.257 325 148 902 025 2	56.049 260 325 755 14	−4.670 838 442 744 955	−0.767 547 770 841 047 2	0.428 904 494 171 659 8	−66.593 372 948 108 14	13.620 085
420 868 763 081 458 816	1.268 996 133 691 608 2	56.047 441 725 702 29	−9.077 437 817 018 067	−9.646 840 954 226 185	2.222 640 369 679 444	−8.914 444 260 264 036	13.221 521
420 868 694 361 987 968	1.237 767 135 399 201 2	56.028 861 697 515 65	2.537 421 075 388 417	−1.706 937 989 149 121 2	0.677 743 046 182 088 6	-	14.987 889
420 868 660 002 250 368	1.229 724 582 887 008 5	56.026 010 768 164 03	4.627 311 066 971 24	−2.152 120 974 795 863 6	1.101 280 356 230 024 8	-	14.730 945
420 868 694 361 991 168	1.254 147 390 384 694	56.025 273 809 112 09	−2.996 766 557 380 365	0.553 994 347 681 535	1.480 079 394 807 257 7	-	14.446 015
420 868 282 045 138 432	1.237 099 654 696 438 3	56.008 254 632 493 056	−1.566 167 423 064 268 6	0.057 652 371 534 519 076	0.333 489 632 326 832 4	-	13.584 623
420 871 236 982 638 336	1.225 990 944 823 044 2	56.005 845 399 038 36	−2.031 781 945 001 157	0.267 121 957 715 476 3	0.258 761 703 916 257 4	-	14.099 56
420 871 065 183 955 840	1.207 618 459 976 065 3	55.982 937 637 298 626	−4.737 627 431 923 207	−2.418 586 556 727 704 3	0.348 302 038 972 541 53	-	14.884 19
420 868 213 325 668 480	1.259 809 195 087 075 3	55.998 032 851 495 374	−0.706 890 497 721 246	−0.325 065 242 433 404 57	0.768 329 470 680 955 7	-	16.139 25
420 862 234 731 211 264	1.244 994 964 638 135 3	55.958 537 608 648 13	−2.982 243 235 147 746	−4.830 350 937 407 229	0.218 432 842 688 565 64	-	14.536 202
420 868 105 945 182 336	1.249 427 391 018 477 2	55.959 887 344 235 916	−3.833 808 808 472 088	−1.545 813 426 153 652 5	0.409 525 719 659 967 2	-	14.755 087
420 862 131 652 010 752	1.272 306 877 126 730 3	55.937 865 912 962 04	−0.374 874 687 546 437 1	0.518 382 537 177 703 4	0.683 840 679 075 86	−48.790 268 887 390 02	10.694 777 5
420 868 007 167 254 656	1.309 553 331 012 288 9	55.975 507 482 391 116	−0.480 749 560 525 196 5	−0.925 500 305 786 13	0.297 607 070 473 155 7	-	13.711 132
420 867 972 807 519 616	1.298 998 655 947 517 7	55.967 967 344 830 89	−10.632 206 830 936 969	−1.191 244 158 248 797	0.790 186 380 291 086 9	-	15.819 694 5
420 867 972 807 524 096	1.307 681 394 580 642 3	55.961 405 186 725 194	−3.988 559 420 810 826	−0.586 801 042 525 284 5	0.279 062 787 811 709 4	-	15.550 452
420 867 801 008 840 960	1.321 932 900 205 118 6	55.949 044 157 435 15	−6.778 941 919 836 803	−9.225 237 840 419 318	1.350 314 505 080 790 5	-	14.818 141
420 867 801 008 838 272	1.324 866 383 549 705 4	55.953 300 795 725 085	−5.500 149 726 710 595	−3.277 921 703 540 996 7	0.362 540 405 024 915 9	-	15.644 194
420 867 079 454 351 232	1.397 620 166 694 192 3	55.932 374 951 456 06	−2.840 890 021 980 642	−6.208 509 174 261 929	0.565 760 986 093 119 5	-	15.279 495
420 866 903 351 769 600	1.423 899 968 965 719 7	55.938 145 178 512 64	−1.130 202 754 314 013 2	−5.015 759 608 987 013	1.178 045 726 227 665 3	-	10.864 799 5
420 867 285 612 779 520	1.421 126 107 971 934 2	55.941 583 726 304 1	0.848 193 348 518 442 3	−2.655 658 479 885 317 6	0.513 390 010 743 759 3	−44.935 269 439 124 91	13.364 601
420 867 212 591 948 544	1.443 383 300 197 713 2	55.935 824 869 382 17	0.035 543 863 320 649 11	−3.650 788 820 139 096 6	0.806 350 457 225 100 2	−17.369 932 592 970 784	12.835 987
420 867 487 469 889 280	1.382 150 510 943 364	55.955 824 772 190 3	−2.147 521 298 023 186	−1.838 381 683 509 069 8	0.473 884 783 999 863 33	-	14.083 479
420 867 491 771 196 544	1.384 686 241 892 524 8	55.960 143 256 638 61	−1.780 437 147 629 562 6	−0.701 587 892 660 571 5	0.185 304 907 086 558 5	-	14.687 607
420 867 526 130 932 864	1.392 323 573 306 737 2	55.964 665 276 371 1	4.448 170 387 596 843	0.085 065 050 420 235 74	1.177 586 139 727 162 8	-	15.216 633
420 867 526 130 932 096	1.395 716 426 652 725	55.966 700 036 706 214	−1.815 977 787 419 203 1	−2.022 426 595 346 608	0.528 030 536 541 087 1	-	15.403 096
420 867 526 130 937 472	1.402 409 687 294 159 6	55.960 748 238 863 4	3.296 651 895 004 657	0.439 492 246 084 499 44	1.739 903 208 188 9	-	13.764 656

Continued on the next page...

... Continuation of table 8

Gaia Source ID	RA in °	Dec in °	pm RA in mas year^{-1}	pm Dec in mas year^{-1}	parallax in mas	RV in km s^{-1}	mag$_g$
420 867 418 747 843 072	1.439 835 152 067 198	55.969 083 220 755 75	−3.054 595 303 988 599 6	4.792 128 652 092 86	1.700 839 990 344 272 6	−32.412 353 205 491 06	12.487 401
420 868 866 160 725 888	1.444 333 938 596 876 3	55.981 140 550 737 734	−4.218 429 719 912 393	−1.119 575 228 222 849 7	0.287 334 750 657 956 8	-	14.468 263
420 867 594 843 854 208	1.368 147 679 818 379 4	55.982 615 511 932 266	−4.980 727 515 900 498	−1.626 826 122 892 772 5	0.423 896 688 025 269 5	−57.473 810 362 989 96	11.172 018
420 869 141 038 619 136	1.399 783 751 190 681 9	55.997 352 481 843 76	2.873 709 510 089 606 4	0.769 699 411 968 711 6	0.661 283 354 907 261 6	-	13.961 436
420 867 663 569 868 288	1.394 789 533 519 63	55.998 925 023 272 67	−3.060 758 609 590 646 3	−5.708 812 990 008 179	0.928 633 493 118 234 4	-	13.791 844
420 869 141 038 616 448	1.394 198 715 296 994 8	56.004 006 103 482 05	−3.129 311 880 985 549	−1.636 903 532 911 165 2	0.757 003 135 084 763 2	-	13.203 005
420 869 141 038 614 016	1.389 100 914 769 640 7	56.007 652 374 343 82	0.320 504 157 964 740 85	−0.806 714 004 493 664 7	0.556 449 356 733 834 2	-	15.272 344
420 869 209 758 084 992	1.362 384 974 800 027 4	56.013 345 672 359 9	7.394 924 062 753 184	−1.362 868 803 009 084 8	0.827 365 013 133 770 6	-	15.295 614
420 869 141 038 617 344	1.407 133 335 198 108	56.003 334 928 964 54	−2.728 533 710 633 582	−5.510 822 120 694 128	0.943 278 083 035 658 5	-	14.252 408
420 868 591 282 790 016	1.286 306 267 097 980 8	56.004 909 763 570 83	0.460 821 720 659 711 55	−2.227 098 536 908 157 7	0.715 737 293 331 596 1	-	14.624 305
420 868 522 563 308 928	1.305 501 821 733 276 8	56.017 499 020 041 74	2.407 846 122 444 939 2	−4.040 623 803 047 157	0.616 538 604 196 456 8	−29.478 002 256 557 96	13.582 946
420 868 556 923 042 304	1.298 302 671 216 584 8	56.025 719 491 312 02	3.243 387 002 232 240 4	−1.383 644 598 459 032 9	0.795 065 280 356 450 6	-	14.794 025
420 870 068 751 517 184	1.297 311 611 465 271 4	56.052 149 710 818 13	−0.685 013 343 970 128 9	−1.201 742 351 084 129 2	0.265 764 247 354 085 77	-	14.465 325
420 870 167 529 611 392	1.302 523 681 092 182 8	56.060 010 000 564 986	−0.035 364 148 902 211 07	−3.841 375 434 778 460 6	0.457 043 658 096 072 2	-	15.012 246
420 870 137 470 996 224	1.347 472 201 540 226 3	56.058 767 387 609 49	−3.698 100 121 862 433 6	−1.312 410 211 546 624	0.256 569 970 671 191 4	-	14.235 304
420 870 103 111 263 488	1.344 490 142 819 326 6	56.046 326 716 749 48	7.595 448 626 156 939	1.864 340 661 106 644 4	0.669 661 903 172 391 5	-	14.825 337
420 869 347 197 023 616	1.357 807 954 912 136 2	56.041 247 572 974 76	−0.133 718 700 927 094 26	−2.385 038 050 084 844	1.239 587 544 796 595 4	-	14.801 231
420 869 278 477 562 624	1.409 667 466 744 654 7	56.020 906 193 319 306	−1.184 699 445 657 159 8	−0.078 380 402 517 105 03	0.284 702 616 368 690 04	-	15.681 424
420 869 072 319 131 008	1.418 493 174 249 349 2	56.026 120 785 923 32	−4.574 609 779 864 831	5.431 465 126 247 52	1.142 057 003 439 580 5	-	14.393 742
420 869 415 916 515 968	1.455 661 897 599 844	56.030 633 691 341 68	−3.789 541 026 745 210 3	−1.155 327 668 700 236 3	0.347 769 468 600 502 7	−38.808 960 927 144 21	13.115 114
420 869 450 276 248 320	1.460 369 385 974 291 4	56.042 605 755 879 96	8.312 620 506 430 779	−2.162 758 667 758 893	1.120 969 469 335 581	-	15.492 434 5
420 869 450 276 244 992	1.445 648 842 214 762 9	56.046 351 106 097 6	−2.520 332 508 786 880 4	−0.934 128 055 578 079 1	0.176 787 359 385 650 38	-	14.973 309 5
420 869 518 995 713 408	1.419 195 166 684 515	56.057 880 239 476 97	0.388 445 897 743 831 54	2.419 160 650 733 551	0.554 028 909 530 419	-	15.072 03
420 869 725 154 141 056	1.413 440 504 470 122 1	56.061 076 602 025 636	1.837 843 799 441 576 2	−2.131 222 639 196 489 7	0.524 926 062 845 145 8	-	14.550 065
420 869 656 434 657 024	1.427 926 892 122 055	56.079 423 345 940 28	−4.119 661 555 102 147	−0.829 598 562 088 564 2	0.199 321 856 406 804 36	-	13.899 075 5
420 870 549 787 844 096	1.338 889 976 788 360 9	56.091 129 264 537 32	−4.981 271 648 258 922 5	3.434 965 458 025 727 6	0.299 431 866 785 783 93	-	13.779 522
420 869 931 312 547 712	1.355 122 320 801 667 4	56.106 480 167 531 274	2.592 351 137 295 428 7	5.866 365 290 397 565	1.522 961 336 331 231 3	-	14.927 658
420 964 523 671 177 088	1.340 778 338 539 277 3	56.119 754 041 842 924	0.497 242 155 849 253 6	−2.170 506 903 241 712	1.005 795 227 644 615 6	-	14.722 212
420 964 523 671 176 960	1.344 355 151 453 423	56.123 123 671 696 44	−1.745 598 911 905 923	−1.444 537 024 461 107 3	0.183 646 840 065 187 3	-	15.292 637
420 964 558 030 914 304	1.350 159 508 749 455 6	56.137 244 918 975 675	−2.908 689 553 942 526	−3.445 872 052 160 286 4	0.624 136 013 179 416 6	-	14.895 134
420 964 725 531 434 624	1.324 489 518 873 169 1	56.149 334 627 020 416	−2.162 460 069 516 465 3	0.055 258 848 815 285 91	0.178 100 106 544 780 98	-	15.316 231
420 964 695 469 863 552	1.329 142 611 235 404 3	56.170 027 418 339 56	−2.010 661 601 590 831 6	−0.972 397 981 773 914 6	0.210 774 843 146 442 85	-	15.861 542
420 965 107 786 724 096	1.351 777 440 686 242 4	56.174 463 556 484 54	3.364 830 752 864 644 4	−3.773 349 980 691 309	0.484 288 631 331 201 54	-	15.586 416
420 964 454 951 694 592	1.369 738 407 905 881 9	56.181 203 854 864 336	−2.817 669 310 920 339 2	−2.238 107 788 819 623	0.481 953 758 537 164 54	-	15.430 484
420 964 386 232 348 928	1.390 752 671 405 250 5	56.182 224 605 920 474	−7.250 152 114 688 483 5	−5.214 927 028 154 954	0.401 299 848 547 869 9	-	16.004 461
420 964 386 232 219 648	1.390 747 677 917 309 4	56.170 723 690 589 36	−12.226 548 941 923 587	−2.340 870 905 544 736 8	1.013 635 650 935 396	−30.622 825 255 753 003	10.349 059
420 963 836 476 410 112	1.402 775 860 931 276 2	56.127 238 900 188 09	−6.394 112 930 694 184	−2.241 491 664 745 733	0.915 614 750 504 188 7	-	15.357 492
420 963 664 677 718 528	1.418 128 420 108 000 2	56.129 694 523 656 18	−0.649 659 182 830 303 2	−3.237 343 475 419 594 4	0.698 647 364 153 630 2	-	14.332 453
420 963 973 915 527 168	1.459 473 808 050 193 7	56.120 767 008 583 8	−2.204 499 773 825 860 5	−1.945 209 044 054 611 3	0.401 373 164 673 417 66	-	14.495 299
420 963 595 958 408 448	1.452 646 204 939 608 5	56.111 377 671 966 28	−4.558 716 661 440 407	−6.992 245 128 017 76	0.520 312 606 173 192 4	-	14.872 522
420 963 699 037 458 048	1.386 867 944 839 878 6	56.099 865 071 494 186	−8.976 470 831 643 109	−4.652 756 491 153 736	0.596 249 005 140 107 4	-	16.282 337
420 964 111 354 467 584	1.468 960 728 131 094 6	56.148 740 940 945 04	−4.391 643 287 191 348	−2.129 927 449 257 916 5	0.493 978 573 944 754 53	-	15.180 276
420 964 145 714 196 992	1.449 500 143 247 404 2	56.161 401 918 911 956	−1.910 253 314 701 009 2	−0.002 336 437 773 866 349 7	0.365 670 840 103 258 45	-	14.039 215
420 964 214 433 667 456	1.434 642 093 609 995 7	56.167 303 977 729 32	2.859 353 322 096 227 5	−1.123 638 573 853 820 6	0.319 076 235 882 266 8	-	14.997 808
420 964 214 433 667 712	1.443 079 465 860 981 3	56.168 727 646 898 76	−0.890 095 347 052 016 4	−1.705 944 799 833 979 6	0.434 185 797 649 209 3	-	14.009 269
420 964 145 714 334 464	1.457 587 388 896 762 3	56.162 426 258 370 36	−3.664 706 184 374 096 7	−6.653 325 916 273 027	1.119 986 326 676 795	-	14.254 127 5
420 965 623 182 941 824	1.466 712 429 002 268 2	56.171 634 699 243 13	0.557 379 955 242 574 9	−2.640 497 406 312 216 6	0.194 497 917 379 939 27	-	14.576 595
420 965 623 182 937 344	1.458 491 930 262 585 8	56.179 813 725 129 705	−1.510 364 730 555 865 2	−3.229 371 464 126 677	0.477 142 450 499 912 1	−50.848 957 601 768 01	13.1949
420 954 009 591 365 248	1.484 484 492 617 411 9	56.192 966 049 492 81	1.975 118 732 485 443	−1.833 966 305 479 603 4	0.635 871 642 673 285 8	-	13.384 901

End of table 8

Table 9: *Gaia Source ID* and various other properties of the non CMs of Stock 19.

Gaia Source ID	RA in °	Dec in °	pm RA in mas year^{-1}	pm Dec in mas year^{-1}	parallax in mas	RV in km s^{-1}	mag$_g$
420 874 982 194 047 872	1.052 771 716 494 700 4	56.185 936 050 354 53	−2.005 711 497 046 519	−0.699 538 949 496 157	0.079 496 057 643 318 6	−77.372 141 860 081 48	13.200 895
420 874 982 194 048 128	1.058 974 560 465 921	56.186 025 437 768 41	15.634 094 820 413 141	−3.088 466 633 659 699 3	1.868 787 846 239 006 6	-	11.059 405
420 875 080 974 492 416	1.083 444 759 776 848 8	56.206 477 260 014 46	−1.747 195 974 202 328 4	−0.167 747 847 598 346 85	0.102 182 081 995 065 69	−51.147 167 697 556 1	12.958 017

Continued on the next page...

... Continuation of table 9

Gaia Source ID	RA in °	Dec in °	pm RA in mas year^{-1}	pm Dec in mas year^{-1}	parallax in mas	RV in km s^{-1}	mag$_g$
420 968 097 083 952 384	1.160 745 562 128 716 6	56.192 831 894 336 905	−4.218 952 643 742 107	−1.394 040 889 121 871 4	0.132 081 260 399 809 03	−83.036 981 628 643 08	11.420 302
420 874 535 517 455 232	1.096 713 402 746 596 6	56.157 906 037 073 59	−2.207 140 804 988 649 4	−1.479 690 258 608 730 8	0.100 013 092 079 877 55	-	15.023 648
420 874 604 236 930 816	1.078 067 102 693 902 8	56.160 256 271 731 57	−2.456 994 424 572 532 6	−0.259 412 908 702 931 4	0.149 687 850 103 253	-	15.027 268
420 873 058 048 713 984	1.014 071 463 087 598	56.104 281 927 979 166	−1.909 706 982 007 779	−1.596 411 078 377 541 6	0.155 765 985 726 686 82	-	14.196 004
420 872 954 969 497 600	1.072 695 013 865 420 8	56.121 759 560 083 376	−1.581 571 064 303 458 4	−0.583 281 901 955 853	0.017 934 127 129 253 054	-	13.984 155
420 872 508 292 912 512	0.991 281 073 748 046 5	56.064 485 490 755 615	−29.170 641 313 822 06	−40.373 391 110 877 684	16.093 373 595 170 252	−26.446 296 383 326 07	10.903 09
420 866 564 058 185 344	1.030 364 481 430 583 7	56.045 450 215 900 765	5.444 063 975 717 419	−12.590 753 126 594 203	1.131 045 952 325 797 2	-	14.791 661
420 866 564 058 185 728	1.023 636 765 939 656 1	56.043 476 685 470 82	−1.352 476 850 874 528 6	−0.925 082 930 991 816 9	0.131 173 581 507 312 4	-	15.008 316
420 866 460 978 978 944	0.990 802 579 037 417 5	56.016 971 356 897 41	−0.610 689 042 398 065 1	−0.384 566 457 787 832 16	0.139 978 334 679 535 66	-	14.282 475
420 912 880 987 436 672	0.969 370 156 055 990 9	55.996 422 501 838 25	12.270 278 259 742 2	−0.845 665 017 239 414 2	1.727 523 336 506 174 4	−15.164 366 399 836 746	11.700 828
420 866 426 619 243 648	1.037 706 353 437 736	56.013 467 970 869 18	0.379 179 598 891 222 16	−11.230 542 686 996 174	2.087 337 237 187 621 3	-	15.024 322 5
420 865 533 266 258 560	1.134 404 860 989 091	56.004 262 809 936 016	−5.131 673 607 985 859	−9.902 390 290 301 664	2.416 182 297 235 166 3	−18.460 326 783 156 233	13.602 06
420 871 374 421 576 320	1.141 101 625 528 378 6	56.017 595 892 472 364	−1.266 652 848 544 967 7	−0.764 612 074 093 828 7	0.125 471 799 701 820 43	-	14.678 754
420 871 683 659 218 688	1.195 512 193 176 814 7	56.035 160 074 809 82	−0.037 555 824 712 971 565	−1.095 492 721 137 440 8	0.097 750 559 092 921 24	-	14.765 095
420 873 328 622 834 432	1.180 584 036 299 432 9	56.091 578 620 200 16	3.276 095 893 483 205 4	6.574 744 754 063 53	2.252 865 610 263 447	−20.710 229 104 263 82	11.608 679
420 968 028 364 475 008	1.202 977 354 057 721 8	56.205 254 000 965 645	12.940 332 778 200 606	1.745 902 016 571 379 9	1.029 628 555 005 490 2	-	15.527 997
420 965 039 067 239 680	1.238 695 552 168 23	56.201 233 542 052 314	−1.198 403 288 557 885 2	−1.450 888 540 752 209	0.143 049 832 163 252 32	-	15.069 262 5
420 870 893 385 206 016	1.244 777 998 615 263	56.126 019 044 227 31	24.032 407 763 520 965	−7.528 998 996 609 262	3.258 399 229 780 823	-	10.564 37
420 873 436 005 847 168	1.200 606 064 995 536	56.112 216 922 488 65	9.383 256 135 076 515	−17.072 931 335 002 348	2.107 321 571 506 034 3	13.377 168 992 840 389	13.067 697
420 868 763 081 461 376	1.265 148 465 450 764 3	56.041 654 375 150 58	7.119 529 535 601 507	22.622 201 127 554 632	3.053 323 317 375 784	-	15.362 148
420 868 586 978 944 768	1.259 127 140 471 287 2	56.011 863 294 733 15	27.812 059 002 115 323	−3.516 590 611 642 959 3	3.095 597 551 808 248 6	0.393 911 727 333 076 56	11.720 077
420 871 065 183 959 936	1.210 557 120 414 368 1	55.976 342 253 505 29	14.529 153 353 071 141	−13.466 454 079 813 774	2.049 151 877 117 639 6	-	14.045 153
420 868 247 685 405 824	1.239 526 069 684 836 7	55.995 753 485 837 874	−2.581 553 949 806 077 8	0.255 355 893 636 035 84	0.065 550 540 733 823 03	-	14.090 218
420 868 007 167 253 376	1.301 307 629 645 413 6	55.976 011 223 128 985	14.504 818 452 727 66	0.633 800 691 326 589 6	1.527 204 033 045 027 4	−26.825 841 566 933 317	11.881 409
420 867 869 728 312 704	1.315 615 241 701 721 3	55.954 938 809 854 68	33.098 477 333 211 52	3.796 903 967 922 897	2.065 060 577 182 24	-	15.629 95
420 867 526 130 931 072	1.399 594 446 096 313 7	55.969 301 075 399 43	19.905 313 868 200 27	−10.326 548 388 924 905	2.015 840 907 940 034	-	14.997 961
420 868 350 764 636 544	1.346 688 805 250 265 7	55.986 799 399 042 255	63.801 497 223 855 286	−26.253 876 022 484 828	3.203 350 178 140 021 8	-	14.125 177
420 867 659 268 629 504	1.403 807 959 987 918	55.991 948 114 367 624	−1.629 992 100 138 531 1	−0.211 115 926 296 018 94	0.084 611 807 760 545 64	-	15.060 613
420 868 419 484 095 360	1.291 246 370 649 785 6	56.010 815 328 088 526	14.338 256 651 693 447	7.533 618 885 700 806	1.213 597 205 461 306	-	14.702 634
420 869 347 197 022 720	1.367 297 015 491 891 8	56.045 340 015 919 26	11.339 109 342 369 433	−21.132 339 890 105 165	2.011 411 780 834 497 3	-	13.250 489
420 869 484 635 986 048	1.431 891 839 471 276	56.037 654 567 056 84	−2.524 094 213 493 533 4	−0.679 079 518 865 085 7	0.130 952 065 703 573 2	-	13.733 88
420 963 424 159 736 192	1.468 400 614 710 591 2	56.076 284 883 104 97	−0.323 725 543 015 530 14	−12.827 667 627 997 437	2.012 921 981 429 333 3	-	14.366 641
420 964 317 512 743 808	1.376 592 357 088 968	56.158 154 139 426 28	−3.224 980 844 023 847	−0.185 775 901 238 044 33	0.100 289 901 509 091 03	-	14.500 54
420 963 905 195 885 824	1.373 080 616 505 904 4	56.134 898 728 071 526	−1.634 876 802 815 959	−0.654 067 818 221 397 3	0.138 710 546 715 083 9	-	14.985 39
420 963 664 677 718 656	1.416 826 707 685 712	56.124 827 932 435 02	−1.837 933 383 996 528 6	−1.613 614 865 446 662 2	0.043 368 310 739 039 92	-	14.728 74
420 963 664 677 878 784	1.442 371 499 273 957	56.123 601 527 901 58	−5.320 682 963 805 631	−15.351 400 068 957 872	1.708 926 034 483 140 5	−36.673 020 632 403 706	12.801 926
420 963 630 318 149 504	1.443 214 390 615 568 3	56.105 402 141 055 81	−10.156 951 246 820 297	12.165 931 549 898 401	1.381 081 079 995 389 2	-	15.620 969

End of table 9

Table 10: *Gaia Source ID* and various other properties of the stars in Stock 19, which were not analysed.

Gaia Source ID	RA in °	Dec in °	pm RA in mas year^{-1}	pm Dec in mas year^{-1}	parallax in mas	RV in km s^{-1}	mag$_g$
420 868 282 045 147 392	1.257 259 714 364 879	55.994 023 280 748 245	−1.398 787 044 662 146 4	−0.413 253 311 014 696 53	−0.021 005 701 011 378 86	-	14.392 95
420 873 161 127 923 328	1.022 191 601 492 38	56.134 918 542 304 41	-	-	-	-	14.936 52
420 963 699 032 102 784	1.399 643 365 633 971 3	56.097 732 203 607 37	−1.367 713 699 284 927 7	0.020 323 465 475 587 81	−0.030 875 870 308 301 49	-	15.802 724
420 911 364 853 215 360	0.967 957 755 446 055 1	55.971 715 521 613 69	-	-	-	−15.501 509 748 932 932	12.686 633

End of table 10